

Tsunami Maritime Response and Mitigation Strategy – Port of Bellingham
Appendix 4: Maritime Tsunami Hazard Assessment for the
Port of Bellingham, Washington - Technical Report

Maritime Tsunami Hazard Assessment for the
Port of Bellingham, Washington

Technical Report

February 1, 2021

Carrie Garrison-Laney
Washington Sea Grant
University of Washington

Randall J. LeVeque & Loyce M. Adams
Department of Applied Mathematics
University of Washington

Contents

1. Introduction	3
2. Earthquake Sources	4
2.1 Cascadia subduction zone earthquake Cascadia-L1, M_w 9.0.	4
2.2 Alaska-Aleutian Subduction Zone Earthquake (AKMaxWA)	5
2.3 Other sources not studied	7
3. Topography and bathymetry	7
3.1 1/9 arc-second DEMs	10
3.2 Coarser DEMs	10
4. Study area	11
5. Model uncertainties and limitations.....	12
5.1 Tide stage and sea level rise.....	12
5.2 Subsidence.....	13
5.3 The built environment	13
5.4 Bottom friction	13
5.5 Tsunami modification of bathymetry and topography.....	13
5.6 Output format.....	13
6. Fgmax results	14
6.1 Maximum onshore flow depths	14
6.2 Maximum speeds.....	17
6.3 HMin results.....	20
7. Gauge output results	22
7.1 Synthetic gauge locations	22
7.2 Synthetic gauge plots.....	26
8. Future studies	65
Acknowledgments.....	66
Data Availability	66
References	67
Appendix A. Complete GeoClaw Model Results	70
Appendix B. GeoClaw technical information	71
Data output format.....	71
GeoClaw Version 5.7.0.....	72
Appendix C. Modifications to Bellingham 1/9 arc-second DEM.....	74

1. Introduction

This Tsunami Hazard Assessment (THA) tests tsunamis from two earthquake sources: the Cascadia subduction zone (CSZ) and the Alaska-Aleutian subduction zone (AASZ) at the Port of Bellingham. The results of this study include modeled flow depths, surface heights (wave amplitudes), current speeds, and times of wave arrival. The data from this study was used to create a maritime guidance document for the Port of Bellingham, the City of Bellingham Emergency Management, and the Bellingham maritime community, to aid in planning and preparing for a tsunami. The maritime guidance document is a collaboration between Washington Sea Grant, Washington Emergency Management Division, the Washington Department of Natural Resources Washington Geological Survey, the Port of Bellingham, and the City of Bellingham.

The tsunami modeling was done using GeoClaw, Version 5.7.0 (Clawpack Development Team, 2020). GeoClaw open source software is available at <http://www.clawpack.org/geoclaw>. GeoClaw simulates tsunami generation, propagation, and inundation. This model, which solves the nonlinear shallow water equations, has undergone extensive verification and validation (Berger and others, 2010; LeVeque and others, 2011), and has been accepted as a validated model by the U.S. National Tsunami Hazard Mitigation Program (NTHMP) after conducting multiple benchmark tests as part of an NTHMP benchmarking workshop (González and others, 2011).

This THA report generally follows the format of reports developed by the University of Washington Tsunami Modeling Group (UWTMG). Some of the text in this report describes modeling methods developed by the UWTMG, and also used in UWTMG reports.

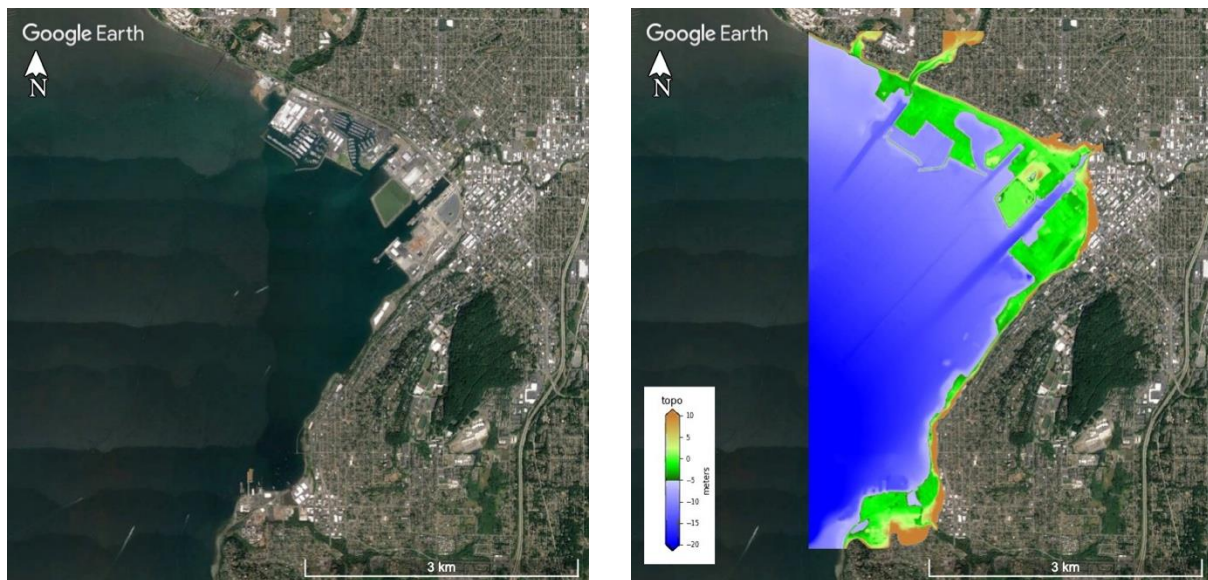


Figure 1. Left, the Bellingham waterfront study area; and right, with a color overlay showing the area of highest resolution topography DEM points used for the study. The Earth tones represent points above mean high water, and blues represent points below mean high water. Elevation and bathymetry values are in meters.

2. Earthquake Sources

This study tests two earthquake sources: a Cascadia subduction zone (CSZ) megathrust event with moment magnitude M_w 9.0 (Cascadia-L1), and an Alaska-Aleutian subduction zone (AASZ) event off the coast of Alaska with magnitude 9.24 (AKMaxWA).

2.1 Cascadia subduction zone earthquake Cascadia-L1, M_w 9.0.

The Cascadia subduction zone (CSZ), which spans from Northern California to British Columbia has been seismically quiet since the year 1700 (Jacoby et al., 1997; Satake and others, 2003; Yamaguchi et al., 1997; Atwater et al., 2005), but geologic evidence of submerged coastal areas and tsunami deposits (Atwater and Hemphill-Haley, 1997; Atwater et al., 2004), in addition to offshore sedimentary evidence (Goldfinger et al., 2012; Goldfinger et al., 2017), reveals that Cascadia has had at least 23 magnitude 9 earthquakes in the last 10,000 years. In addition, global positioning data show that Cascadia is currently building seismic stress, portending a future great earthquake (Burgette et al., 2009; Yousefi et al., 2020). The USGS estimates that there is a 10-14 % chance of a magnitude 9 earthquake, and a 30% chance of a magnitude 8 on the CSZ within the next 50 years (Petersen and others, 2002).

The CSZ earthquake fault model used for this study is the L1 scenario, developed by Witter and others (2011, 2013). This model includes a surface-rupturing splay fault structure that amplifies tsunami waves. Figure 2 displays the crustal and seafloor deformation produced by the L1 model. The L1 source is one of 15 seismic scenarios used in a hazard assessment study of Bandon, OR, based on an analysis of data spanning 10,000 years. Washington State has adopted this scenario as the "maximum considered case" for many inundation modeling studies and subsequent evacuation map development. The Cascadia-L1 has an estimated mean recurrence interval of ~3,333 years (Witter and others, 2013). This is a close and conservative approximation to design requirements for critical facilities in the international building code for seismic hazards that build to the engineering standard of a 2,500-year event (ICC, 2015).

The Cascadia-L1 scenario used in this study is a derivative of the original L1 source developed by Witter and others (2011) was truncated on the northern end at around 48°N. To more accurately represent the maximum considered tsunami for the state of Washington, this source model was extended to north of the entrance to the Strait of Juan de Fuca by the NOAA Center for Tsunami Research at Pacific Marine Environmental Laboratory (PMEL) in Seattle. Recent tsunami hazard assessments for Washington now use the extended version of the Cascadia-L1 (e.g. LeVeque and others, 2018; Adams and others, 2019; LeVeque and others, 2019).

The Cascadia-L1 source creates very large waves along the Pacific coast of Washington, and substantial waves that propagate through the Strait of Juan de Fuca (Sjdf) and into the Strait of Georgia. This source causes initial wave drawdowns in Bellingham about 1 hour and 25 minutes after the earthquake, and wave crest arrival at about 2 hours and 15 minutes after the earthquake. The Cascadia-L1 produces no land level change within this study region.

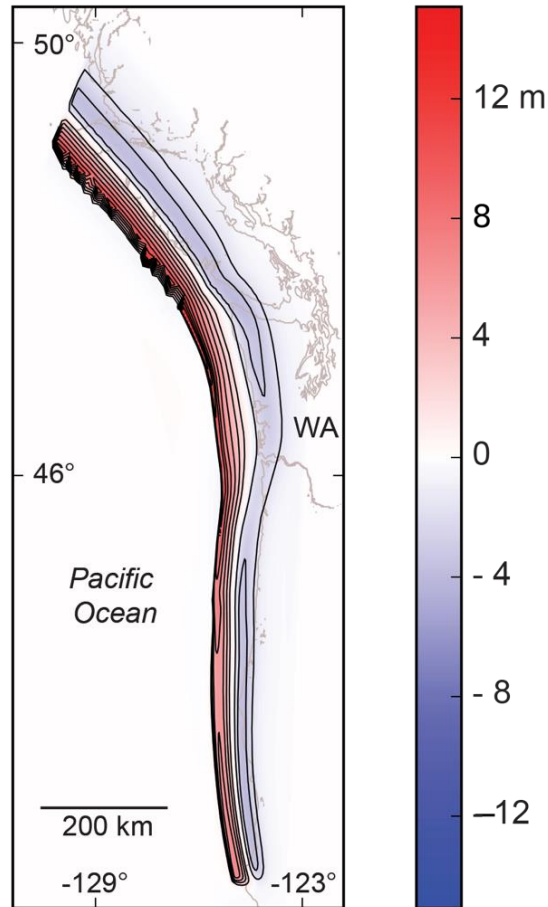


Figure 2. Surface deformation of the Cascadia-L1 tsunami source. This earthquake has a maximum uplift 15.08 meters and a maximum subsidence -3.98 meters. Red shaded areas show uplift, and the blue shaded area shows subsidence (in meters). The contour interval is 2 meters.

2.2 Alaska-Aleutian Subduction Zone Earthquake (AKMaxWA)

The very seismically active Alaska-Aleutian subduction zone has had 82 observed tsunamis since the year 1788 (Wesson et al., 2007), including the tsunami generated by the 1964 magnitude M_w 9.2 Great Alaskan earthquake. The tsunami generated by this earthquake devastated not only the Alaskan coastline (Plafker and Kachadoorian, 1966), but also caused damage and fatalities along coastal areas of British Columbia, Washington, Oregon, and California (Lander et al., 1993).

The NOAA Center for Tsunami Research developed the Alaska-Aleutian subduction zone earthquake source model, AKmaxWA (Figure 3), used in this study (Chamberlain and others, 2009). This source model is a hypothetical earthquake with a similar magnitude as the 1964 Alaska Earthquake (M_w 9.2). This source model has uniform slip of 20 m specified over a set of 20 “unit source” subfaults (Table 1) that correspond to the NOAA SIFT database (2007-2020). A series of tsunami simulations with different combinations of unit sources led to the selection of this specific set of unit sources that produce the maximum tsunami impact to Washington’s waterways. The magnitude of this earthquake source model is a M_w 9.24 (based on the subfault dimensions and slip). Because organizations such as the United

States Geological Survey (USGS) and Pacific Northwest Seismic Network (PNSN) typically report magnitudes with only one decimal place, this scenario is considered the “maximal M_w 9.2” event for impact to Washington (assuming a crustal shear modulus, or rigidity, of 40 GPa). Because organizations such as the United States Geological Survey (USGS) and Pacific Northwest Seismic Network (PNSN) typically report magnitudes with only one decimal place, this scenario is considered the “maximal M_w 9.2” event for impact to Washington.

Table 1. Subfault parameters for the AKMaxWA event used in this study (Chamberlain and others, 2009). All subfaults have a length = 100 km, width = 50 km, dip = 15°, rake = 90°, and slip = 20 m. The subfaults come from the NOAA Unit Source database and SIFT propagation database metadata file (Gica and others, 2008). With crustal rigidity (shear modulus) set to $\mu = 40$ GPa, this gives a M_w 9.24 event (LeVeque and others, 2019).

Unit Source	Longitude	Latitude	Depth (km)	Strike (degrees)
acsza29	-157.7390	55.1330	17.94	247.0000
acsza29	-158.1203	55.4908	30.88	246.2137
acsza30	-156.3960	55.5090	17.94	240.0000
acsza30	-156.8479	55.8534	30.88	240.4869
acsza31	-155.1050	55.9700	17.94	236.0000
acsza31	-155.5685	56.3016	30.88	235.6690
acsza32	-153.7920	56.4730	17.94	236.0000
acsza32	-154.2120	56.8210	30.88	235.4756
acsza33	-152.4630	56.9750	17.94	236.0000
acsza33	-152.8909	57.3227	30.88	235.4119
acsza34	-151.0629	57.5124	17.94	236.0000
acsza34	-151.5802	57.8213	30.88	234.6891
acsza35	-149.7403	58.0441	17.94	230.0000
acsza35	-150.3575	58.3252	30.88	230.1971
acsza36	-148.6751	58.6565	17.94	218.0000
acsza36	-149.4588	58.8129	30.88	217.3327
acsza37	-147.7495	59.2720	17.94	213.7100
acsza37	-148.3921	59.5820	30.88	214.2669
acsza38	-145.3445	60.1351	17.94	260.0800
acsza38	-145.4638	60.5429	30.88	259.0313

The AKmaxWA model produces very large waves along the Aleutian subduction zone. The wave travel across the Pacific Ocean to Washington and propagate into the Strait of Juan de Fuca, Puget Sound, and the Strait of Georgia. The wave crests reach the Bellingham waterfront at approximately 6 hours following the earthquake. With this model, there is no initial drawdown, and the second wave is higher than the first. The AKMaxWA scenario, based on an earthquake in Alaska, produces no land level change within this study region.

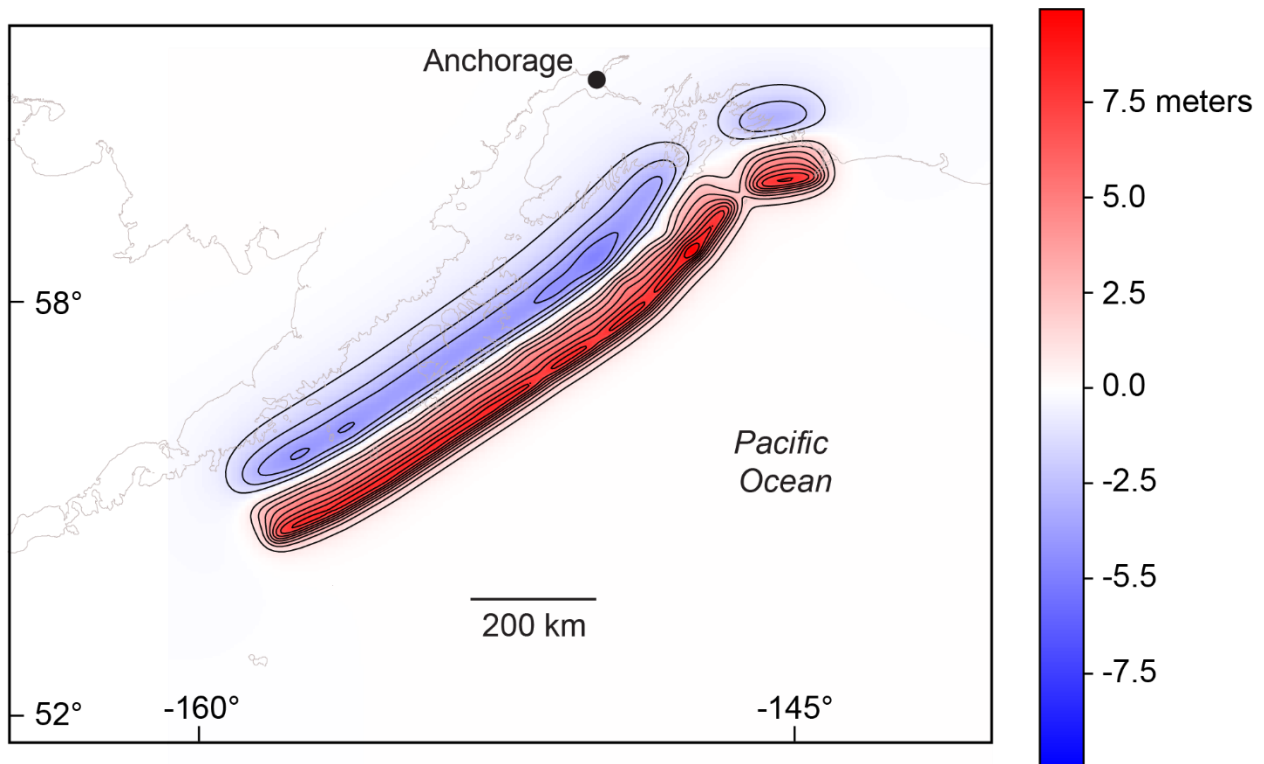


Figure 3. Surface deformation of the AKmaxWA source, with maximum uplift 9.7 m and maximum subsidence -4.9 m. The red shading shows uplift, the blue shading shows subsidence, and the contour interval is one meter.

2.3 Other sources not studied

Washington State faces risk from other potential earthquake sources as well. These include several fault zones that cross the Puget Sound (e.g. Tacoma Fault Zone, South Whidbey Island Fault, and the Devil’s Mountain Fault). However, this study does not consider these faults, as there are no current peer-reviewed deformation models available at this time.

3. Topography and bathymetry

Digital Elevation Models (DEMs) are needed by GeoClaw to effectively track the movement of tsunami waves from the source to the study area. The footprints of the DEMs used in this study are shown in Figure 4, and their resolutions and year of publication are listed in Table 3. All DEMs used in this study are vertically referenced to mean high water (MHW), so that the “0” elevation reference point for model

outputs is MHW. For the Mean Low Water (MLW) simulations, the MHW DEM was also used, but sea level was set to -1.657 m (5.44 feet) below zero. All of the DEMs used in this study are projected in the World Geodetic System 1984 (WGS84, EPSG:4326) coordinate system. Note that published DEMs may have errors, or the landscape may have changed since the DEM was created.

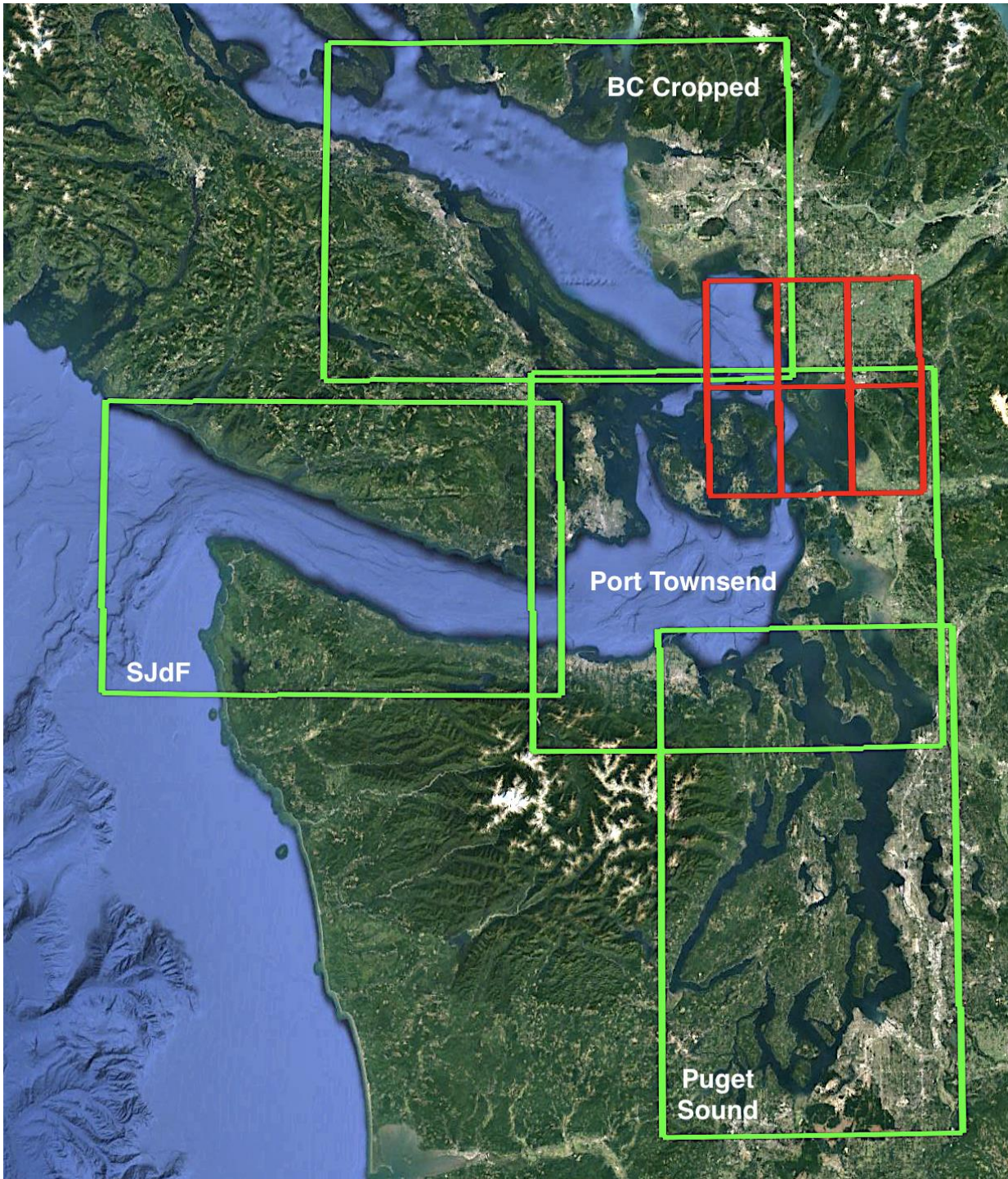


Figure 4. DEMs used in this study (from Adams and others, 2019). The resolution of each of these DEMs is listed in Table 3. The six small regions shown in red, from north to south, west to east are the Bellingham ncei19-UL, ncei19-UM, ncei19-UR, ncei19-LL, ncei19-LM, and ncei19-LR (Table 2). Four of these 1/9 arc-second DEMs were used for the study area. These DEMs were used for both the Cascadia-L1 and AKMaxWA simulations. All simulations also used the

ETOPO1 1-minute resolution DEM (not shown) for the Pacific Ocean and for the part of the Strait of Georgia.

3.1 1/9 arc-second DEMs

The highest resolution model outputs for this study were run on a DEM with 1/9 arc-second grid points (1/9 arc-second both in longitude and latitude). This dataset, developed by NOAA’s National Centers for Environmental Information (NCEI), has six separate tiles for Bellingham Bay that cover the area - 123.00°W to -122.25°W longitude and 48.4998°N to 49.0001°N latitude. Table 2 lists the names of the files for each of the six tiles. For this study, four of the tiles were needed to cover the study area for the Port of Bellingham: UM,UR,LM, and LR. (Figure 4, red tiles.) For this study, some small unpublished edits were made to the Bellingham tiles to correct errors. See Appendix C for more information.

Table 2. The file name and script notation name for the six 1/9” grid tiles for Bellingham Bay.

Notation in script	File name
UM (Upper Middle)	N49x00_w122x75_2020_v3.nc
UR (Upper Right)	N49x00_w122x50_2020_v3.nc
LR (Lower Right)	N48x75_w122x50_2020_v3.nc
LM (Lower Middle)	N48x75_w122x75_2020_v3.nc
LL (Lower Left)	N48x75_w123x00_2020_v3.nc
UL (Upper Left)	N49x00_w123x00_2020_v3.nc

A separate DEM was made from these tiles by coarsening the 1/9 arc-second DEM to 1/3 arc-second by 1/3 arc-second using a pre-processing script that merged and coarsened the tiles by subsampling every third point in each direction. This DEM was used around the study area.

3.2 Coarser DEMs

The Strait of Juan de Fuca, Port Townsend, and Puget Sound DEMs were all coarsened from 1/3 arc-second to 2 arc-second by pre-simulation processing scripts. These coarsened DEMs are more efficient to use in GeoClaw for regions where the detail of a 1/3 arc-second DEMs is not required. The simulations also used ETOPO1 1-minute topography to cover the entire modeling domain; allowing the simulations of the Cascadia-L1 and AKMaxWA that initiate in the Pacific Ocean. Figure 4 displays the extent of all DEMs used in this assessment, with the exception of the 1-minute ETOPO1 DEM used in the Pacific.

Table 3. List of DEMs used in this tsunami modeling study.

Name	Resolution	Publication
ETOPO1 Global Relief Model	1 arc-minute	NOAA NGDC, 2009
Strait of Juan de Fuca	1/3 arc-second, coarsened to 2 arc-second	NOAA NCEI, 2015
Port Townsend	1/3 arc-second, coarsened to 2 arc-second	NOAA NCEI, 2011
Puget Sound	1/3 arc-second, coarsened to 2 arc-second	NOAA NCEI, 2014
British Columbia	3 arc-second	NOAA NCEI, 2013

CUDEM	1/9 arc-second for study area, also coarsened to 1/3 arc-second around the study area	CIRES, 2020*
-------	--	--------------

*Original version published in 2017, with unpublished updates released by NCEI in 2019 and 2020. Additional edits to the DEM were made by Washington DNR in July 2020 for this study (see Appendix C).

4. Study area

Figure 5 shows the Bellingham waterfront area with a color overlay of the highest resolution topography on which the maximum of each quantity of interest is monitored during the course of the simulations. This area is the defined “fgmax” grid, which is a fixed grid (fg) that saves the maximum (max) values of model variables attained during the duration of the simulation. These variables include water depth (h) and water speed (s) derived from the velocity components ($s = \sqrt{u^2 + v^2}$), as well as other quantities of interest derived from the depth (h) and horizontal momenta (hu and hv; the quantities modeled in the shallow water equations). The fgmax grid also monitors the time of the maximum values and the first wave arrival at each grid point.

The fgmax grid points are aligned with the DEM in the regions specified, with 1/9 arc-second spacing in longitude and latitude. An improvement to GeoClaw developed for a previous project (LeVeque and others, 2018) allows selecting only the grid points in each region for which the topography elevation is below some limit. Additional improvements to the code were made by LeVeque and others (2019).

The improvements made helped to reduce the total number of fgmax grid points to a manageable number. The code improvements also helped to reduce the number of fgmax points selected by specifying a certain type of polygon, known as “Ruled Rectangles” (as summarized in LeVeque and others, 2019; Appendix B). Prior to these code improvements, fgmax points were selected by designating a rectangular area. This did not work well for the complicated geometry of Puget Sound waterways, and other Salish Sea areas because rectangular areas included many points on land that were not important to the simulation, but cost a lot in terms of computation (González and others, 2015; see Figure 1). When rectangles were used to define fgmax areas, some computations proved impossible because they contained too many points (maximum points allowed is approximately 6,000,000 (R. LeVeque, Pers. Comm., 2019)). The UW group also improved the AMR procedures in GeoClaw to allow specifying refinement to the finest level only in certain Ruled Rectangles (see Appendix B). Each run uses adaptive mesh refinement (AMR) to focus fine computational grids around the fgmax area.

For this study, the fgmax area was defined by a Ruled Rectangle that contains only points that were either within 10 grid cells of shoreline or have an elevation less than 15m. This reduced the number of grid cells required in the computation. The fgmax area for this study has 1,473,496 points on a 1653 by 1426 grid.

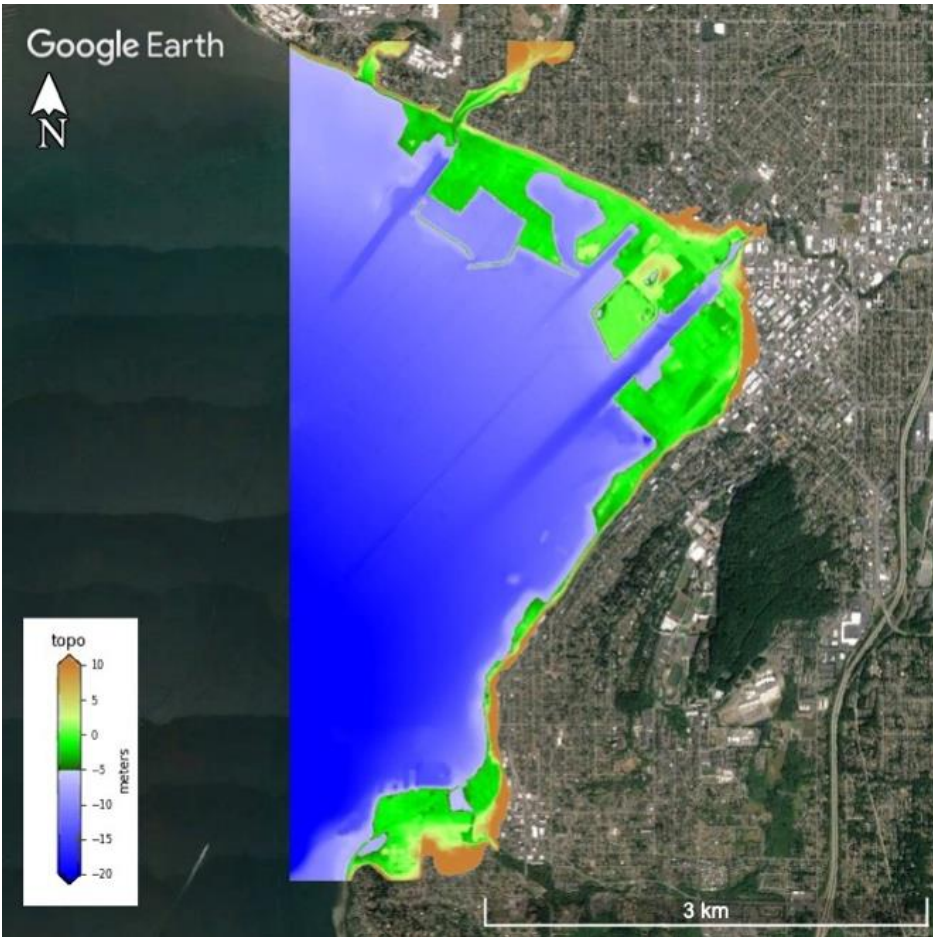


Figure 5. The topographic points that make up the fgmax area (colored areas) overlaid on a Google Earth air photo. Earth tones are land points (at or above MHW), and blue tones are points below MHW.

5. Model uncertainties and limitations

Inputs to the GeoClaw model include the earthquake source, DEMs and fgmax area, as discussed in sections 2-4. In addition other geophysical parameters must be designated. Some physical processes are not included in these simulations, which use the two-dimensional shallow water equations. Each tsunami source and tidal level required a separate job run (two sources at two tidal levels = four runs). See below for the discussion of these parameters and their potential effect on the modeling results.

5.1 Tide stage and sea level rise

The simulations for this study were run at both Mean High Water (MHW) and Mean Low Water (MLW) tidal datums. The MHW datum is conservative for wave heights because the higher tidal stage amplifies the tsunami wave heights. The MLW datum is often conservative for tsunami currents, in that current speeds often increase at lower water levels in shallow areas. Simulations were run at both of these tidal stages to capture the range of variability of expected conditions along the Port of Bellingham waterfront during a tsunami event. The DEMs used near the study location are referenced to the MHW datum (= 0) with the exception of the ETOPO1 and Strait of Juan de Fuca DEMs, which are referenced to NAVD88. This is not a concern because these datasets are far from the study area, and cover parts of the model at coarse resolution. The simulations at MLW used the same DEMs (referenced to MHW), but sea level

was set in GeoClaw at -1.657 m (-5.44 feet) to approximate MLW. The MLW level was obtained from the historical tide gauge datum for MLW for Bellingham Bay.

While sea level rise important for future waterfront planning, this study does not account for potential sea level rise projections.

5.2 Subsidence

Neither earthquake source would produce seismic subsidence in the study area, so no coseismic subsidence is accommodated in the simulations in this study. (In cases where coseismic subsidence occurs within or near the fgmax area, GeoClaw accounts for land level changes from the initial earthquake deformation in the modeling process by modifying the initial DEM provided for the given region.)

5.3 The built environment

The topographic DEMs used in this study are “bare earth” and are created by stripping the land surface of built structures, buildings, and vegetation. The presence of structures and vegetation can alter tsunami flow patterns and generally impede inland flow. To some extent, the lack of structures in the model makes the model results more conservative, because structures can reduce inland penetration of the tsunami wave. Actual tsunami flows are likely to interact with structures that may impede flow, and cause water to pile up in some areas. Bare earth DEMs may lead to simulations with higher flow velocities because there is nothing to slow the flows. Actual tsunami flows may be slowed by structures, or conversely may speed up in areas where the flow is channelized, such as between buildings. Structures also contribute to debris that interacts with tsunami flows.

5.4 Bottom friction

The simulation uses the value 0.025 for Manning’s Roughness Coefficient. This is a standard value used in tsunami modeling and corresponds to a gravelly earth surface material. Using 0.025 is conservative in some sense, because the presence of trees, structures, and vegetation would justify the use of a larger value, which might tend to reduce the inland flow. On the other hand, larger friction values can lead to deeper flow in some areas, since the water may pile up more as it advances more slowly across the topography. There has not been a sensitivity study using other friction values at this moment in time.

5.5 Tsunami modification of bathymetry and topography

Scour, erosion, and deposition all occur in a tsunami. These topographic and bathymetric changes will inherently alter flow patterns of the tsunami wave. The erosion of natural berms or ridges along the coastline (or manufactured levies, dikes, or breakwaters) by the tsunami could increase more extensive flooding. On the other hand, the movement of material in a tsunami also requires an expenditure of tsunami energy, which could reduce the inland extent of inundation. These complex changes to the land are largely uncertain in a tsunami and thus, GeoClaw does not account for erosional or bathymetric/topographic change during simulations. Because there is no active modification to the topography and bathymetry in these results, the modeling dynamics of flow presented here may not entirely predict future tsunami behavior in the study area.

5.6 Output format

The results were stored as netCDF files on a set of points with 1/9 arc-second (1/9") spacing in both longitude and latitude. See Appendix B for further discussion of the data format.

6. Fgmax results

This report contains simple plots of mapped modeling results. The Washington Geological Survey at the Washington State Department of Natural Resources will develop the model results into high-quality graphics for the final maritime guidance publication and products.

In addition to the simple plots in this report, there are also high-resolution png files of these results embedded into kml files that are available for viewing in Google Earth (some of which are reproduced in this report in Figures 6-15), and linked from the URLs in Appendix A. The plots in this report are at a scale that cannot adequately show all results in detail, whereas the high resolution kml files allow zooming in to explore results in greater detail. See Appendix A for details about viewing the results online.

The fgmax plots that follow show the maximum onshore flow depths, maximum speeds, and maximum drawdown (hmin) recorded in the fgmax area over the full simulation time of 10 hours for Cascadia-L1 MHW, 5 hours for Cascadia-L1 MLW, and 12 hours each for AKMaxWA MHW and MLW. To save computing time, the Cascadia-L1 MLW event only simulated five hours of time (as opposed to 10) because the maximum wave height and drawdown had occurred by 5 hours after the earthquake in the MHW simulation. The length of the other simulations was chosen to capture a significant portion of the time that wave activity continued in the study area.

6.1 Maximum onshore flow depths

The greatest onshore flow depths (inundation heights) and inland limits of tsunami flow are from the Cascadia-L1 event at MHW, with flows that cover the low-lying areas seaward of Roeder Avenue; the area around Waypoint Park; and east of Cornwall Avenue to the slope break. Inland limits of tsunami waves exceed these areas in and near stream channels where inland penetration is greater. The Cascadia-L1 MHW simulation has greater onshore flow depths than the MLW simulation, however, the Cascadia-L1 MLW onshore flows still cover nearly the same inland limits as the MHW simulation.

The AKMaxWA event similarly shows greater flow depths for MHW than MLW, where the inland limits and flow depths are similar to the Cascadia-L1 MLW limits. The AKMaxWA MLW simulation produced negligible onshore flows.

Maximum onshore flow depths are shown in Figures 6-9 in separate figures for Cascadia-L1 MHW, Cascadia-L1 MLW, AKMaxWA MHW, and AKMaxWA MLW.

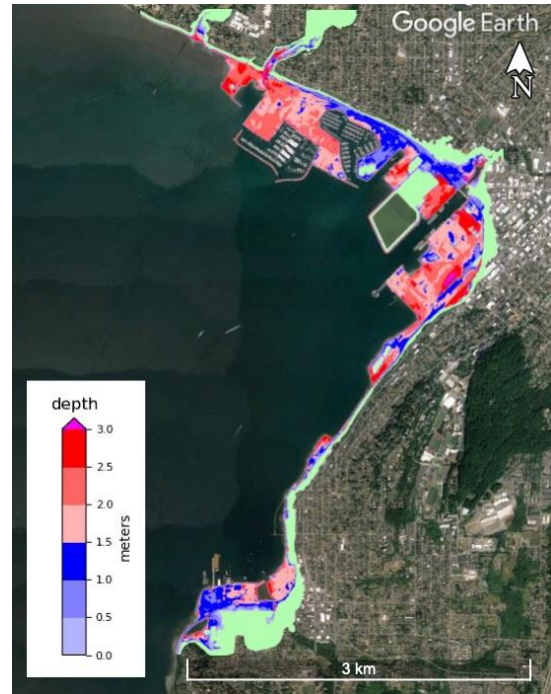
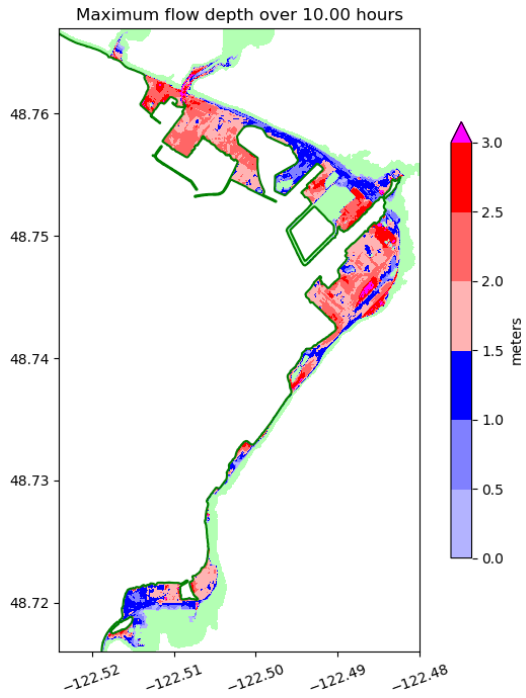


Figure 6. Maximum onshore flow depths for the Cascadia-L1 event at Mean High Water (MHW) plotted alone (left), and as an air photo overlay in Google Earth (right). These are the maximum values over 10 hours of simulated time. Areas in green remained dry for the duration of the simulation.

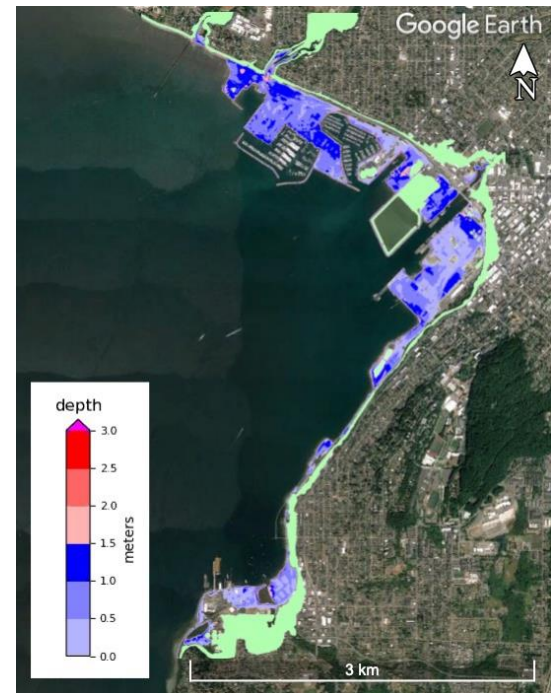
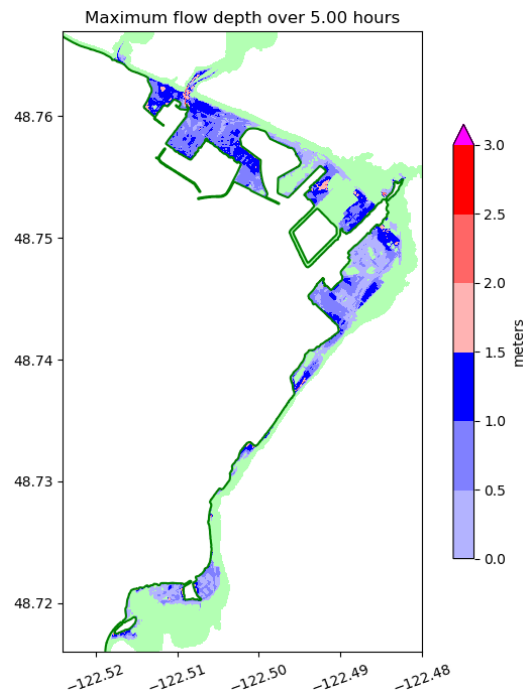


Figure 7. Maximum onshore flow depths for the Cascadia-L1 event at Mean Low Water (MLW) plotted alone (left), and as an air photo overlay in Google Earth (right). These are the maximum

values over 5 hours of simulated time. Areas in green remained dry for the duration of the simulation.

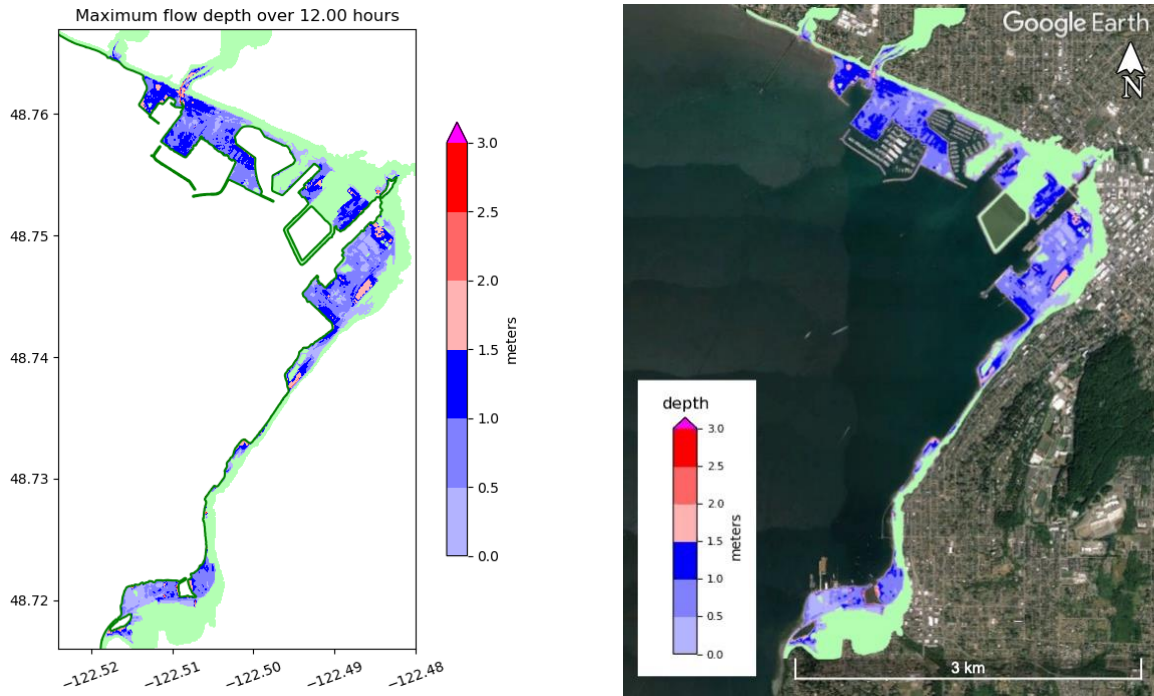


Figure 8. Maximum onshore flow depths for the AKMaxWA event at Mean High Water (MHW) plotted alone (left), and as an air photo overlay in Google Earth (right). These are the maximum values over 12 hours of simulated time. Areas in green remained dry for the duration of the simulation.

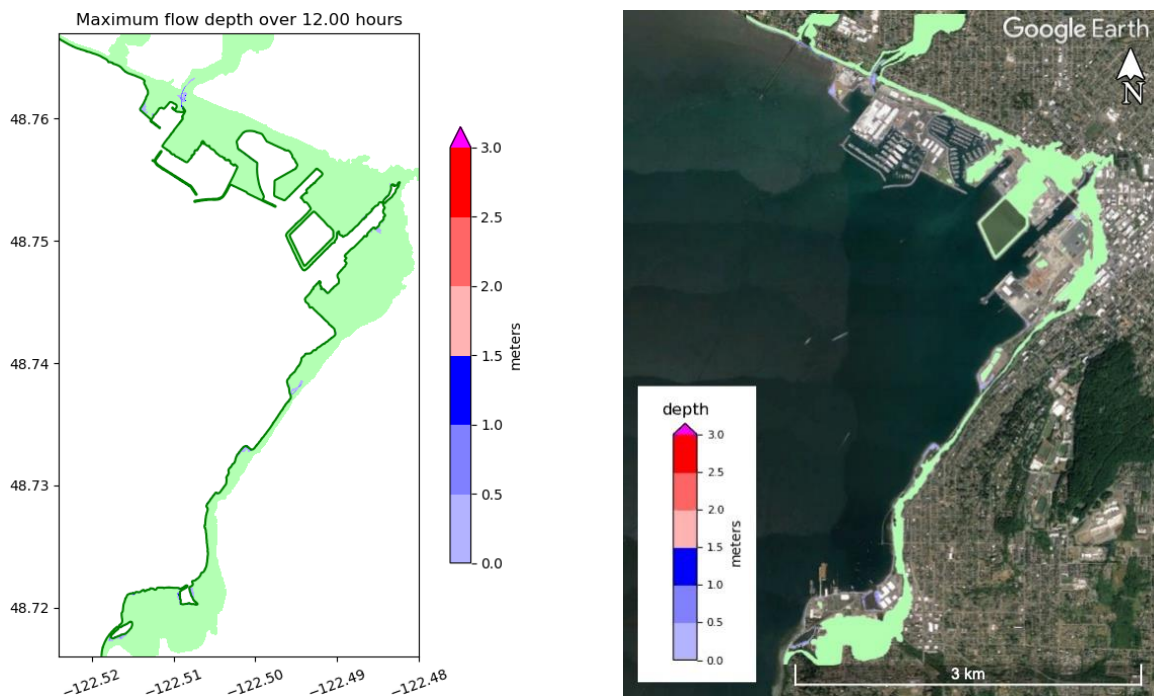


Figure 9. Maximum onshore flow depths for the AKMaxWA event at Mean Low Water (MLW) plotted alone (left), and as an air photo overlay in Google Earth (right). These are the maximum values over 12 hours of simulated time. Areas in green remained dry for the duration of the simulation.

6.2 Maximum speeds

Maximum speeds are shown in Figures 10-13 for both the Cascadia-L1 and AKMaxWA events, at Mean High Water (MHW) and Mean Low Water (MLW) tidal stages. The fastest simulated currents are in and at the entrances to Squalicum Harbor. Higher current areas were also observed near the Bellingham Cruise Terminal and the Fairhaven Shipyard. Higher current speeds occurred in Squalicum Harbor for both the Cascadia-L1 and AKMaxWA simulations at MLW in comparison to the same events at MHW.

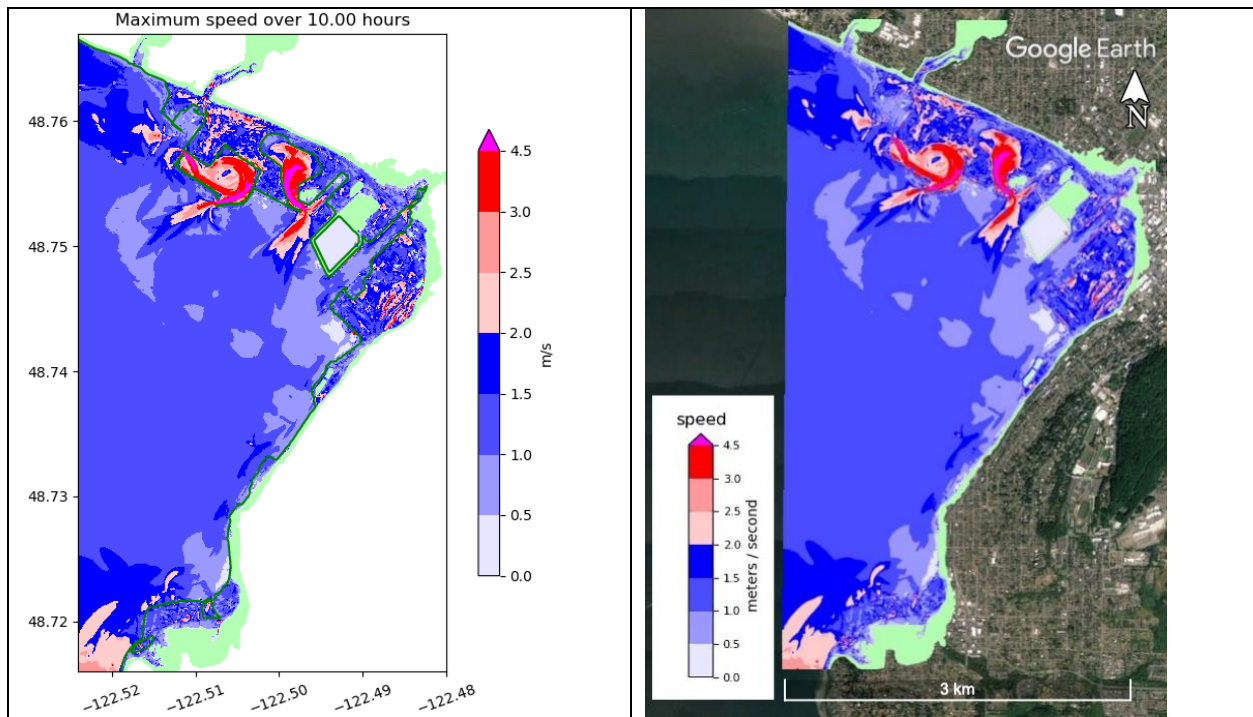


Figure 10. Maximum current speeds for the Cascadia-L1 event at Mean High Water (MHW) plotted alone (left), and as an air photo overlay in Google Earth (right). These are the maximum values over 10 hours of simulated time. Areas in green remained dry for the duration of the simulation.

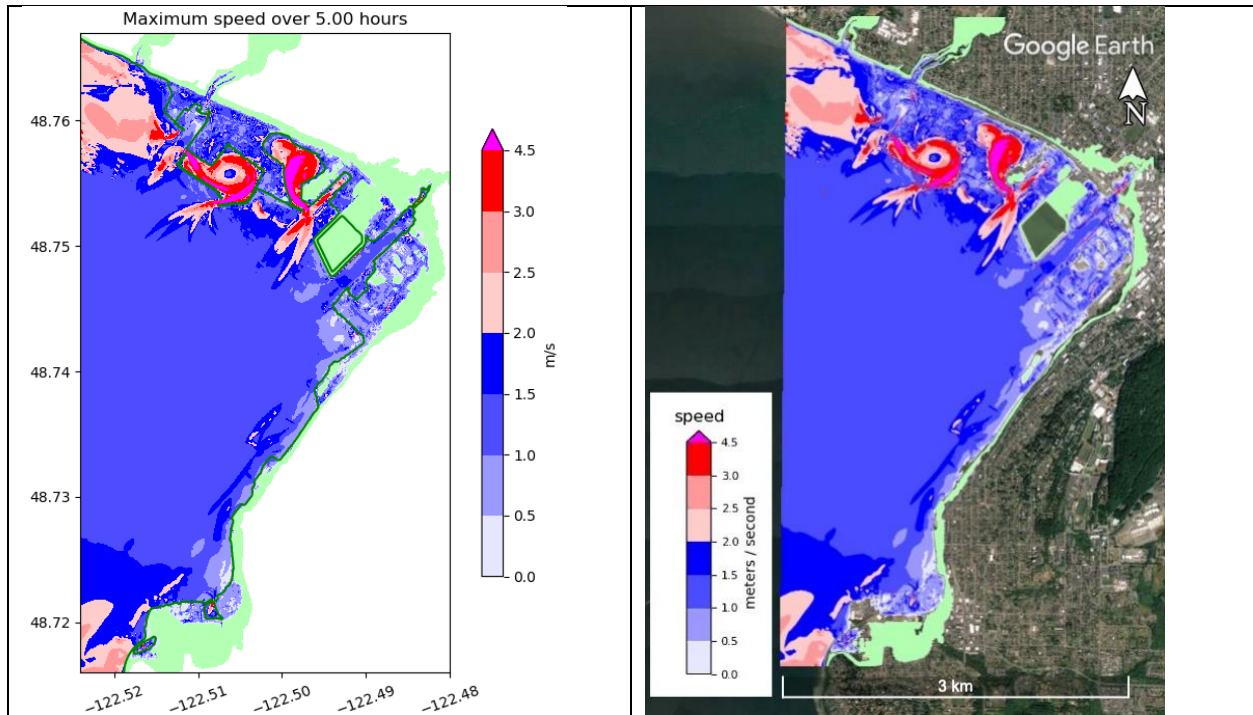


Figure 11. Maximum current speeds for the Cascadia-L1 event at Mean Low Water (MLW) plotted alone (left), and as an air photo overlay in Google Earth (right). These are the maximum values over 5 hours of simulated time. Areas in green remained dry for the duration of the simulation.

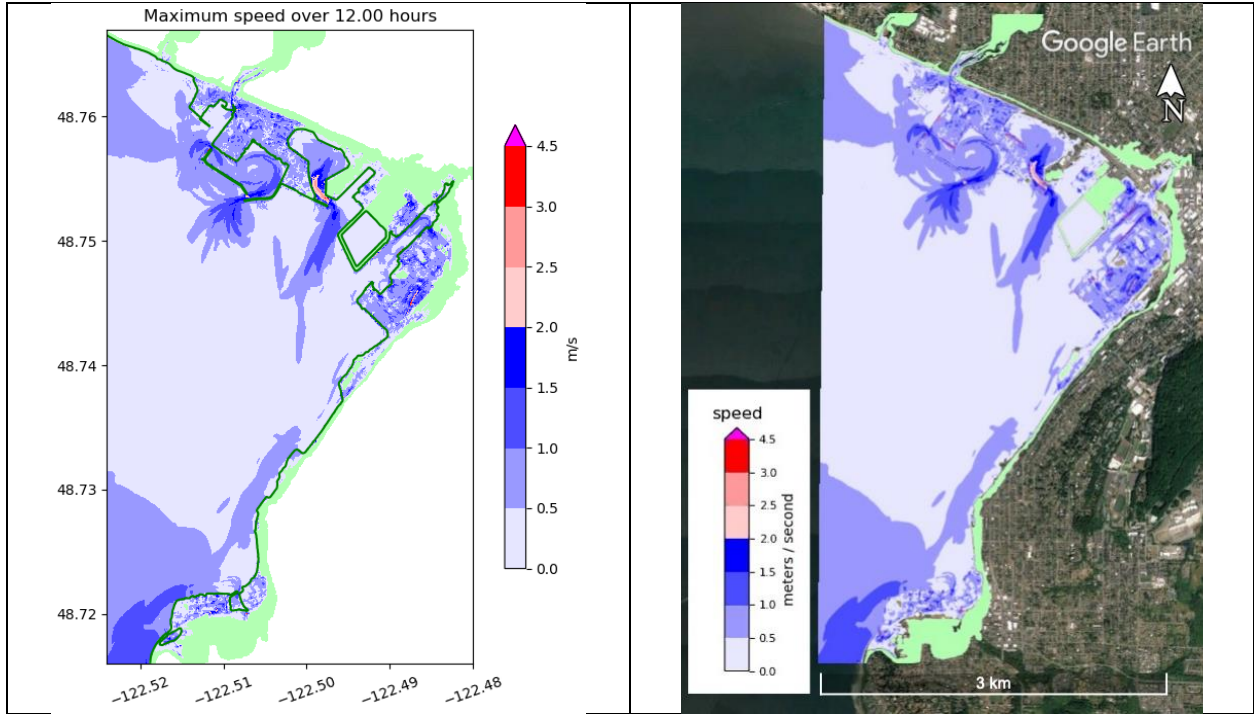


Figure 12. Maximum current speeds for AKMaxWA event at Mean High Water (MHW) plotted alone (left), and as an air photo overlay in Google Earth (right). These are the maximum values over 12 hours of simulated time. Areas in green remained dry for the duration of the simulation.

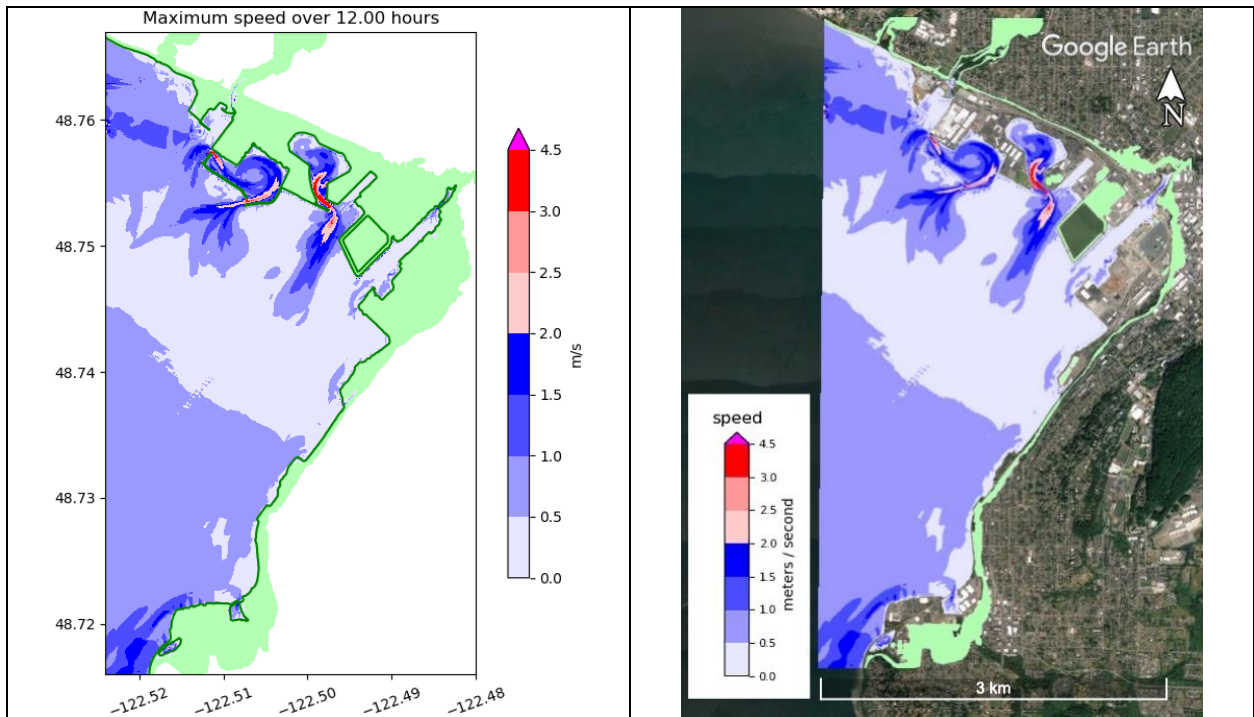


Figure 13. Maximum current speeds for AKMaxWA event at Mean Low Water (MLW) plotted alone (left), and as an air photo overlay in Google Earth (right). These are the maximum values over 12 hours of simulated time. Areas in green remained dry for the duration of the simulation.

6.3 HMin results

Maximum drawdown (hmin) values are important for understanding the drawdown of water preceding or between tsunami wave crests. In marinas, this can result in vessels becoming stranded and possibly tipped prior to wave crest arrival.

As expected, the low tide simulations resulted in greater drawdown for both the Cascadia (Figure 14) and Alaska (Figure 15) sources. The Cascadia source produced a greater drawdown than the Alaska source (roughly twice as much). The Squalicum marina shows some of the greatest drawdown hazards (dark brown areas). Gauge plots (Section 7.2) show the timing of the maximum drawdown for each event.

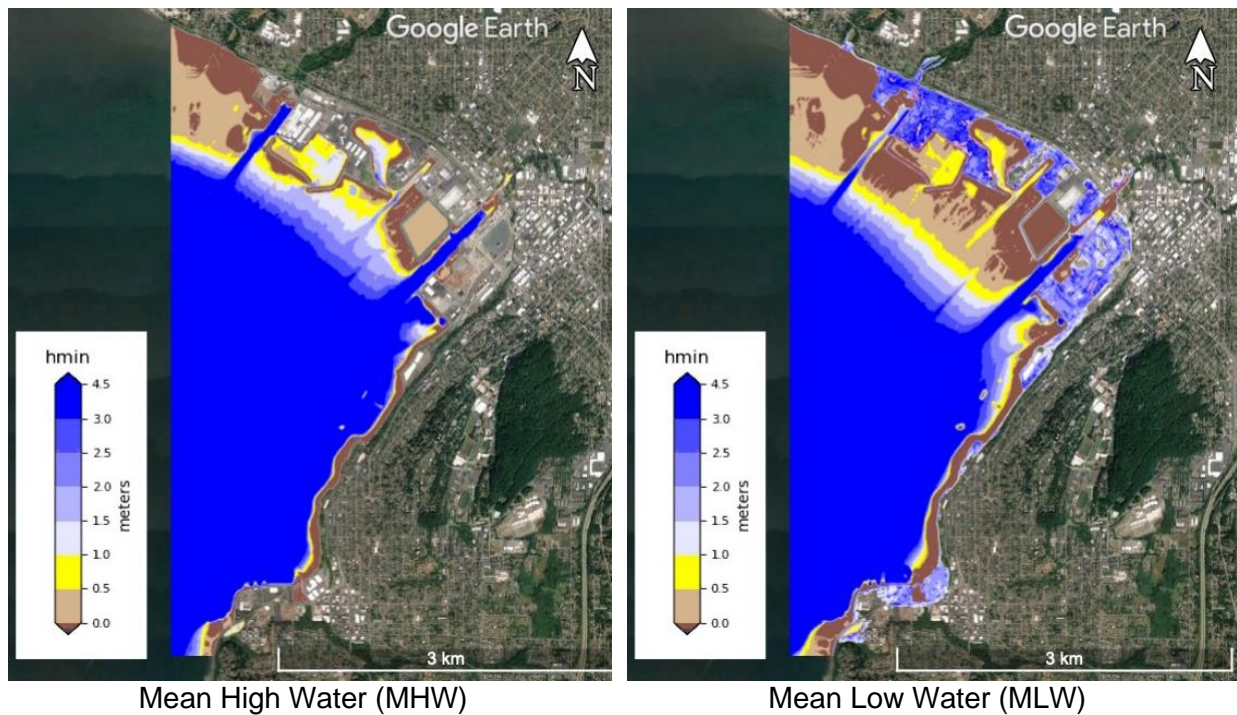


Figure 14. Cascadia-L1 source, minimum height (hmin) of water attained over 10 hours for MHW simulation (left) and 5 hours, MLW simulation (right).

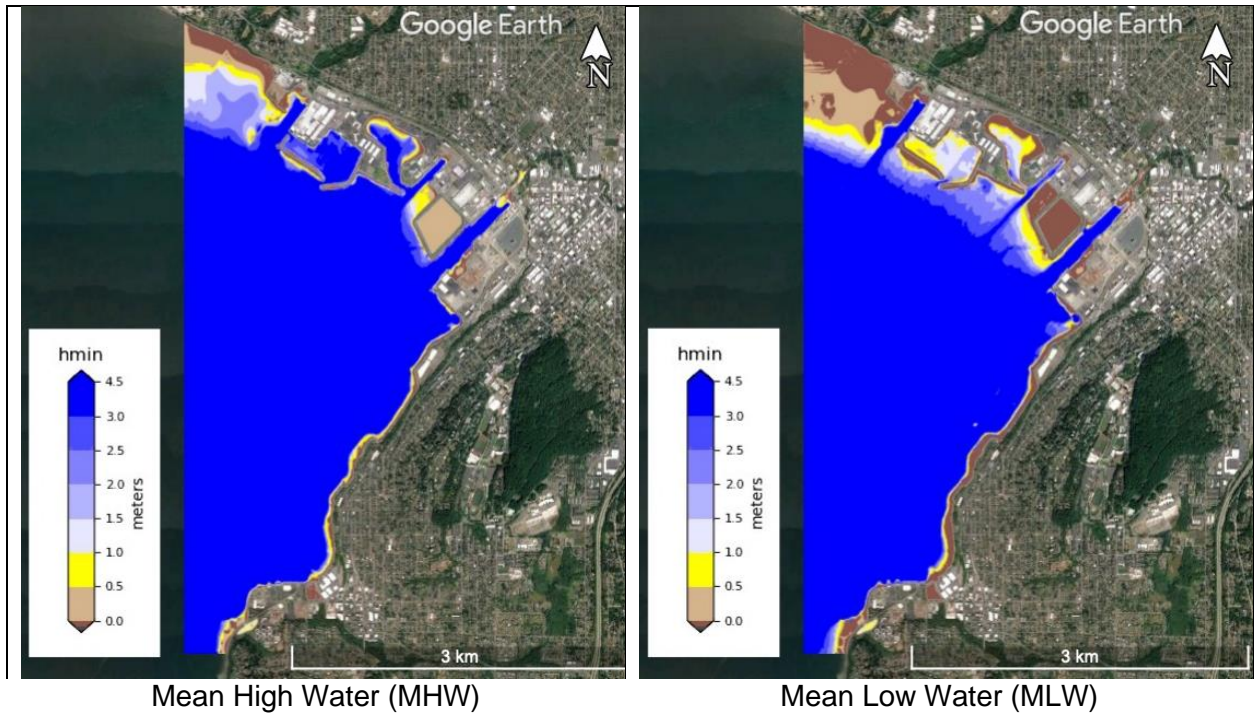


Figure 15. AKMaxWA source, minimum height (hmin) of water attained over 12 hours for MHW simulation (left), and MLW simulation (right).

7. Gauge output results

7.1 Synthetic gauge locations

Figure 16 shows the locations of the 36 simulated gauges used to capture time series of the flow depth/surface elevation, and current velocity at specified locations for each simulation. All 36 gauges were used in simulations of both the Cascadia-L1 and AKMaxWA events, at both MHW and MLW. The Cascadia-L1 MHW event was a 10 hour simulation; the Cascadia-L1 source at MLW was a 5 hour simulation; and the AKMaxWA source at MHW and MLW were both 12 hour simulations. Figure 17 shows the gauges closest to the Bellingham waterfront and the outline of the fgmax study region in yellow. Gauges 1-16 are within the fgmax region that records the highest resolution output on the 1/9 arc-second grid. The remaining gauges used coarser resolution, so their time series are likely less accurate. All study gauges are located in water (no land gauges). Figure 18 shows the locations of gauges in Squalicum Harbor. Table 4 summarizes location and resolution of each gauge.



Figure 16. The 36 synthetic gauge locations used for this study.

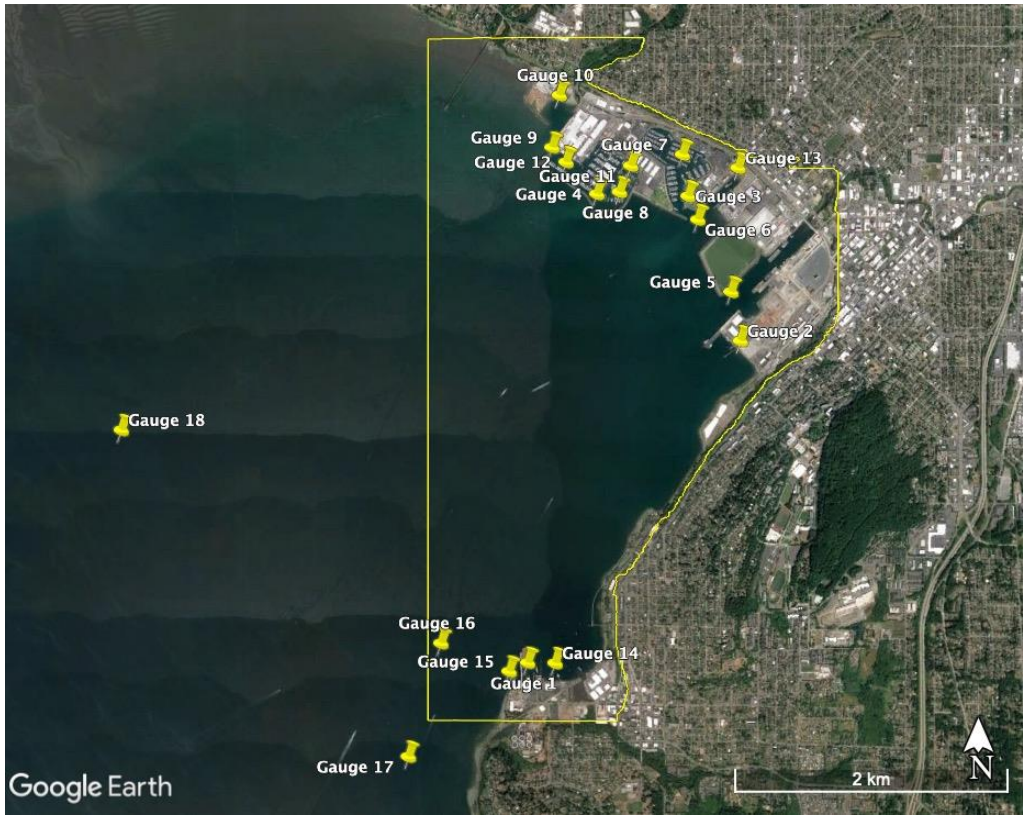


Figure 17. Port of Bellingham synthetic gauges. Fgmax area outlined in yellow.



Figure 18. Synthetic gauges in the Squalicum Harbor area.

Table 4. Locations of the synthetic gauges used in this study. These gauges are also shown in map view in Figures 16-18. Each gauge records both the results for Cascadia-L1 and AKMaxWA. The grid resolution of gauges 1-16 in the fgmax area is 1/9 arc-second, and 1/3 arc-second for the others.

Gauge Number	Location	Longitude	Latitude	Grid resolution
1	East of Fairhaven Shipyard	-122.514209	48.721997	1/9"
2	Bellingham Shipping Terminal	-122.492420	48.743690	1/9"
3	East entrance to Inner Squalicum Harbor	-122.497747	48.753459	1/9"
4	South entrance Outer Squalicum Harbor	-122.507093	48.753613	1/9"
5	Whatcom Creek Waterway	-122.493366	48.746997	1/9"
6	East entrance to Inner Squalicum Harbor	-122.496749	48.751874	1/9"
7	Inner Squalicum Harbor	-122.498323	48.756263	1/9"
8	Inside Outer Squalicum Harbor	-122.504776	48.753748	1/9"
9	Near West entrance Outer Squalicum Harbor	-122.511679	48.756759	1/9"
10	West of Bellingham Cold Storage	-122.510936	48.760253	1/9"
11	Inside Outer Squalicum Harbor	-122.503625	48.755511	1/9"
12	Inside Outer Squalicum Harbor	-122.510248	48.755767	1/9"
13	US Coast Guard dock	-122.492643	48.755354	1/9"
14	East of Bellingham Cruise Terminal	-122.511409	48.721972	1/9"
15	West of Fairhaven Shipyard	-122.516104	48.721407	1/9"
16	Bellingham Bay	-122.523089	48.723304	1/9"
17	Bellingham Bay	-122.526428	48.715655	1/3"
18	Bellingham Bay	-122.555810	48.737701	1/3"
19	Mouth of Nooksack River	-122.559720	48.770523	1/3"
20	Southeast of Portage Island	-122.608857	48.692264	1/3"
21	Northwest of Portage Island	-122.652248	48.711536	1/3"
22	East of Lummi Point	-122.680788	48.733904	1/3"
23	North of Eliza Island	-122.588247	48.667907	1/3"
24	Between Lummi and Eliza Islands	-122.601622	48.649414	1/3"
25	North of Lummi Island	-122.710731	48.755271	1/3"

26	Georgia Strait northeast of Orcas Island	-122.784010	48.786211	1/3"
27	South of Eliza Island	-122.590922	48.639505	1/3"
28	West of Lummi Rocks	-122.683563	48.669637	1/3"
29	North Samish Bay	-122.521124	48.622877	1/3"
30	Bellingham Bay	-122.541183	48.681227	1/3"
31	Rosario Strait between Orcas and Lummi Islands	-122.726594	48.687371	1/3"
32	Northeast of Sinclair Island	-122.646199	48.630372	1/3"
33	North end of Chuckanut Bay	-122.501249	48.693407	1/3"
34	Chuckanut Bay east of Chuckanut Island	-122.497173	48.676544	1/3"
35	Pleasant Bay	-122.503358	48.667507	1/3"
36	West of Chuckanut	-122.512174	48.662343	1/3"

7.2 Synthetic gauge plots

The gauge plots that follow show flow depth (fluctuations in the water depth at the gauge location during the simulation), the gauge surface eta (the variation in the height of the water surface at the gauge location), and current speeds for both the Cascadia-L1 and AKMaxWA events, at both MHW and MLW.

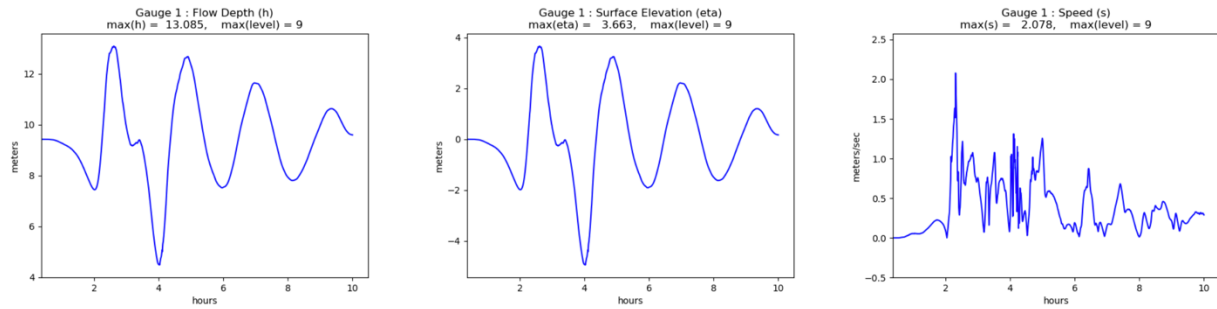
Note that the vertical and horizontal axes on the gauge plots vary by location, parameter, and duration. The vertical scale is set by the maximum amplitude value in each plot to better show the results.

The Cascadia -L1 event creates very large waves along the Pacific coast, and substantial waves that flow into the Strait of Juan de Fuca, Puget Sound, the Strait of Georgia, and Bellingham Bay. An initial drawdown begins about an hour after the earthquake, and is at its lowest about two hours after the earthquake. The first wave crest follows at about two hours and 15 minutes after the earthquake. The lowest drawdown is the second one (at some gauges bottoming out), which happens at about four hours after the earthquake. At most gauges, the first wave was the largest in the series of waves during the simulation.

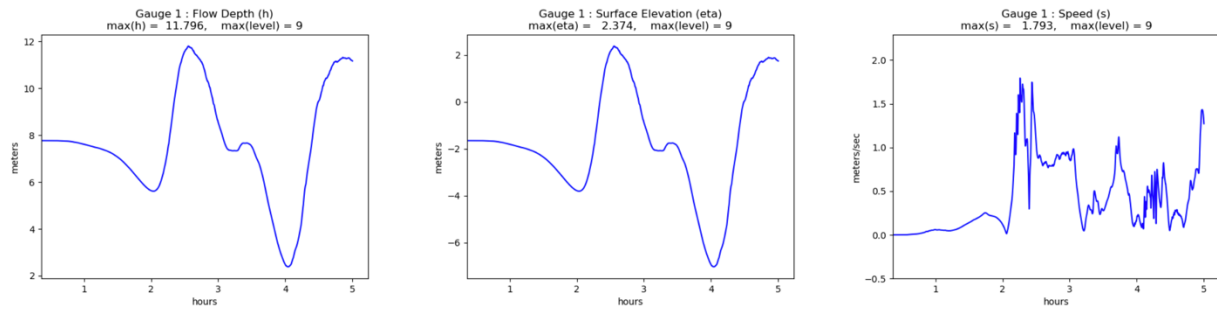
The AKmaxWA event produces very large waves along the Alaska-Aleutian subduction zone. The waves travel across the Pacific Ocean to Washington, into the Strait of Juan de Fuca, Puget Sound, the Strait of Georgia, and Bellingham Bay. With this event, there is no initial water drawdown. The first waves reach the Bellingham waterfront at about 5 hours and 45 minutes after the earthquake. At most gauges, the second wave was the largest in the series of waves in the simulation. The first drawdown occurs about 7 hours after the earthquake (after the first wave), and is roughly half as much drawdown as occurs for the Cascadia -L1 event.

Gauge 1: East of Fairhaven Shipyard

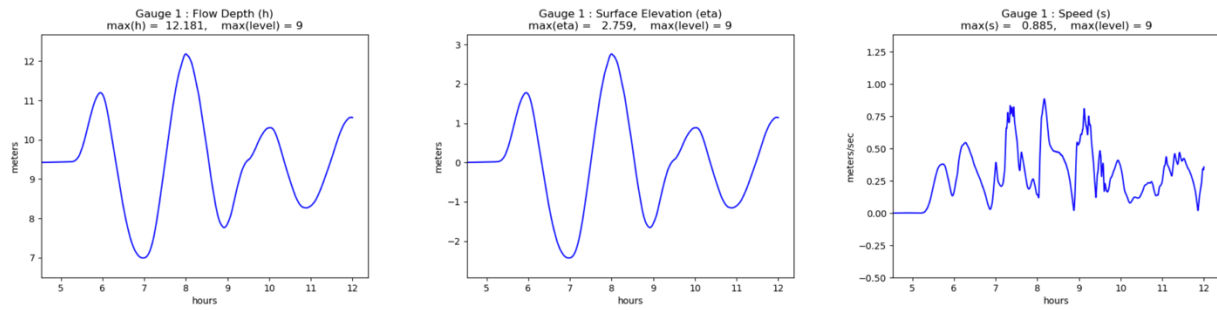
Cascadia-L1 MHW:



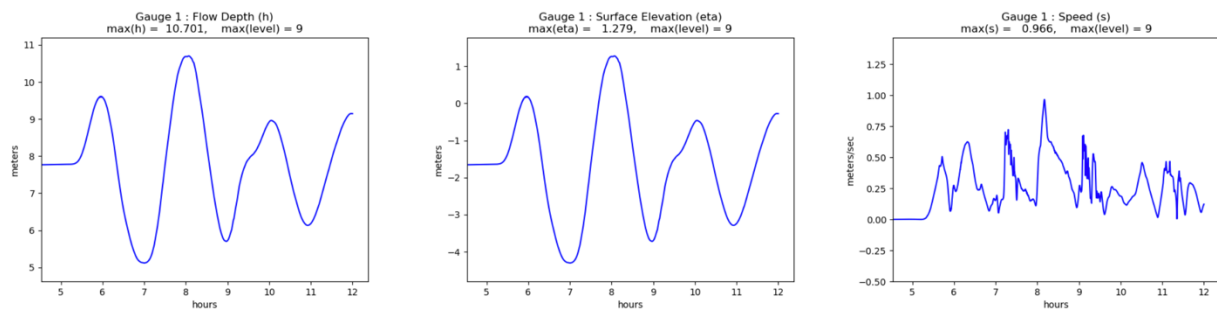
Cascadia-L1 MLW:



AKMaxWA MHW:

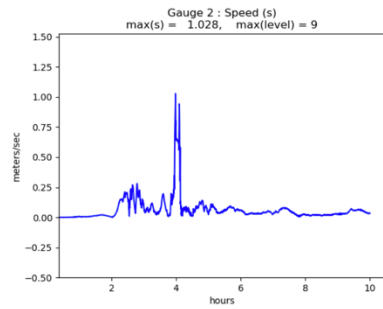
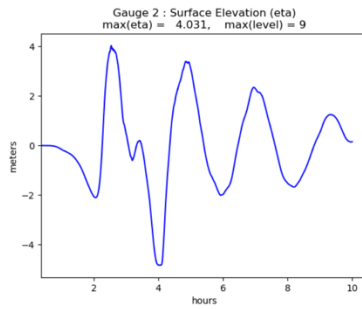
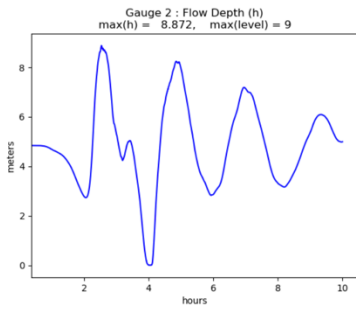


AKMaxWA MLW:

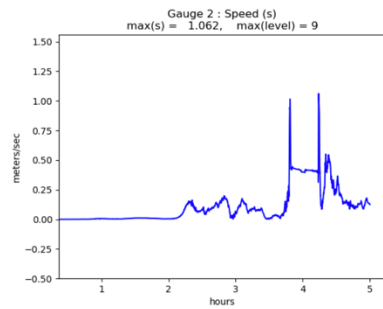
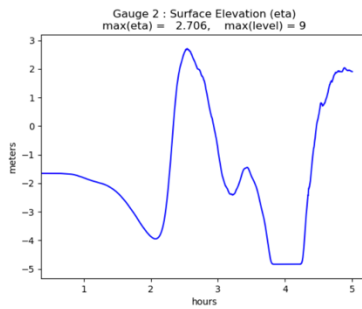
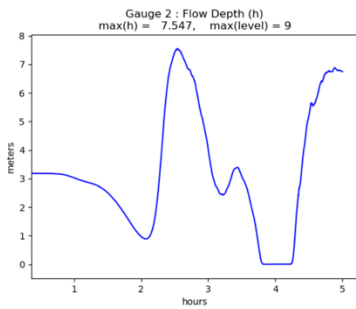


Gauge 2: Bellingham Shipping Terminal

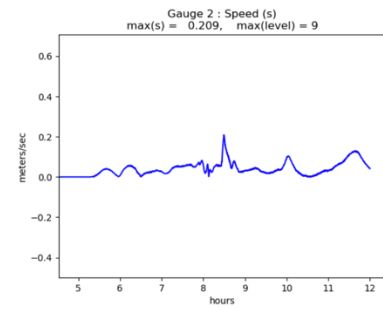
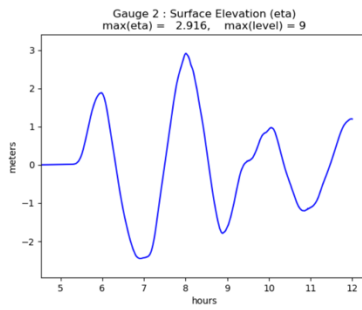
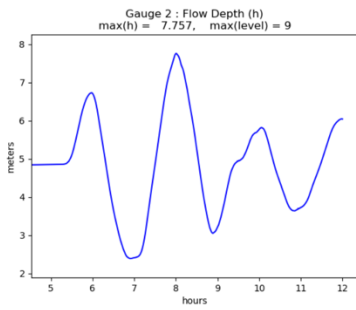
Cascadia-L1 MHW:



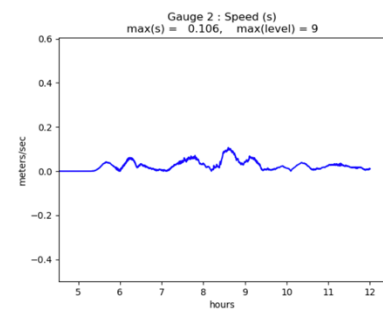
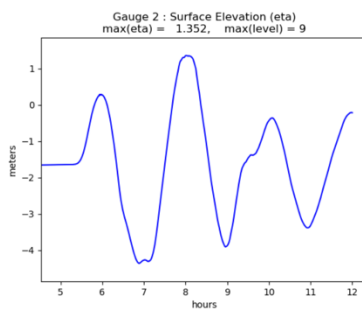
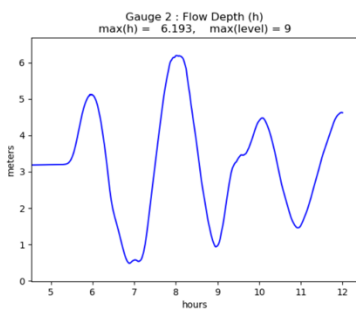
Cascadia-L1 MLW:



AKMaxWA MHW:

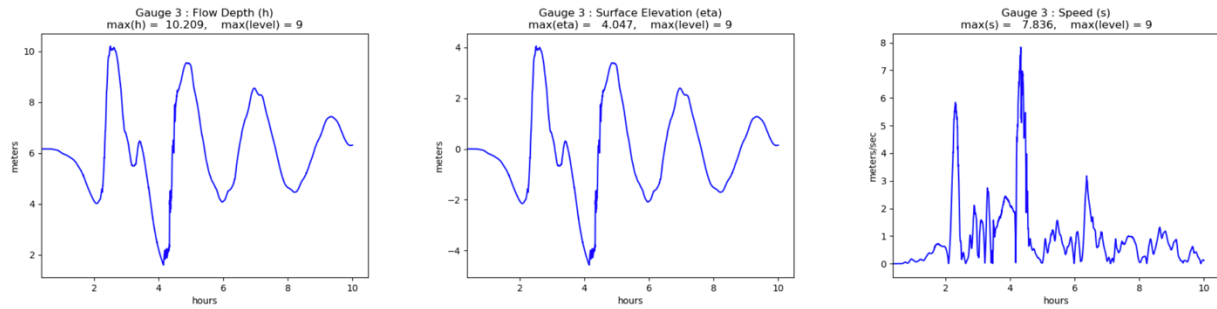


AKMaxWA MLW:

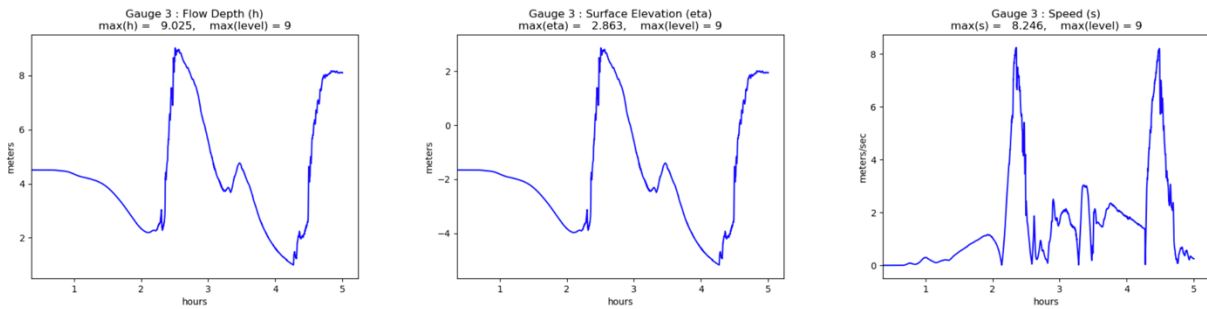


Gauge 3: East entrance to Inner Squilicum Harbor

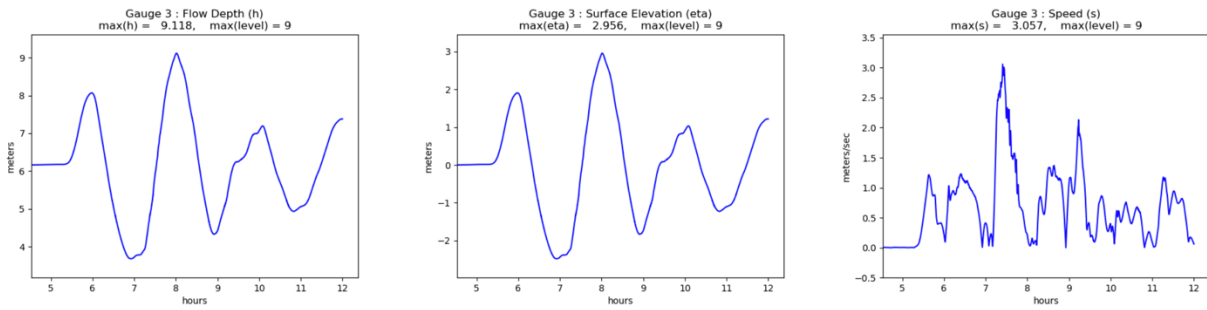
Cascadia-L1 MHW:



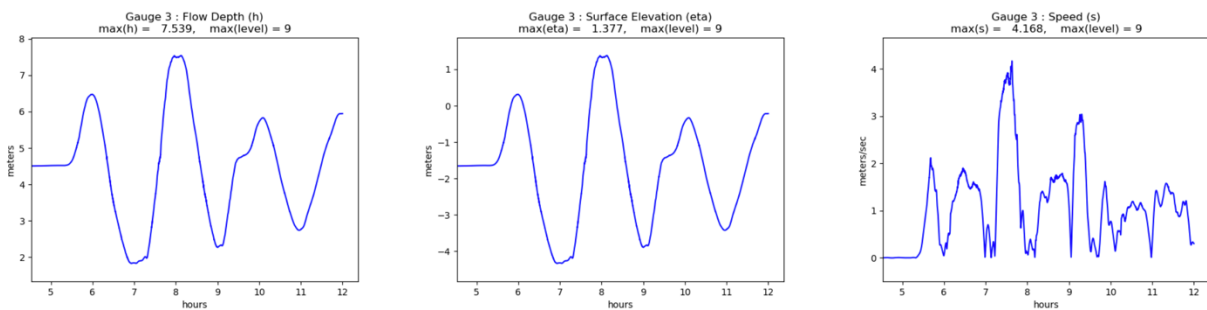
Cascadia-L1 MLW:



AKMaxWA MHW:

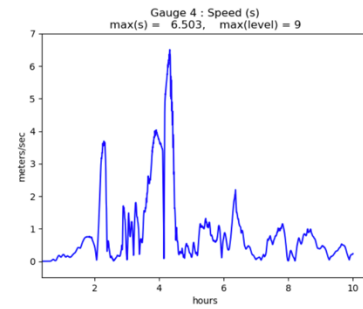
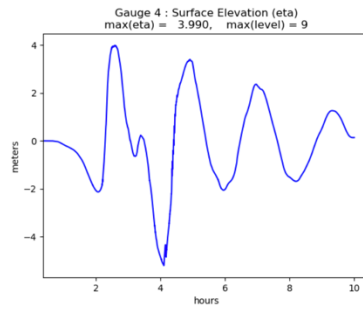
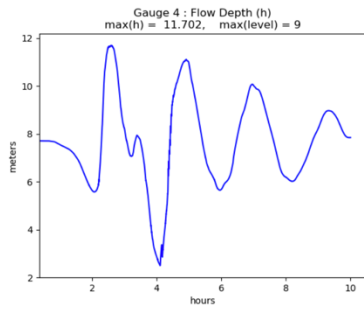


AKMaxWA MLW:

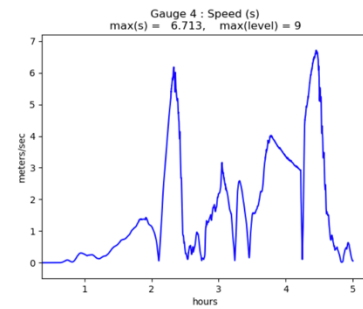
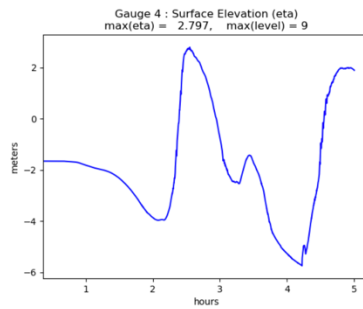
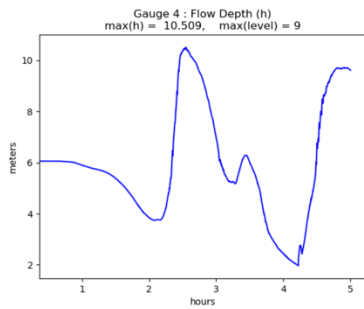


Gauge 4: South entrance Outer Squalicum Harbor

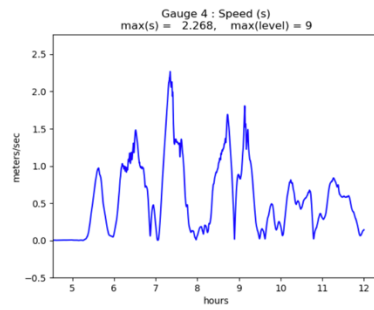
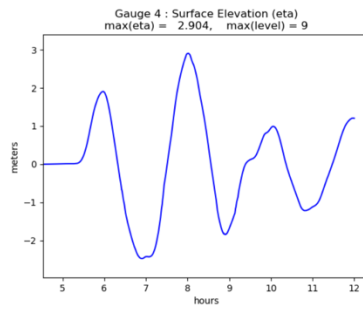
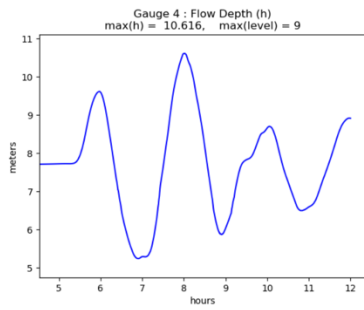
Cascadia-L1 MHW:



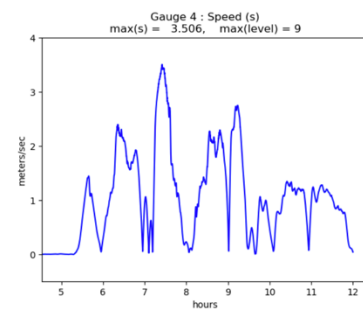
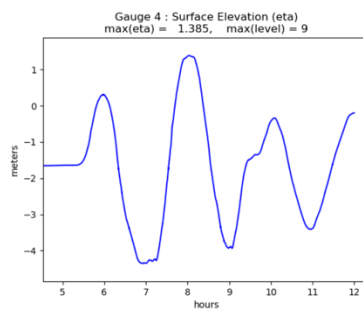
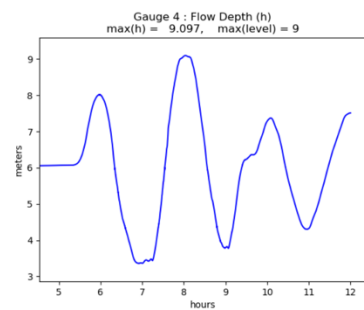
Cascadia-L1 MLW:



AKMaxWA MHW:

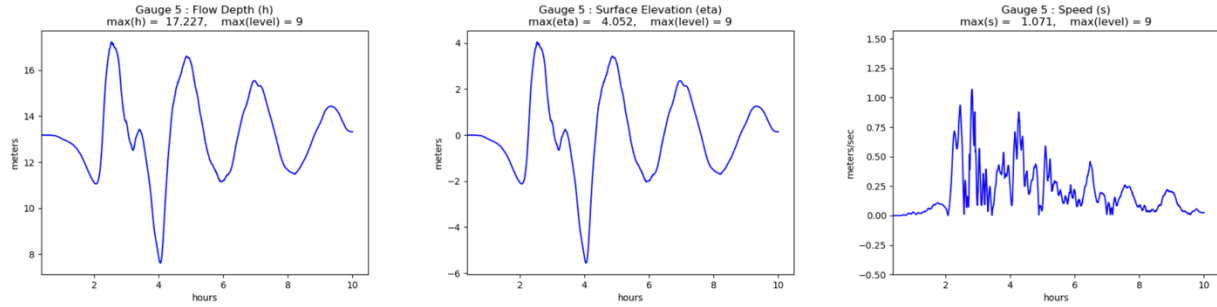


AKMaxWA MLW:

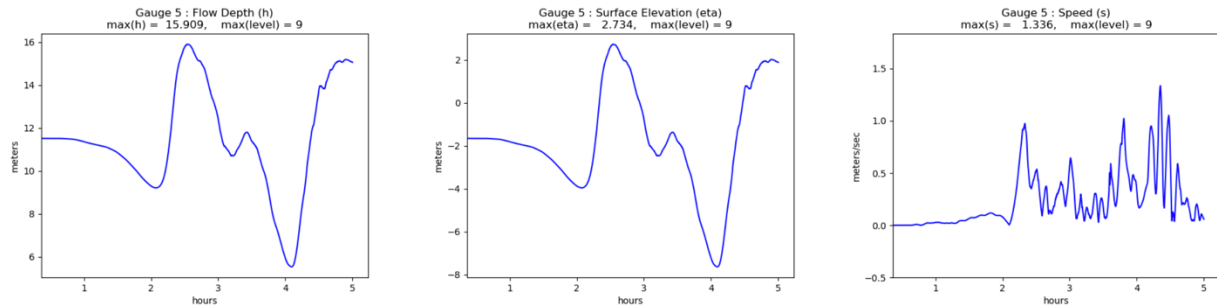


Gauge 5: Whatcom Creek waterway

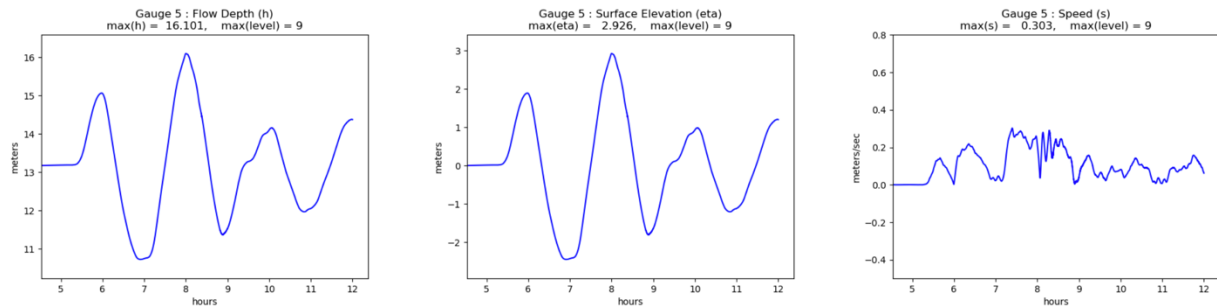
Cascadia-L1 MHW:



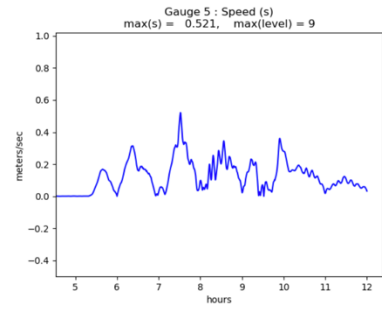
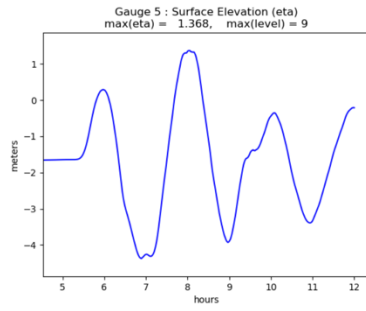
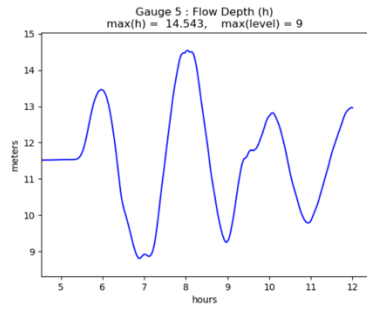
Cascadia-L1 MLW:



AKMaxWA MHW:

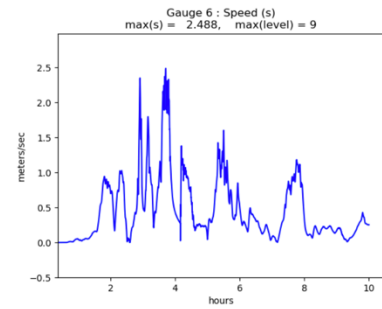
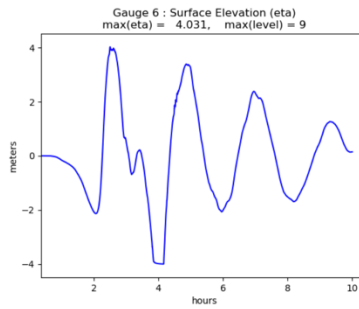
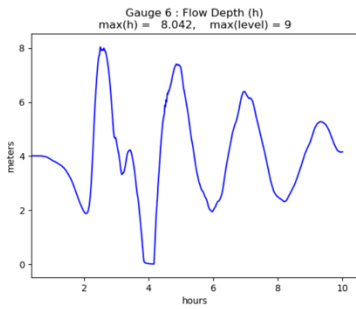


AKMaxWA MLW:

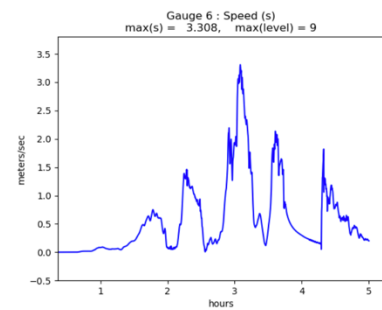
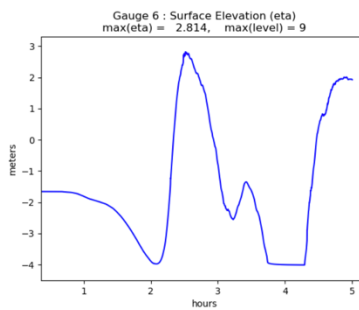
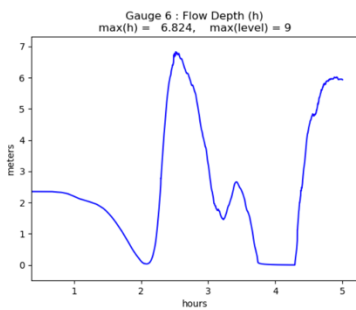


Gauge 6: East entrance to Inner Squalicum Harbor

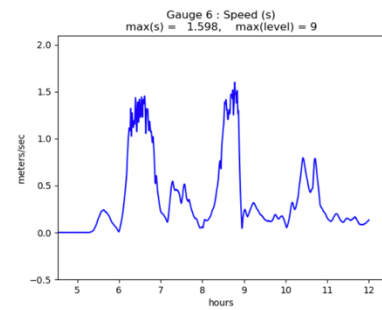
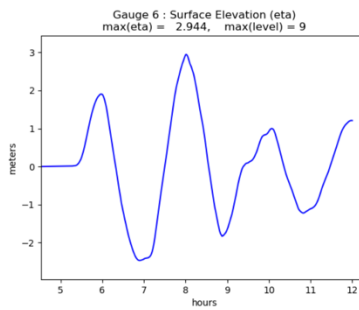
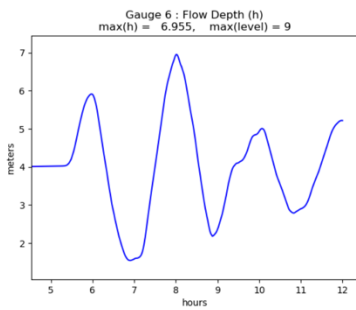
Cascadia-L1 MHW:



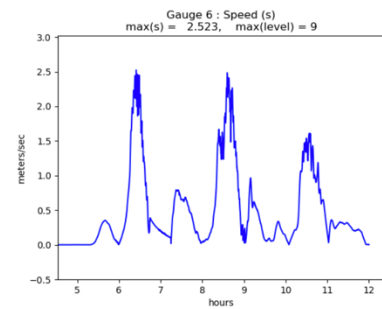
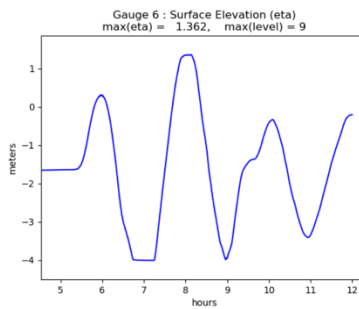
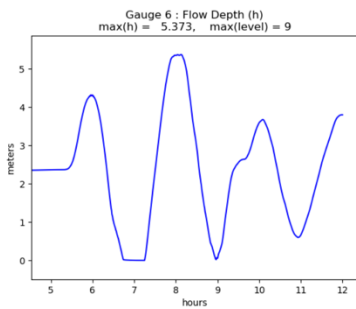
Cascadia-L1 MLW:



AKMaxWA MHW:

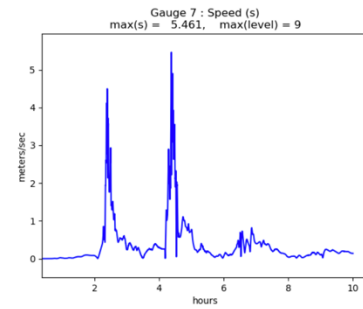
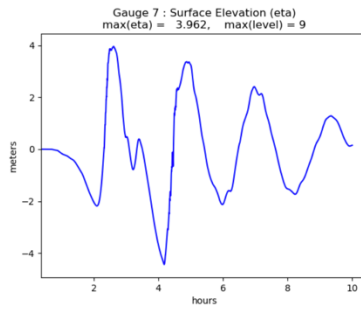
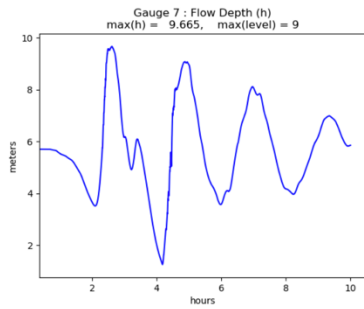


AKMaxWA MLW:

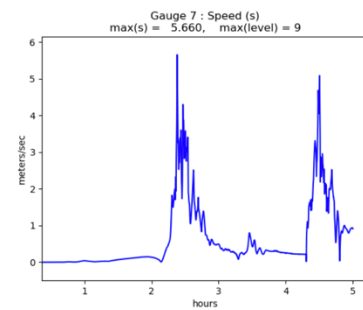
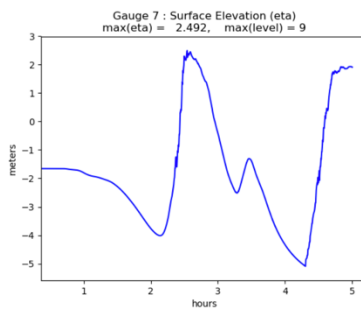
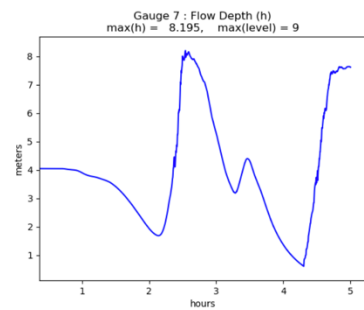


Gauge 7: Inner Squalicum Harbor

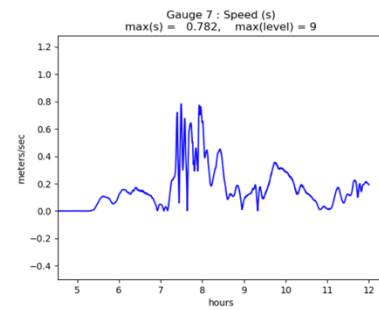
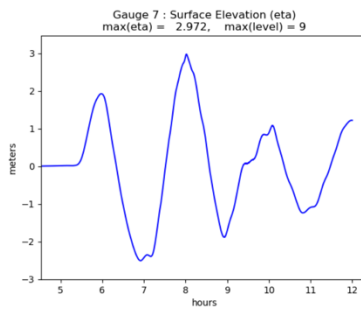
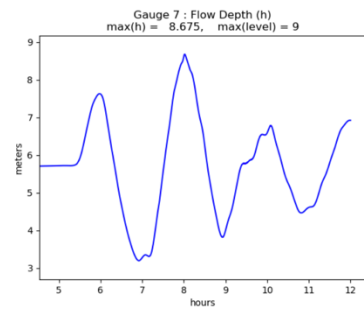
Cascadia-L1 MHW:



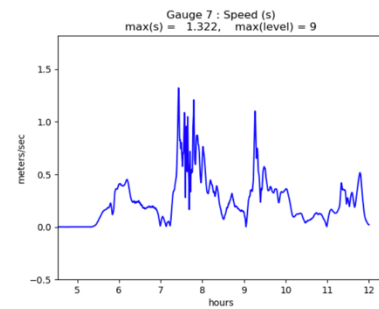
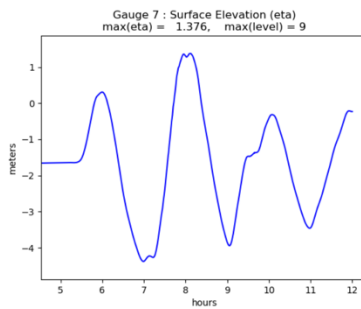
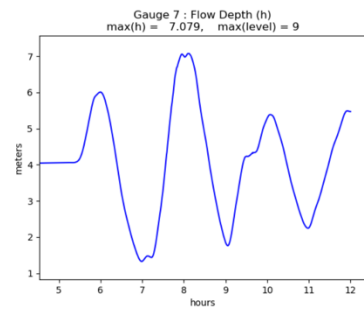
Cascadia-L1 MLW:



AKMaxWA MHW:

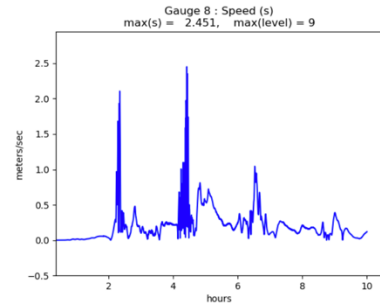
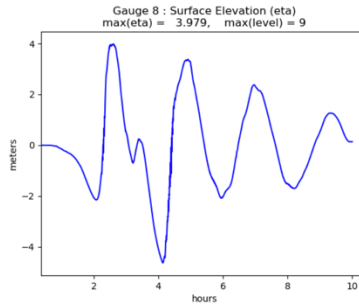
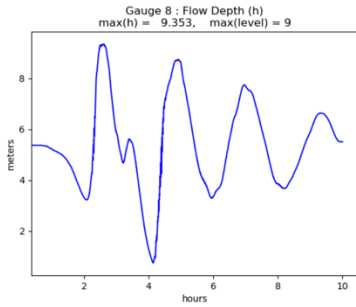


AKMaxWA MLW:

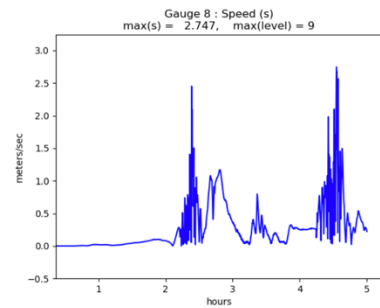
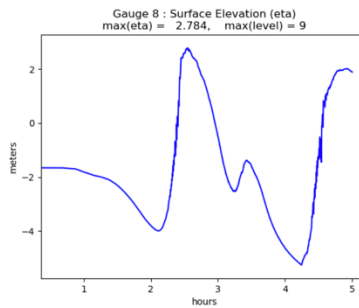
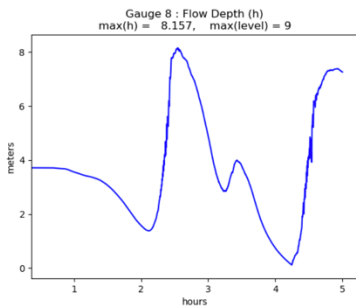


Gauge 8: Inside Outer Squalicum Harbor

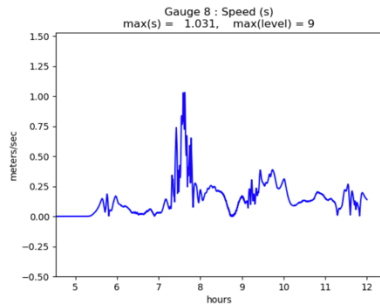
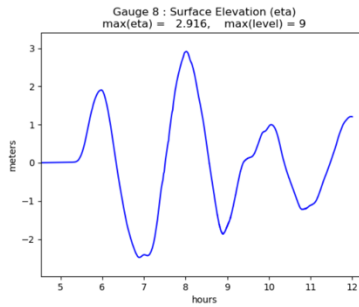
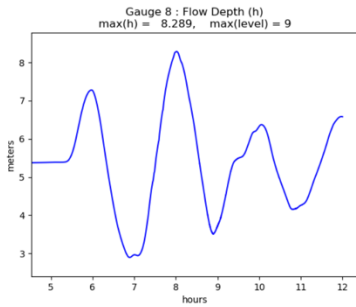
Cascadia-L1 MHW:



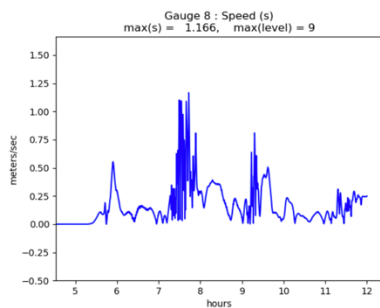
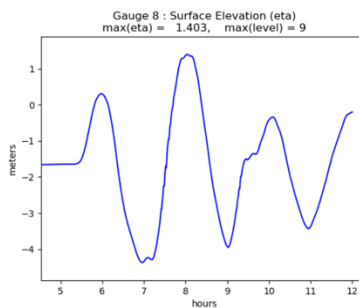
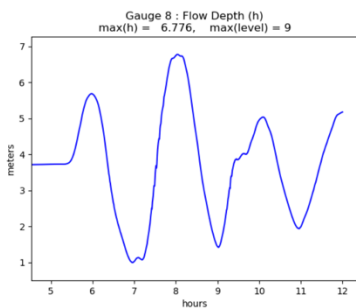
Cascadia-L1 MLW:



AKMaxWA MHW:

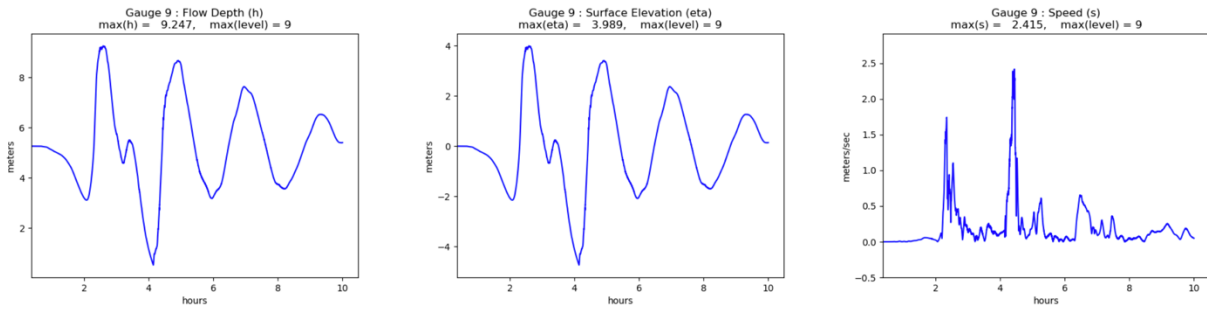


AKMaxWA MLW:

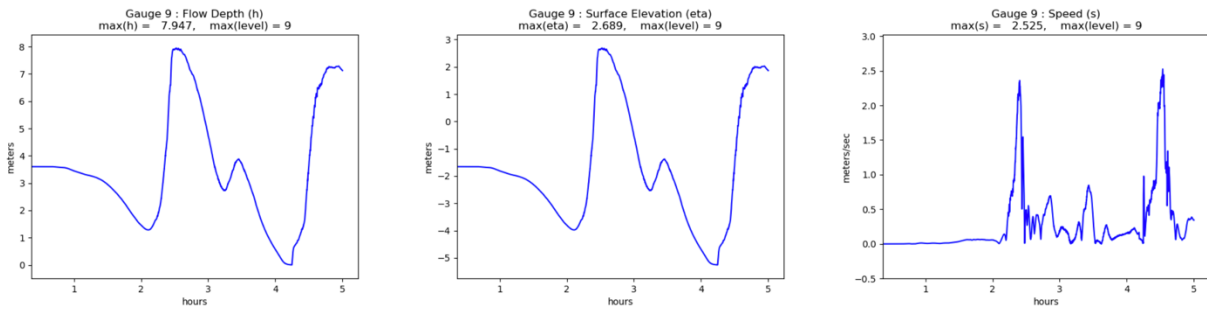


Gauge 9: Near West entrance Outer Squalicum Harbor

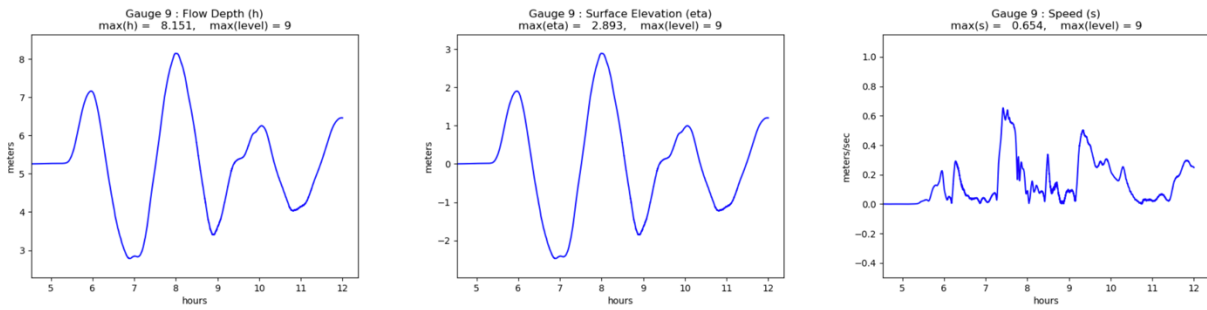
Cascadia-L1 MHW:



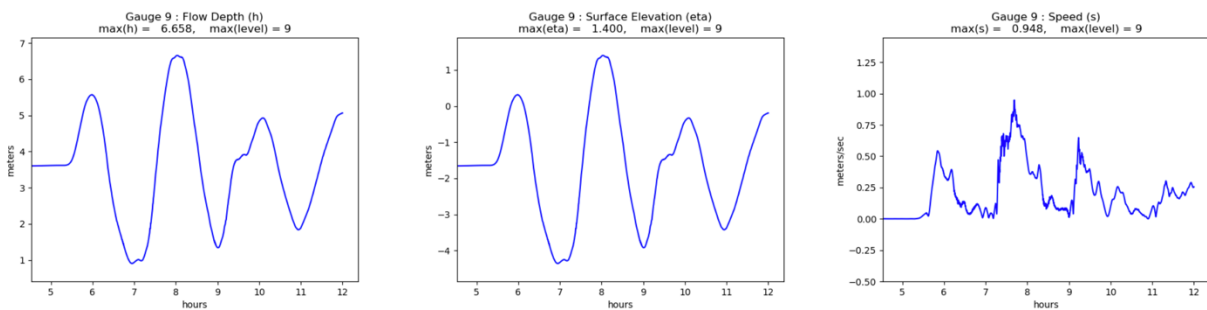
Cascadia-L1 MLW:



AKMaxWA MHW:

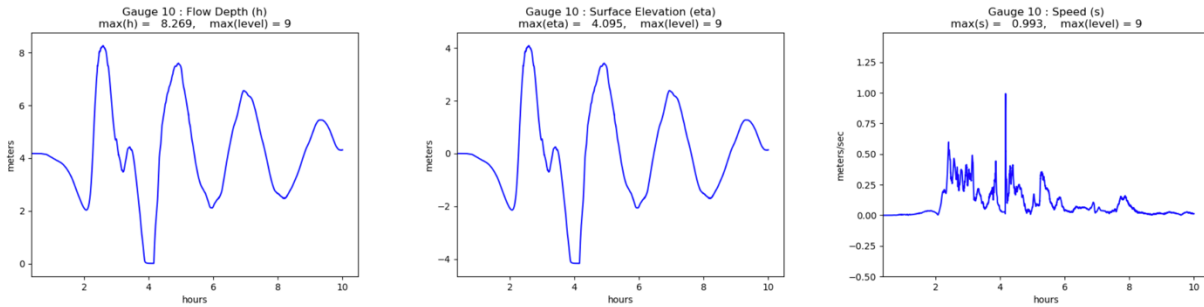


AKMaxWA MLW:

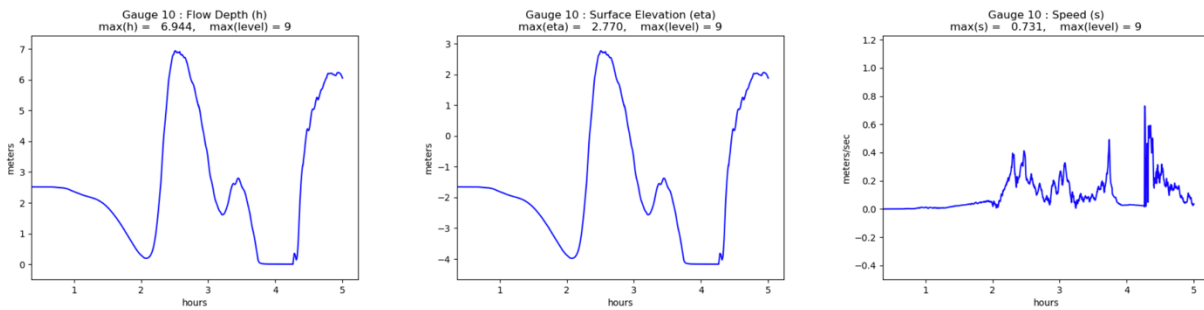


Gauge 10: West of Bellingham Cold Storage

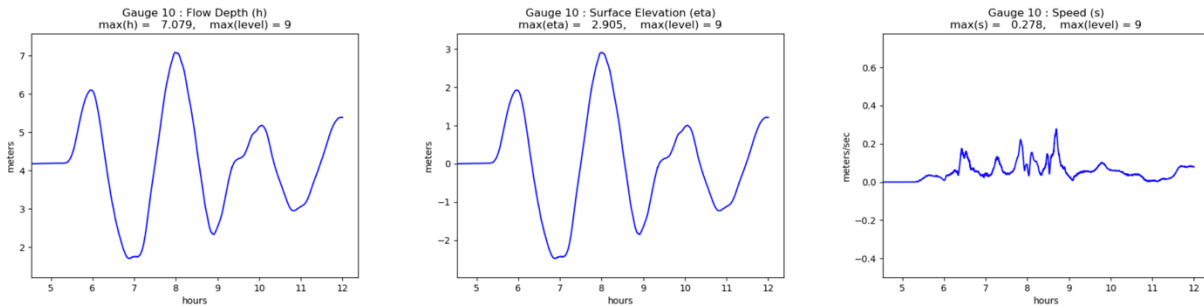
Cascadia-L1 MHW:



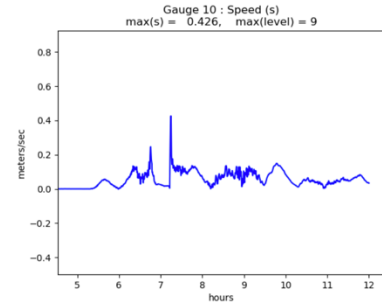
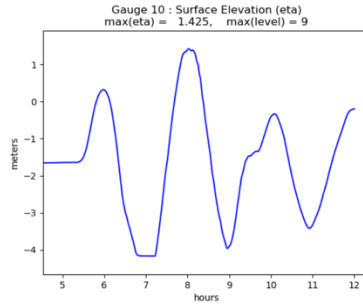
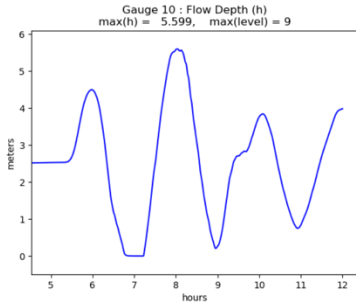
Cascadia-L1 MLW:



AKMaxWA MHW:

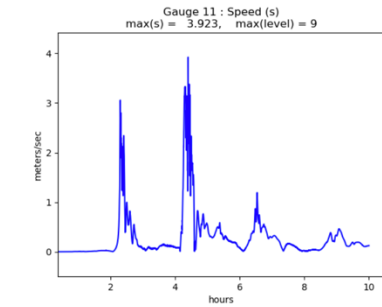
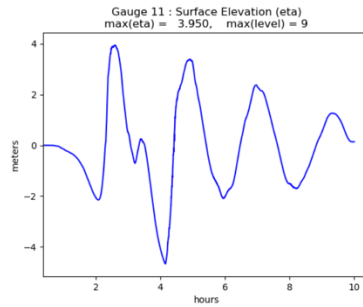
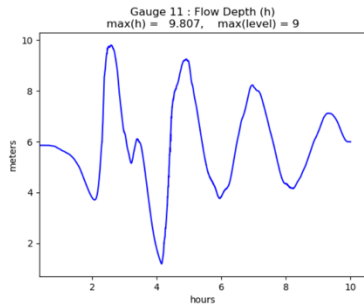


AKMaxWA MLW:

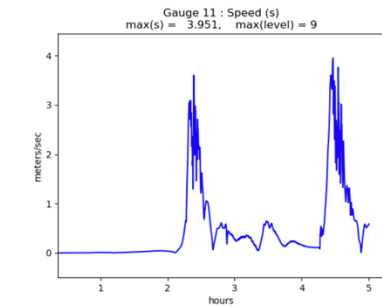
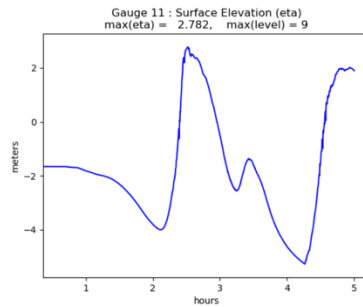
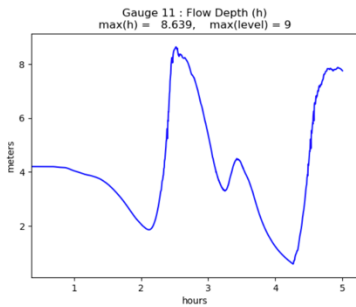


Gauge 11: Inside Outer Squalicum Harbor

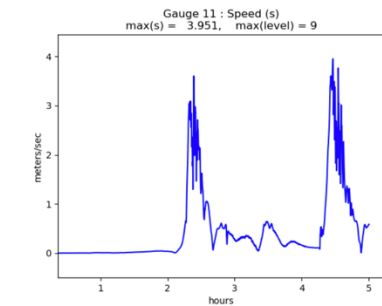
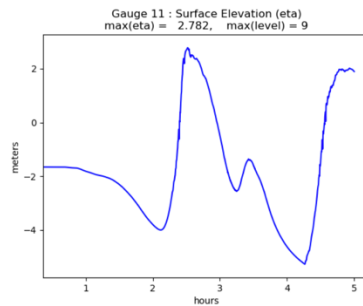
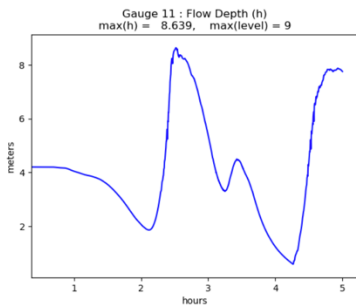
Cascadia-L1 MHW:



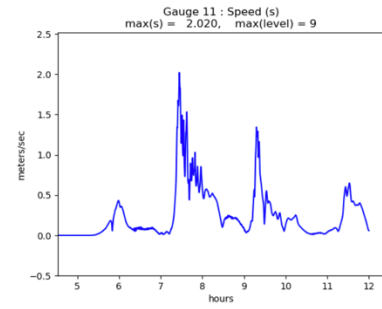
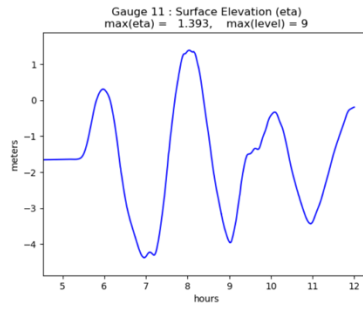
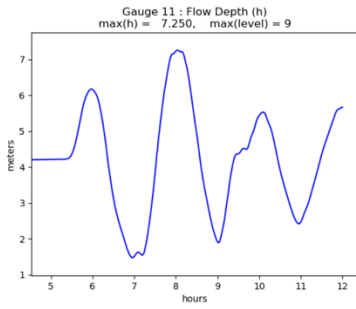
Cascadia-L1 MLW:



AKMaxWA MHW:

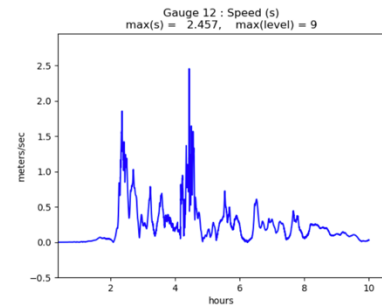
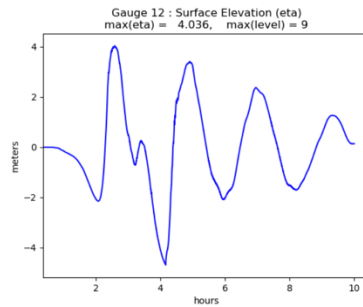
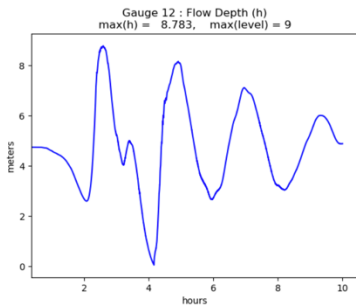


AKMaxWA MLW:

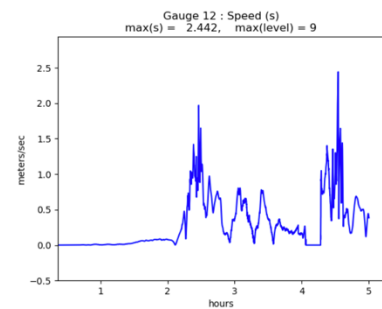
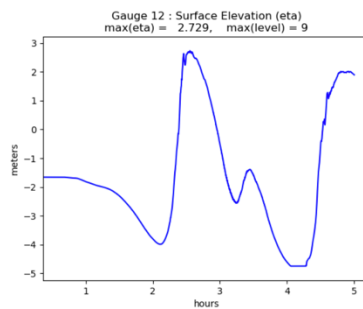
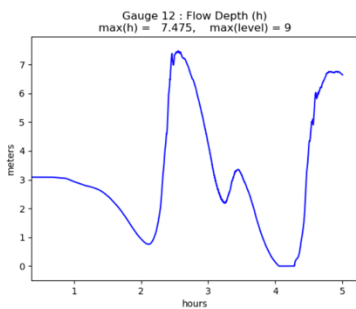


Gauge 12: Inside Outer Squalicum Harbor

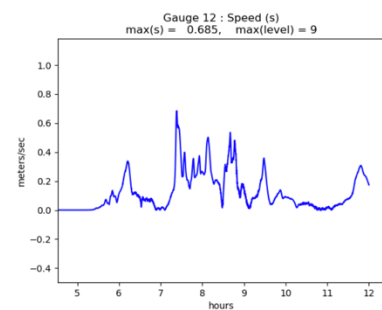
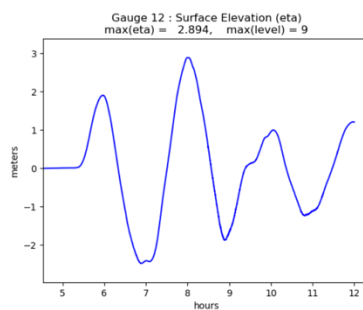
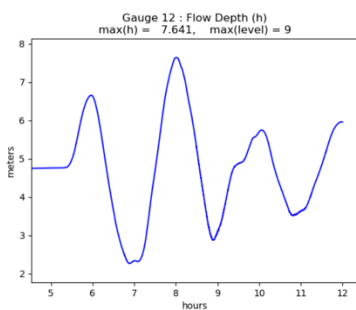
Cascadia-L1 MHW:



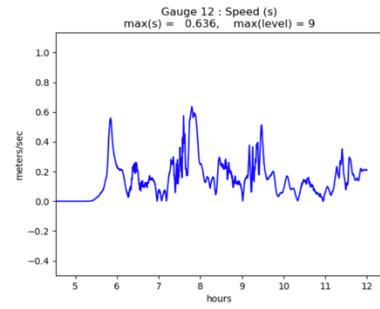
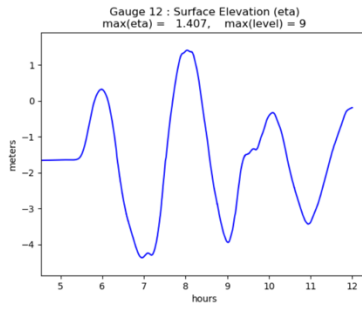
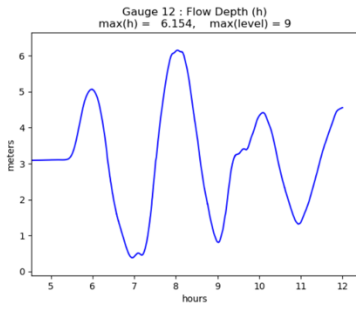
Cascadia-L1 MLW:



AKMaxWA MHW:

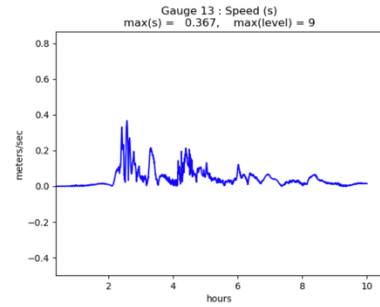
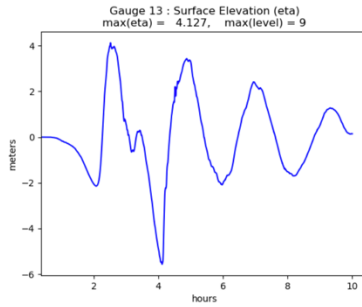
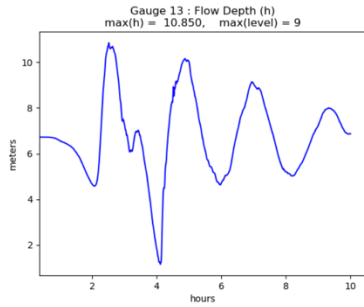


AKMaxWA MLW:

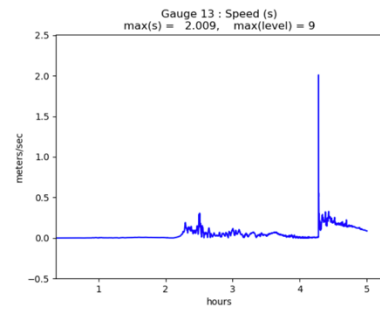
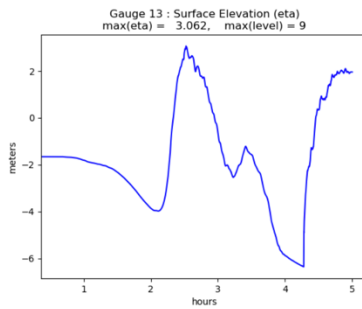
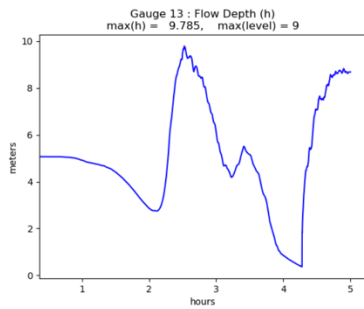


Gauge 13: US Coast Guard dock

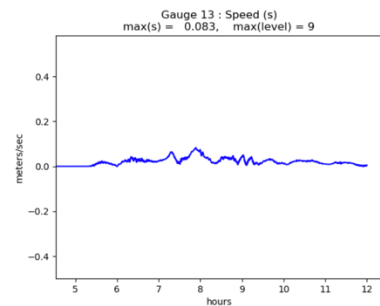
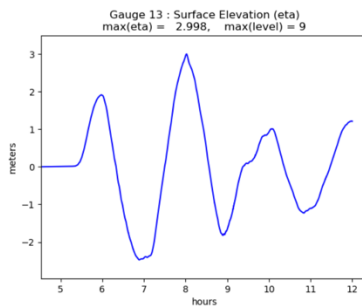
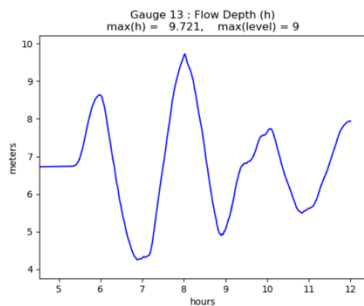
Cascadia-L1 MHW:



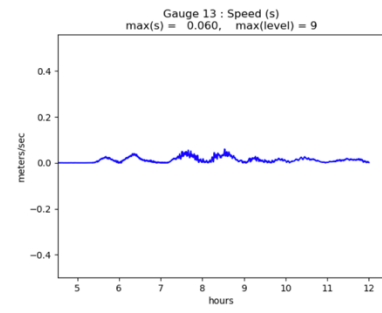
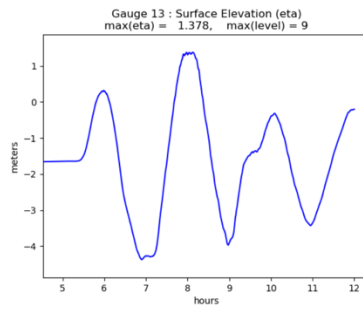
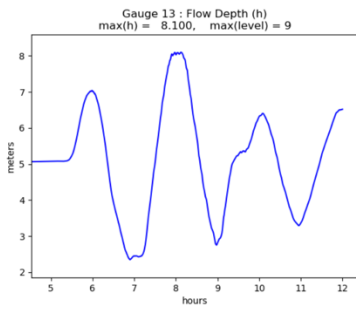
Cascadia-L1 MLW:



AKMaxWA MHW:

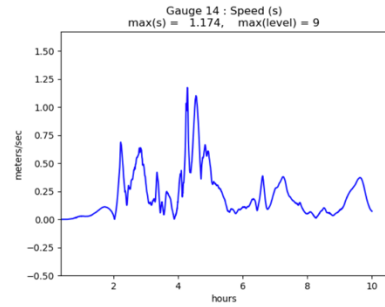
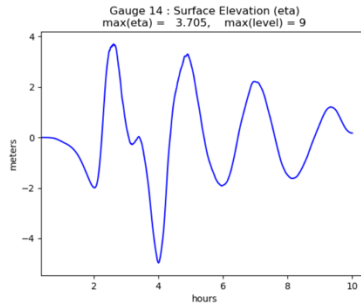
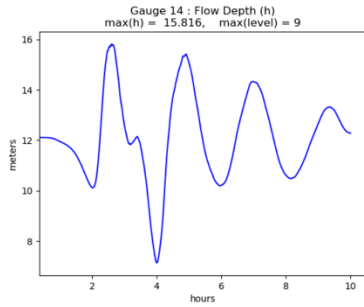


AKMaxWA MLW:

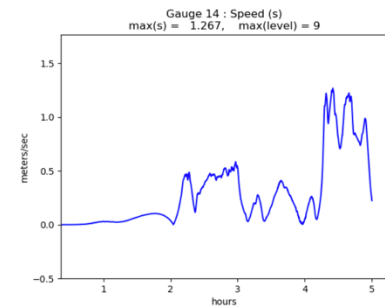
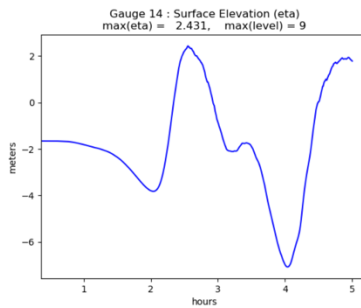
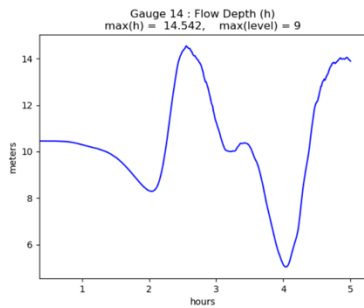


Gauge 14: East of Bellingham Cruise Terminal

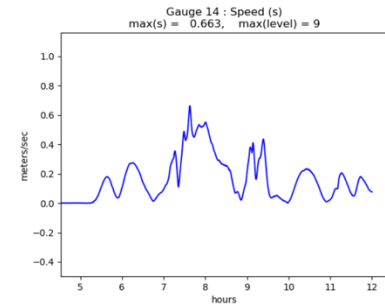
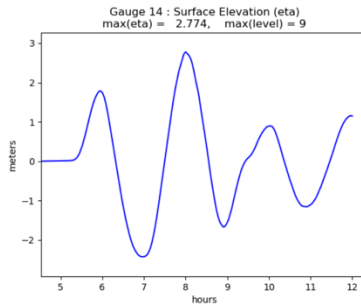
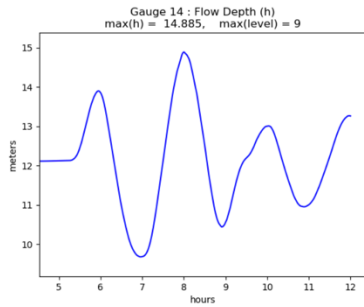
Cascadia-L1 MHW:



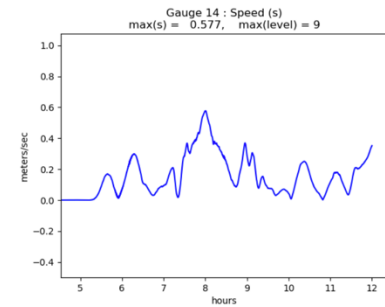
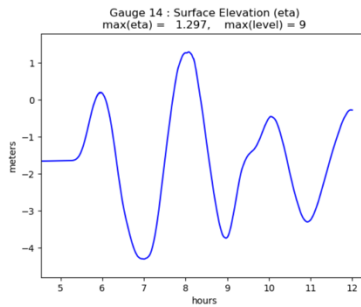
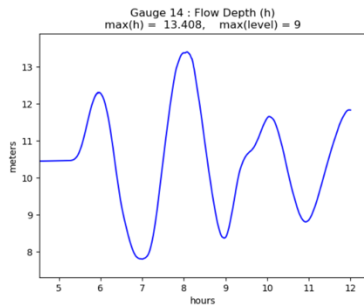
Cascadia-L1 MLW:



AKMaxWA MHW:

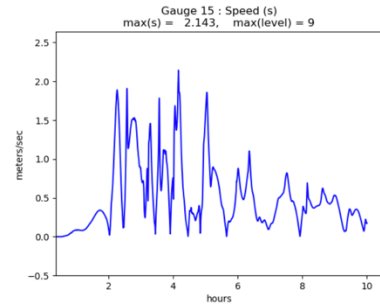
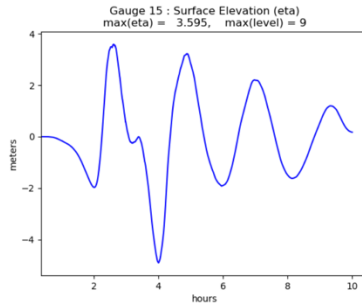
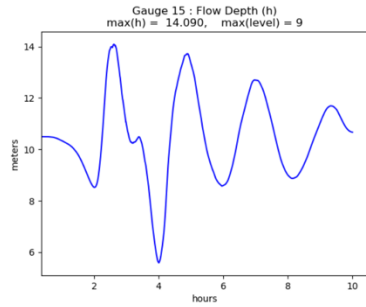


AKMaxWA MLW:

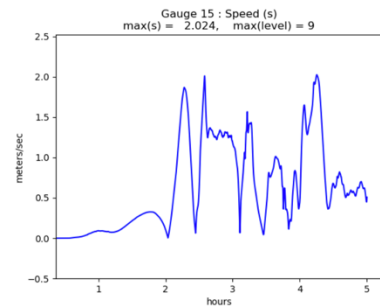
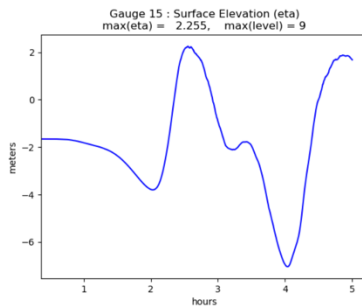
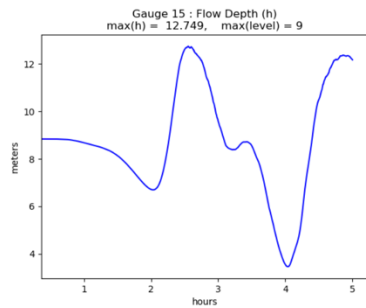


Gauge 15: West of Fairhaven Shipyard

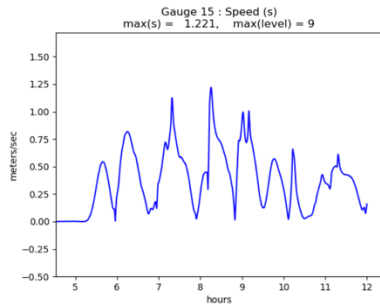
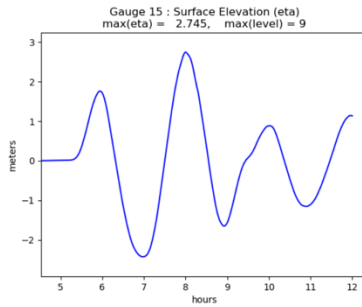
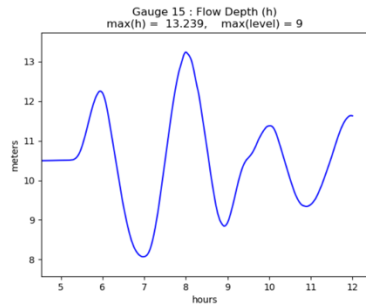
Cascadia-L1 MHW:



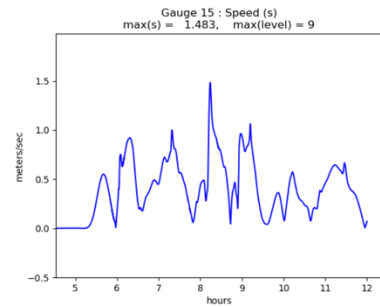
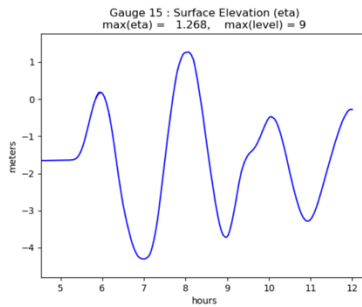
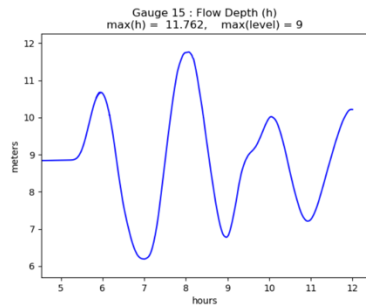
Cascadia-L1 MLW:



AKMaxWA MHW:

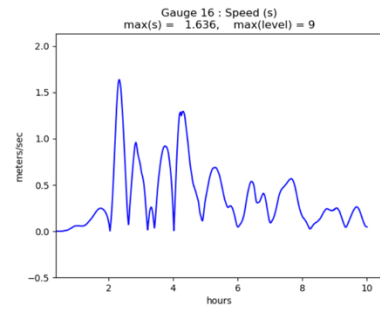
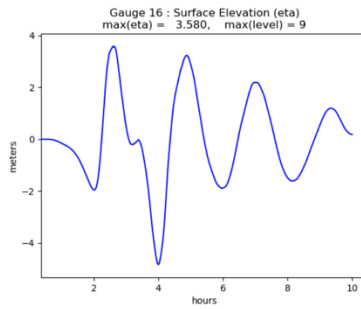
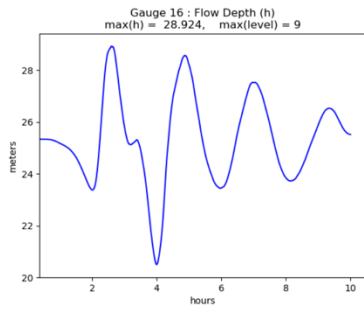


AKMaxWA MLW:

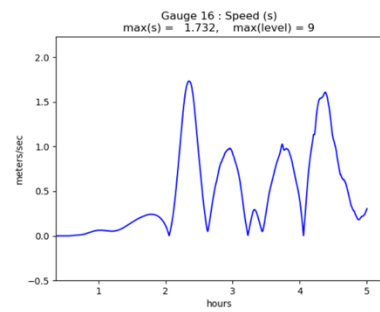
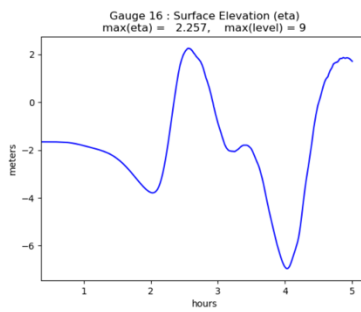
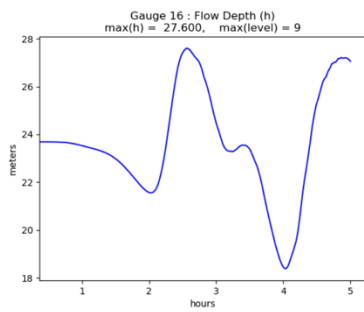


Gauge 16: Bellingham Bay

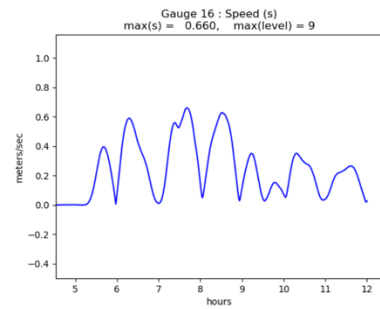
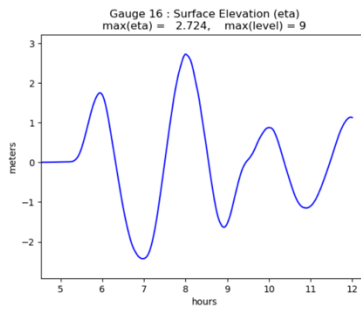
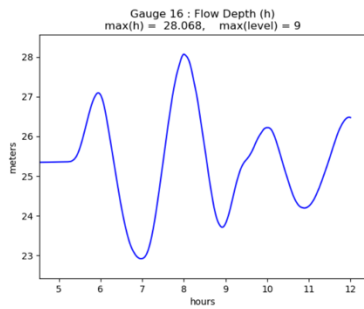
Cascadia-L1 MHW:



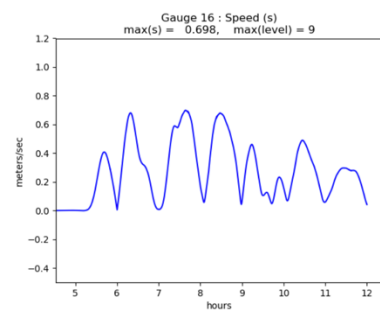
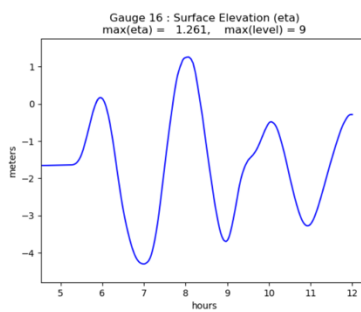
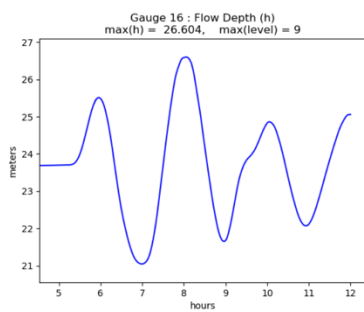
Cascadia-L1 MLW:



AKMaxWA MHW:

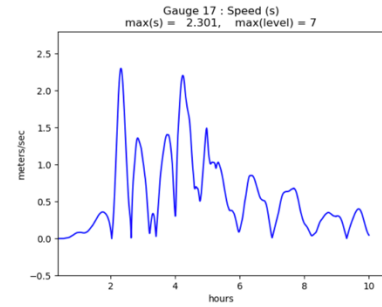
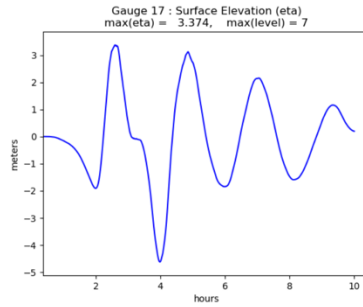
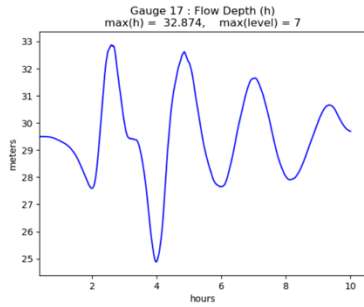


AKMaxWA MLW:

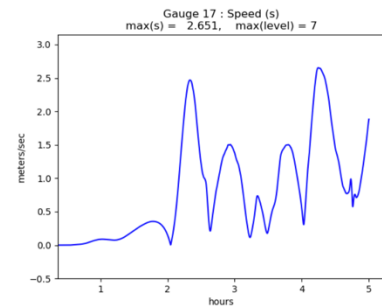
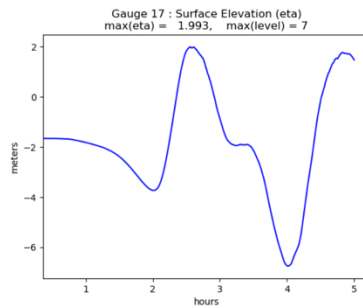
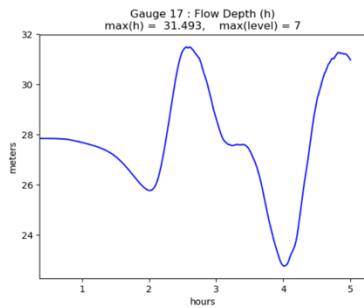


Gauge 17: Bellingham Bay

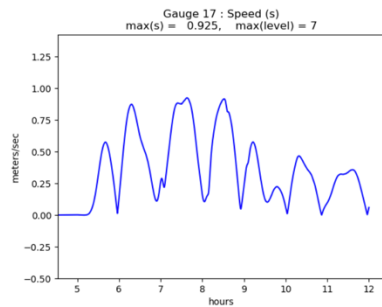
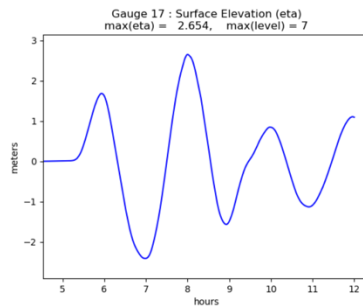
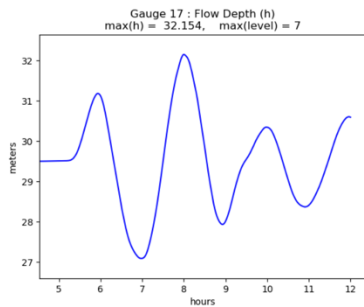
Cascadia-L1 MHW:



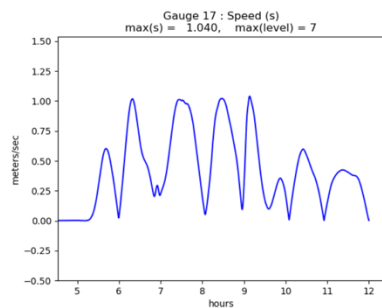
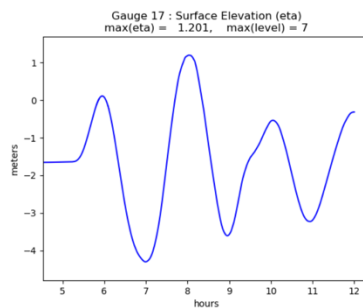
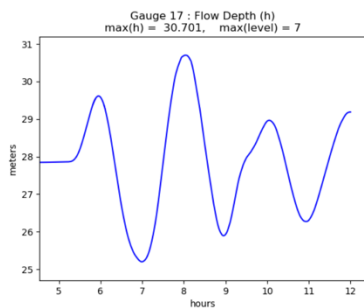
Cascadia-L1 MLW:



AKMaxWA MHW:

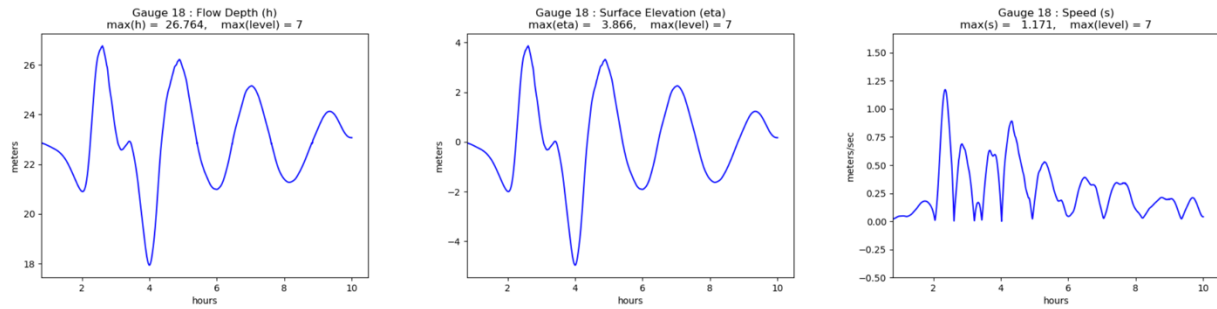


AKMaxWA MLW:

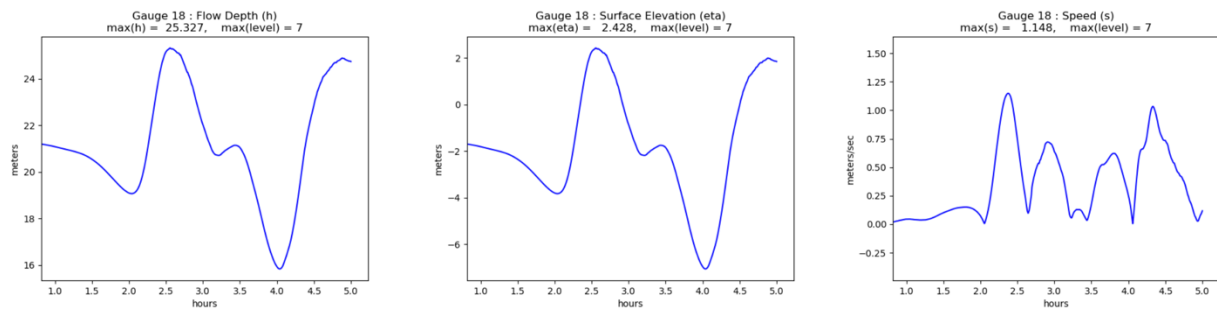


Gauge 18: Bellingham Bay

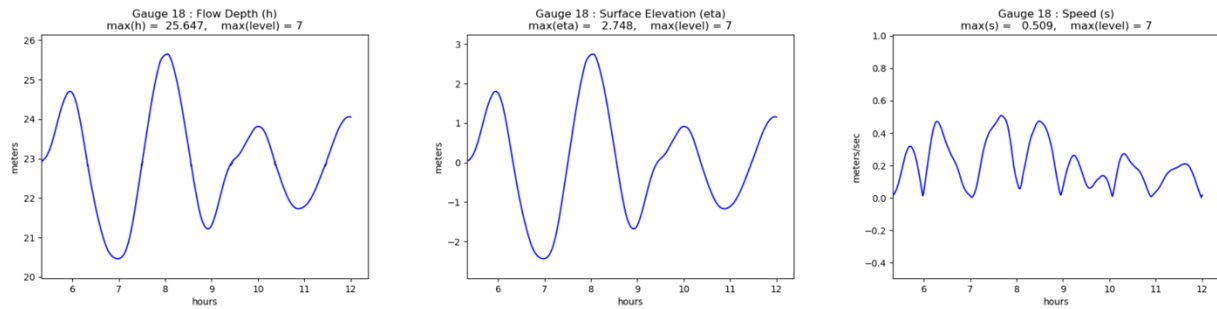
Cascadia-L1 MHW:



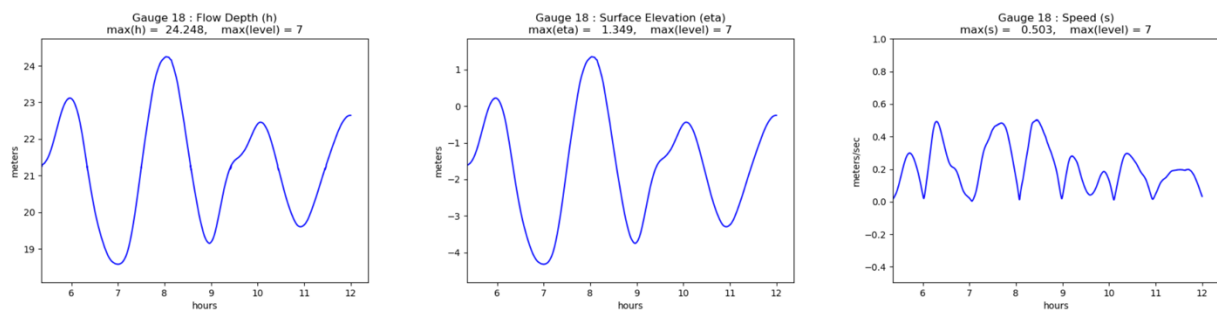
Cascadia-L1 MLW:



AKMaxWA MHW:

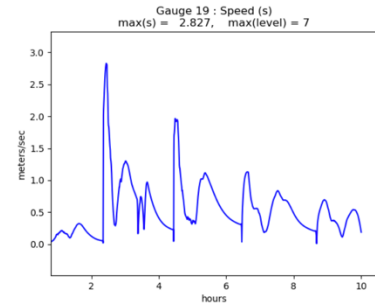
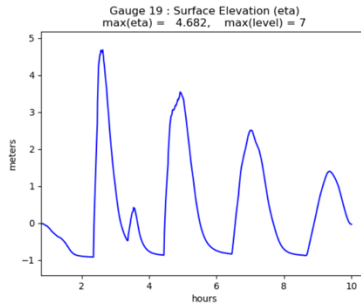
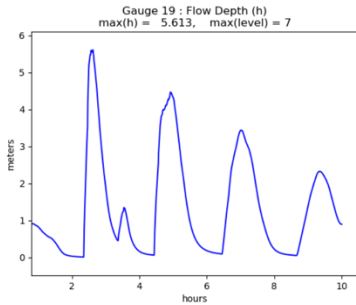


AKMaxWA MLW:

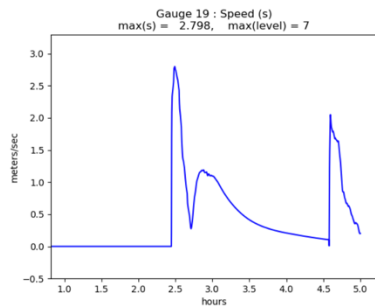
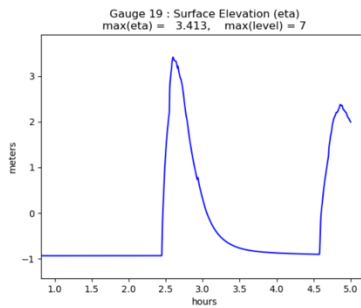
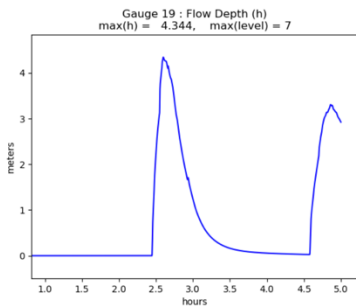


Gauge 19: Mouth of Nooksack River

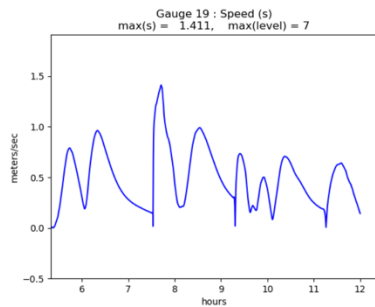
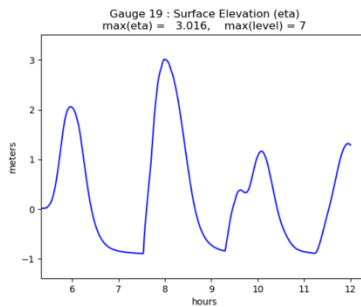
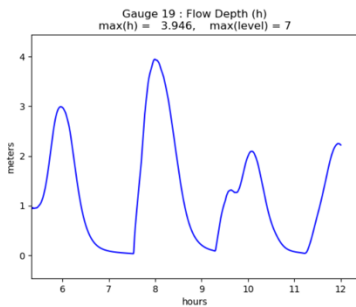
Cascadia-L1 MHW:



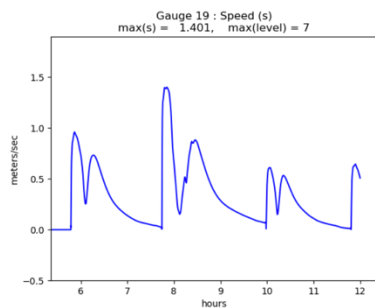
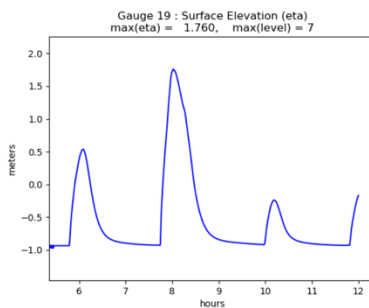
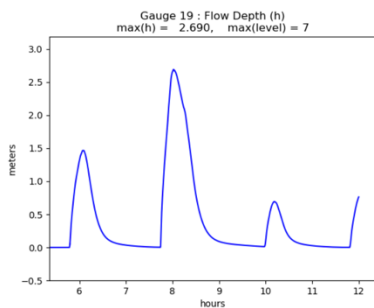
Cascadia-L1 MLW:



AKMaxWA MHW:

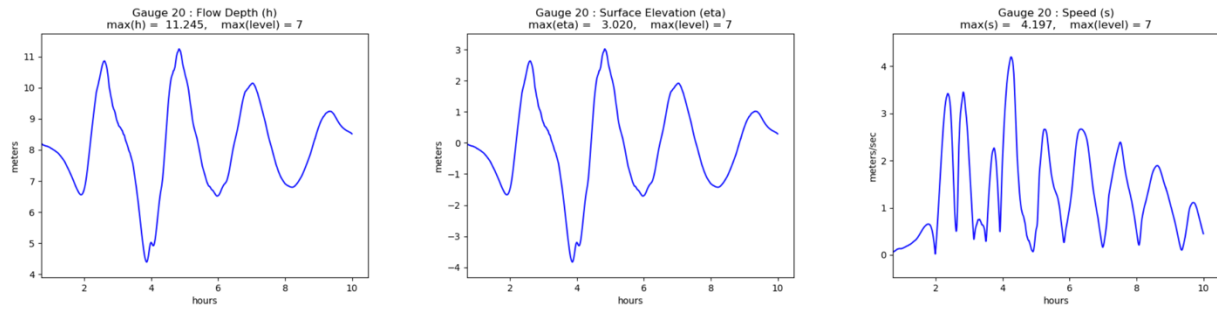


AKMaxWA MLW:

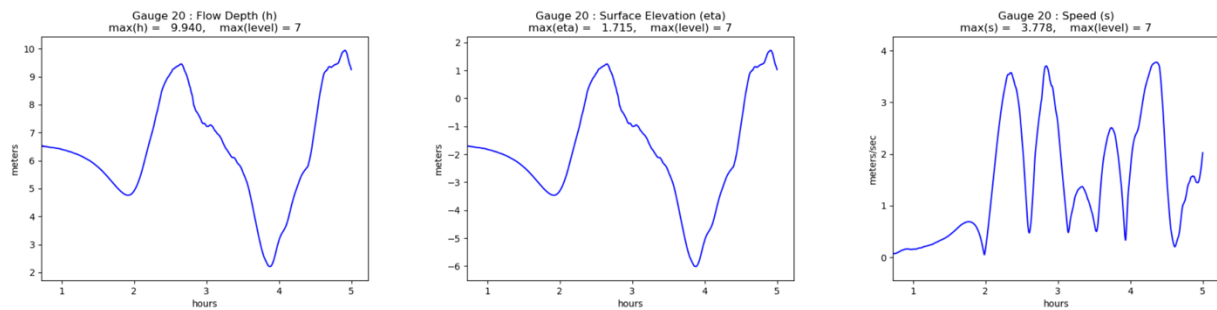


Gauge 20: Southeast of Portage Island

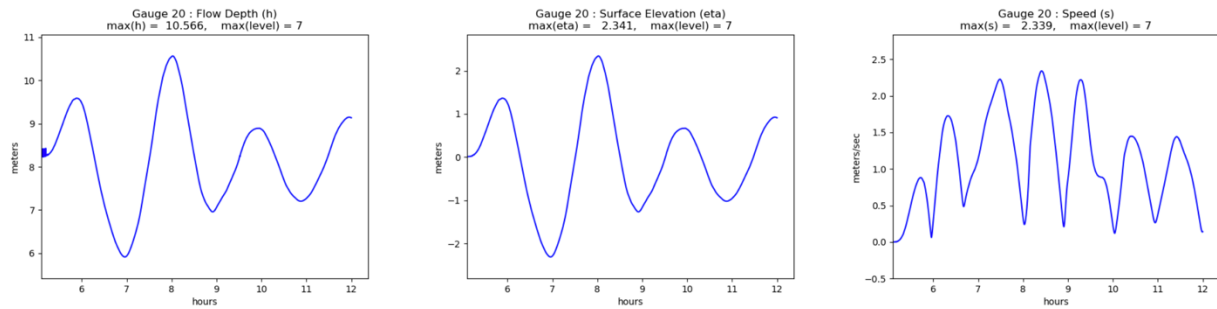
Cascadia-L1 MHW:



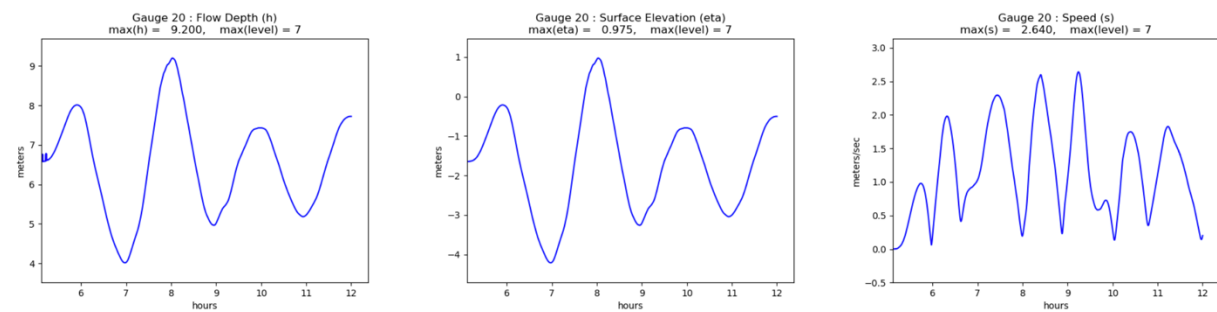
Cascadia-L1 MLW:



AKMaxWA MHW:

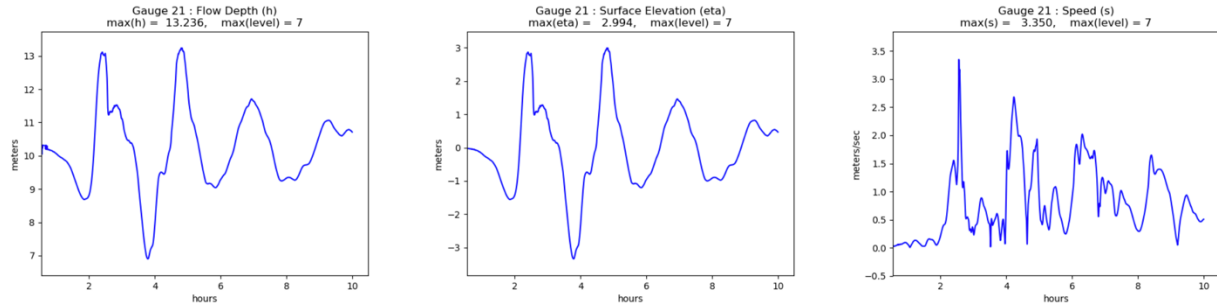


AKMaxWA MLW:

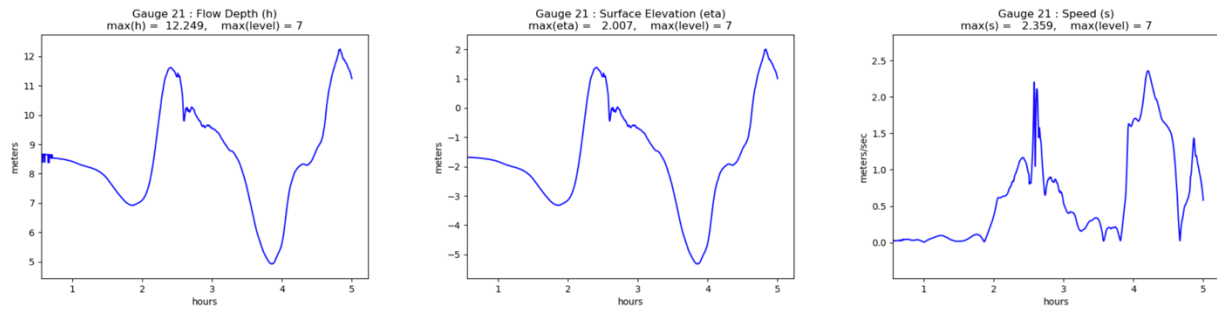


Gauge 21: Northwest of Portage Island

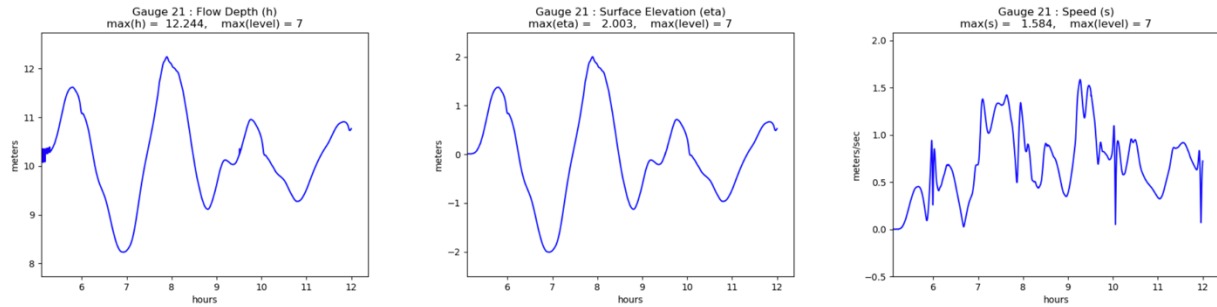
Cascadia-L1 MHW:



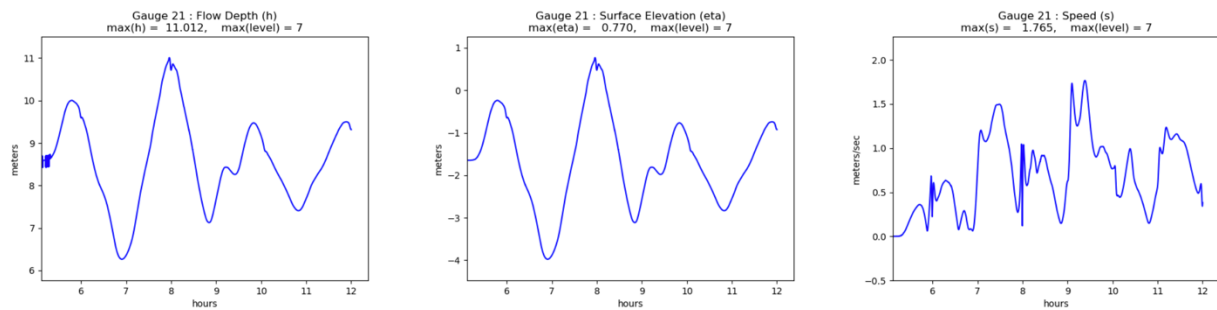
Cascadia-L1 MLW:



AKMaxWA MHW:

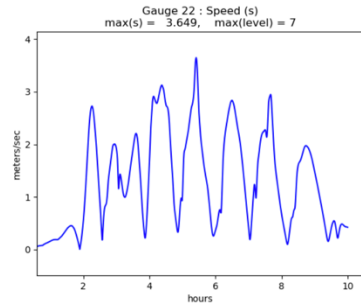
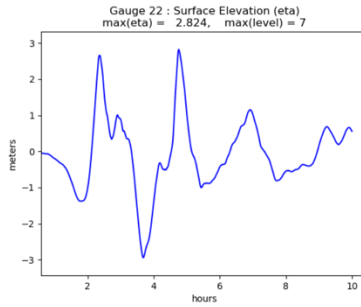
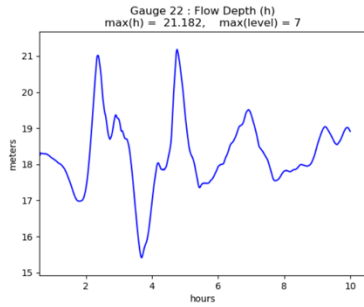


AKMaxWA MLW:

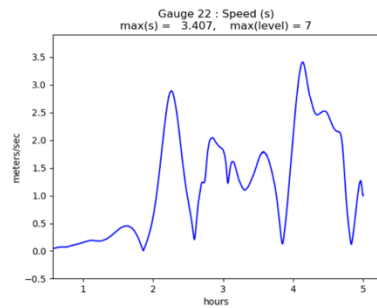
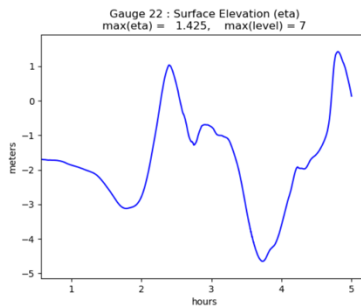
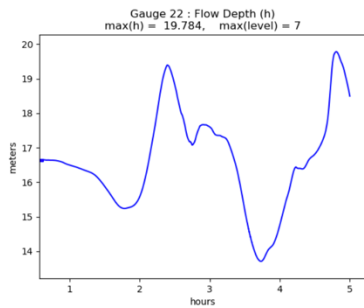


Gauge 22: East of Lummi Point

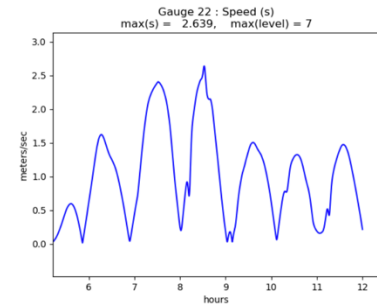
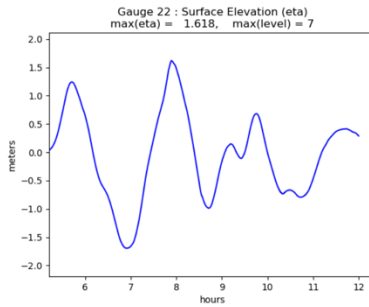
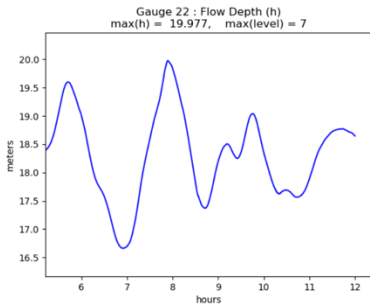
Cascadia-L1 MHW:



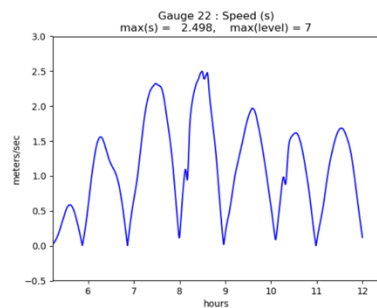
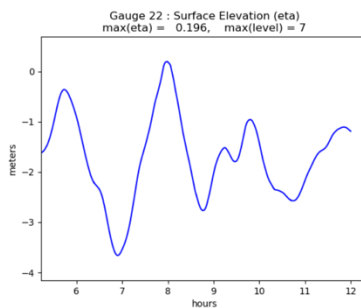
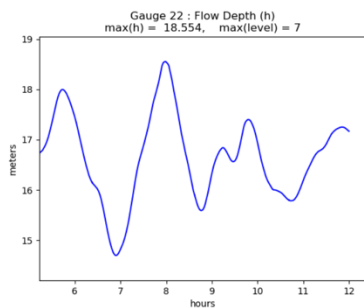
Cascadia-L1 MLW:



AKMaxWA MHW:

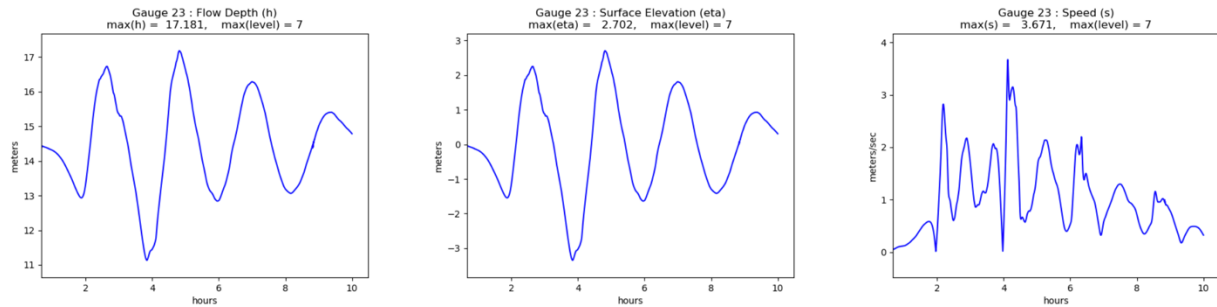


AKMaxWA MLW:

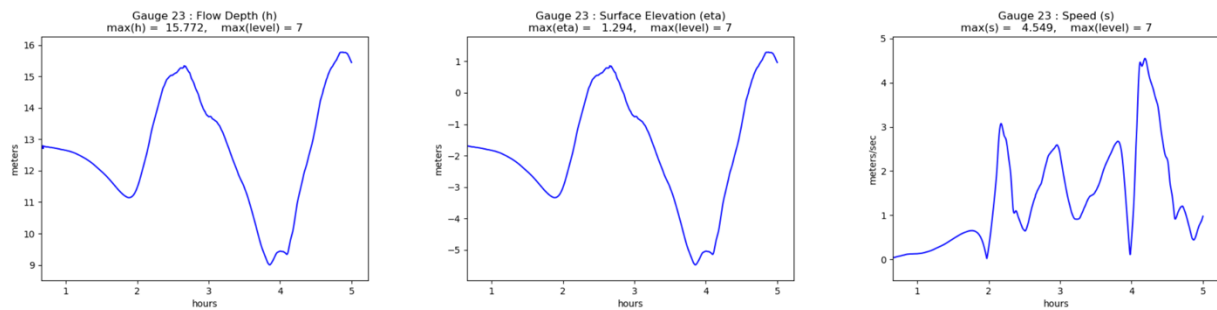


Gauge 23: North of Eliza Island

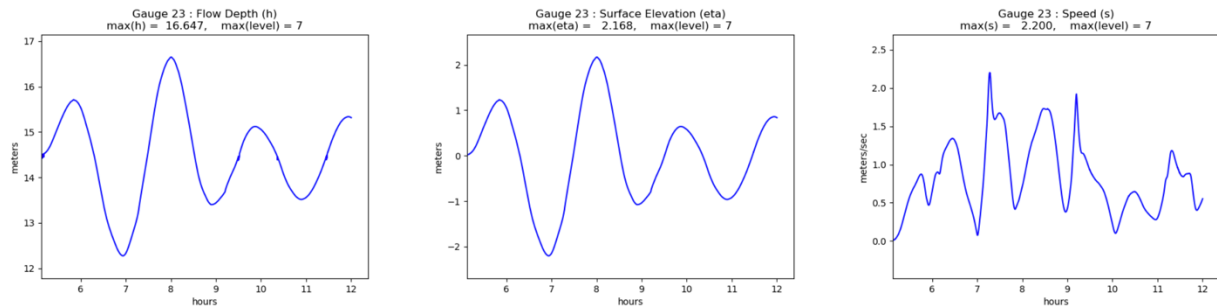
Cascadia-L1 MHW:



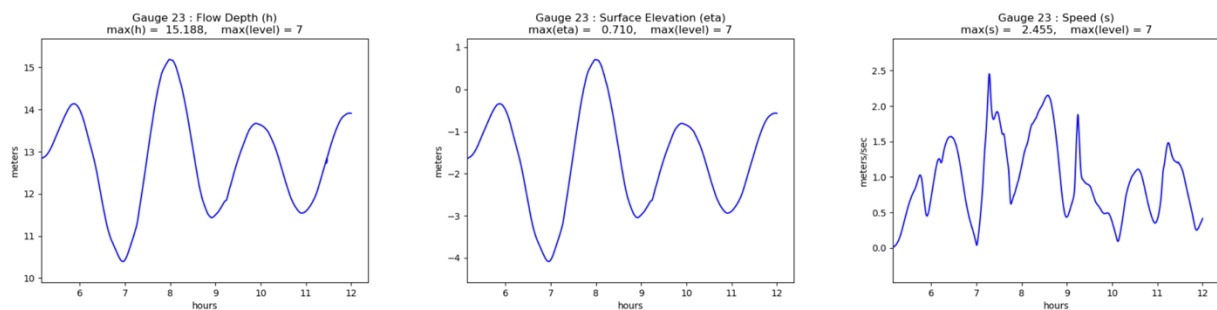
Cascadia-L1 MLW:



AKMaxWA MHW:

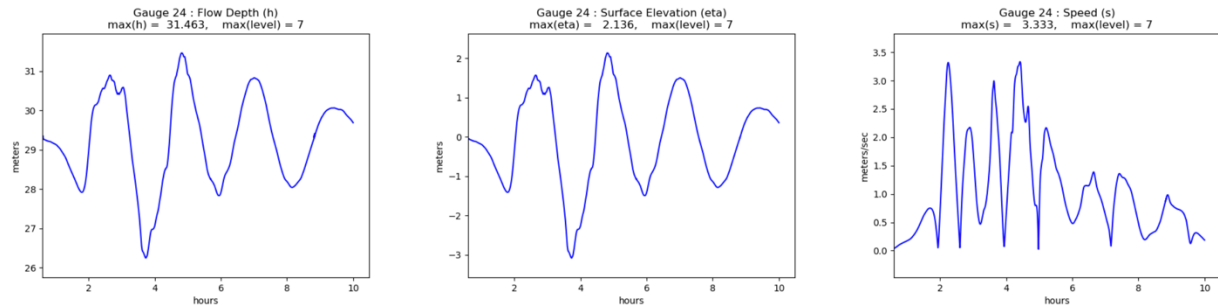


AKMaxWA MLW:

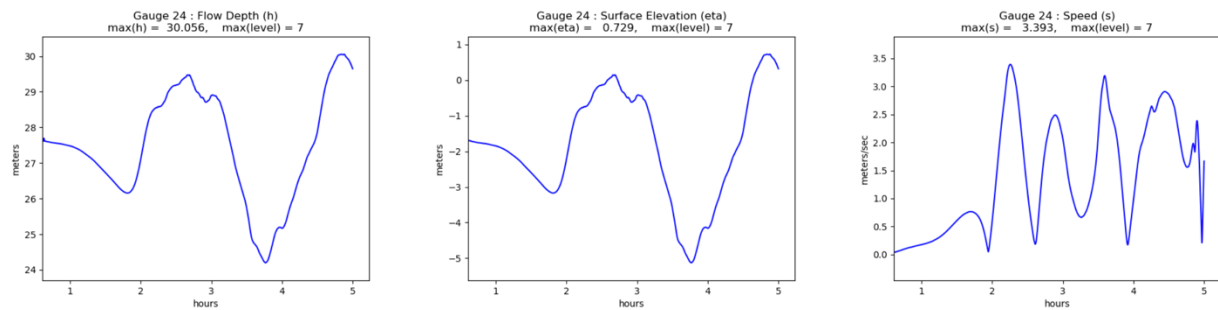


Gauge 24: Between Lummi and Eliza Islands

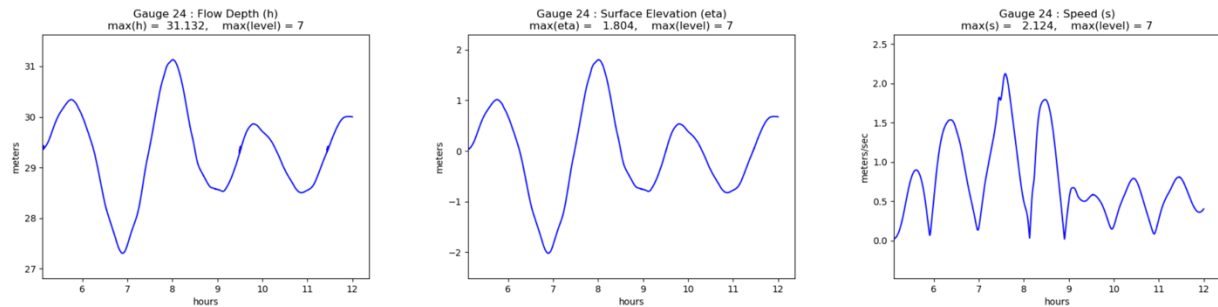
Cascadia-L1 MHW:



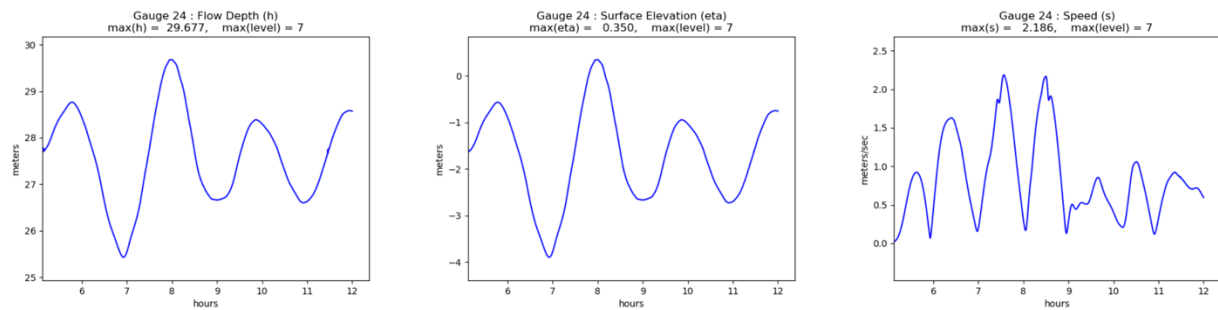
Cascadia-L1 MLW:



AKMaxWA MHW:

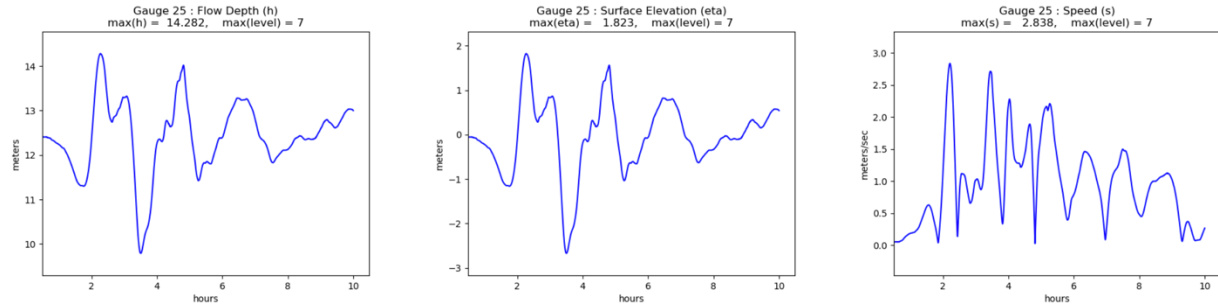


AKMaxWA MLW:

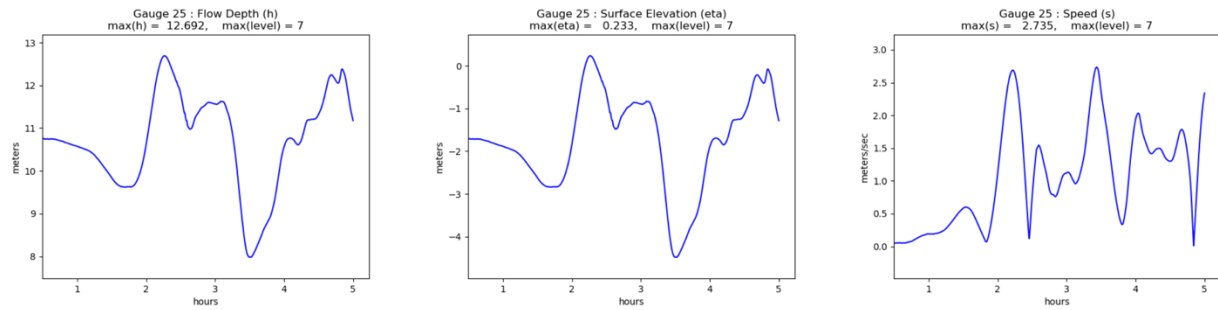


Gauge 25: North of Lummi Island

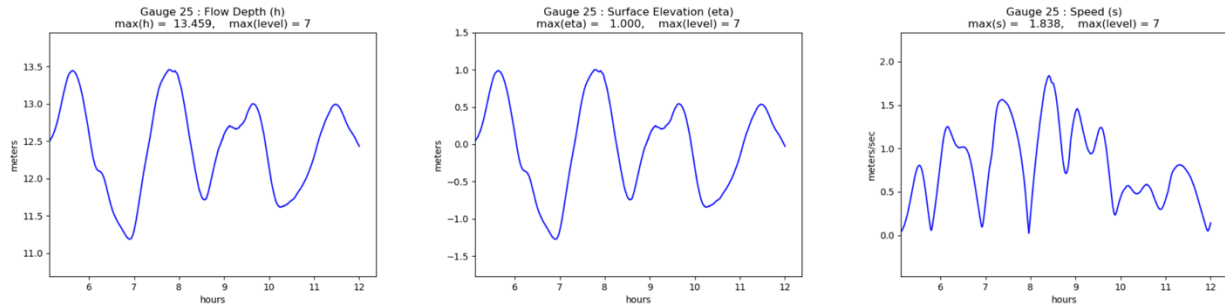
Cascadia-L1 MHW:



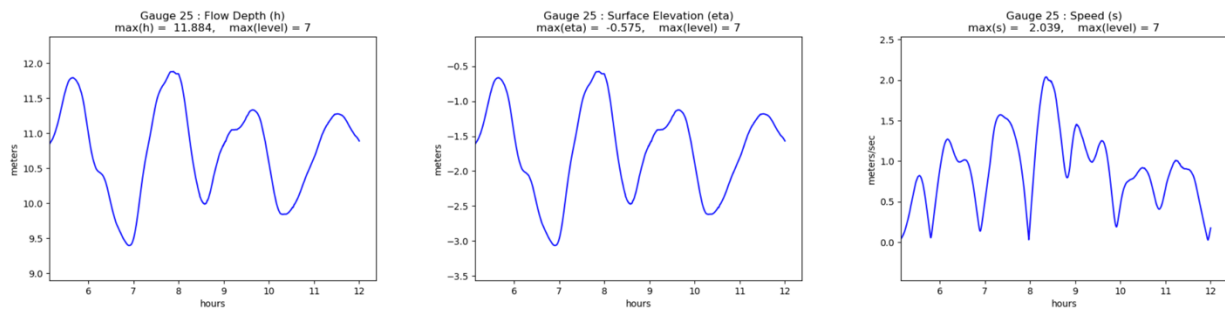
Cascadia-L1 MLW:



AKMaxWA MHW:

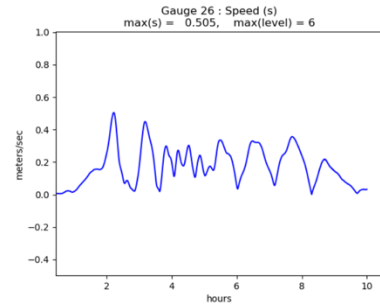
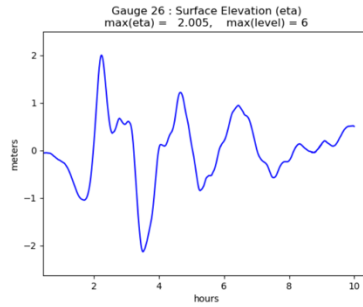
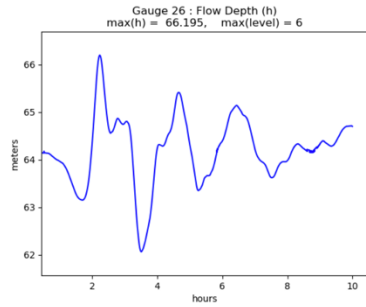


AKMaxWA MLW:

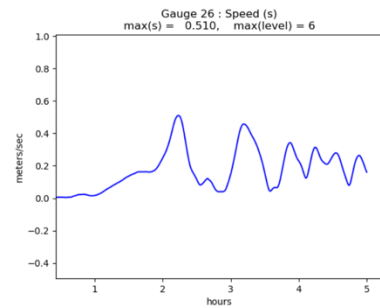
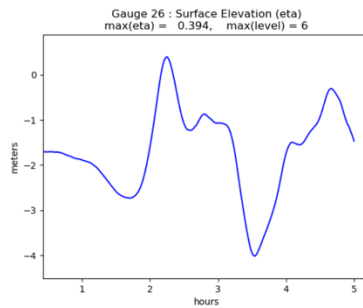
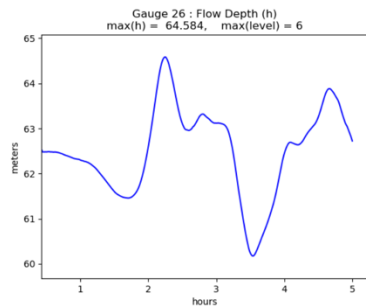


Gauge 26: Georgia Strait northeast of Orcas Island

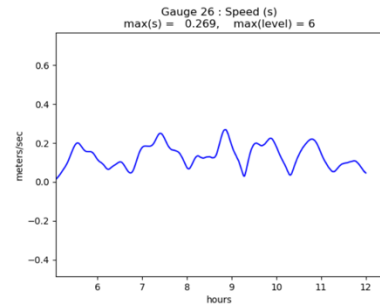
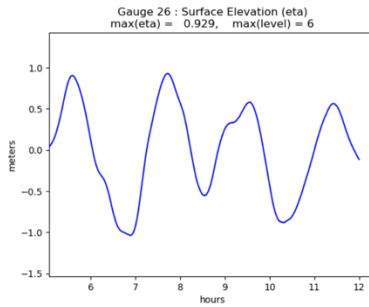
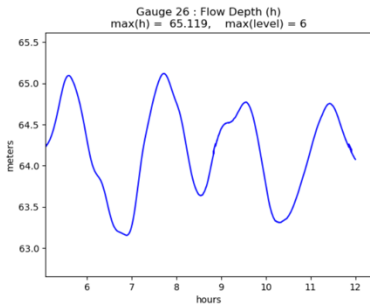
Cascadia-L1 MHW:



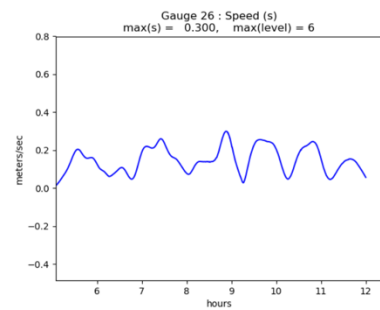
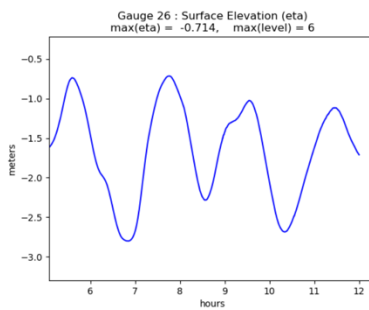
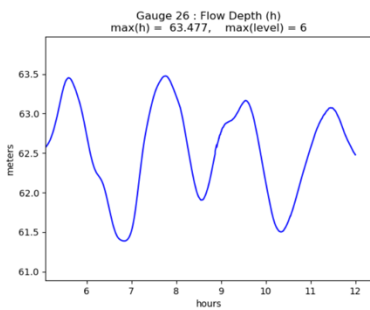
Cascadia-L1 MLW:



AKMaxWA MHW:

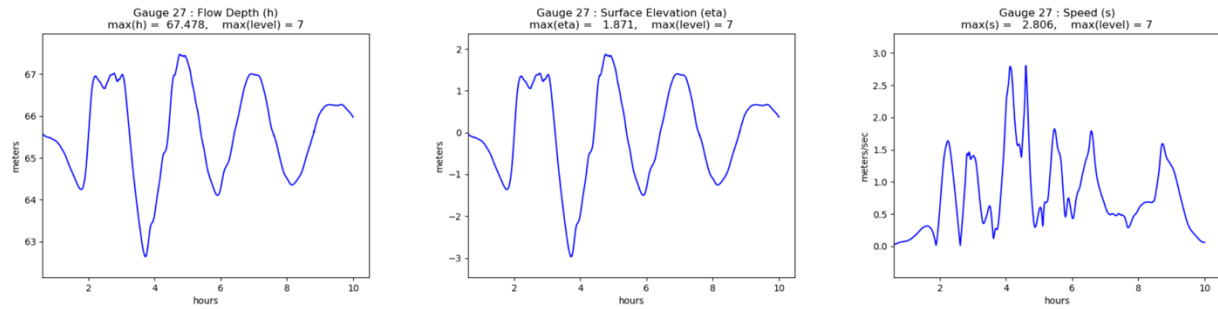


AKMaxWA MLW:

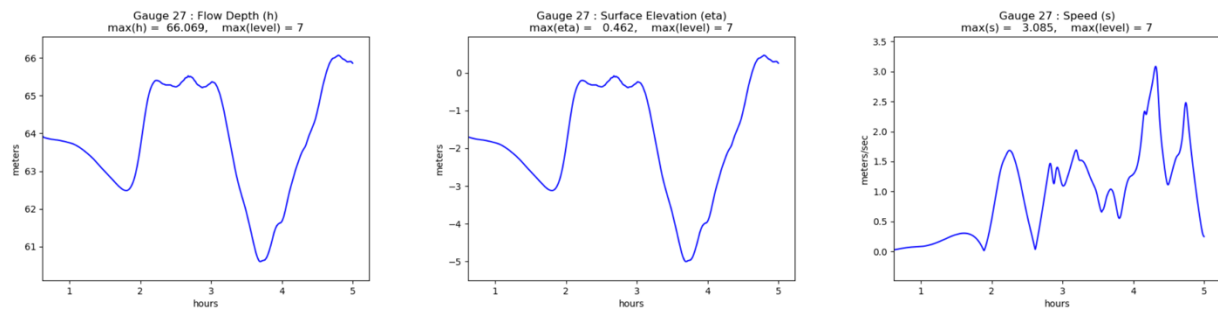


Gauge 27: South of Eliza Island

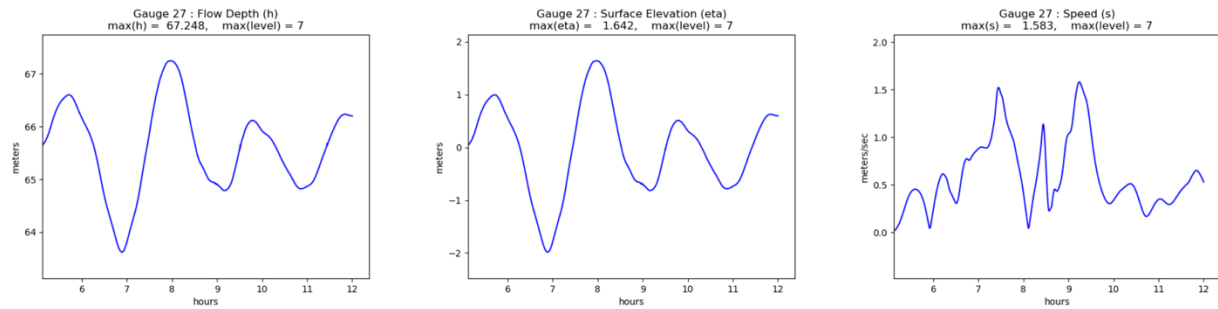
Cascadia-L1 MHW:



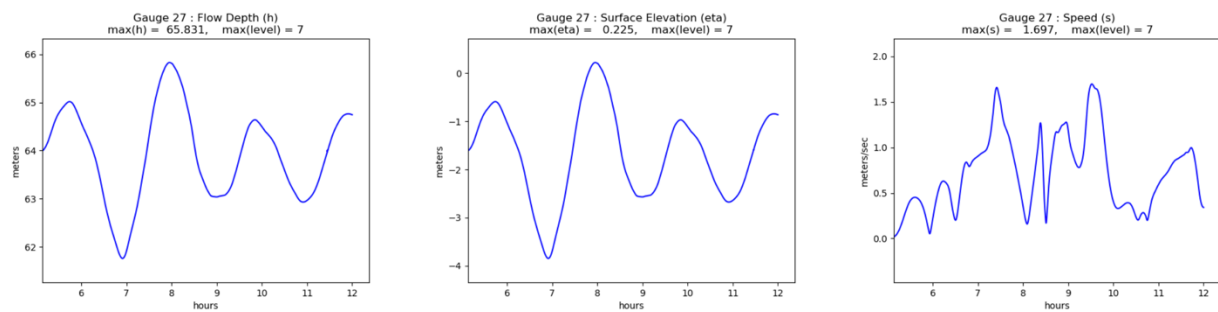
Cascadia-L1 MLW:



AKMaxWA MHW:

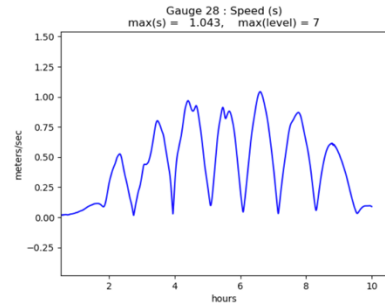
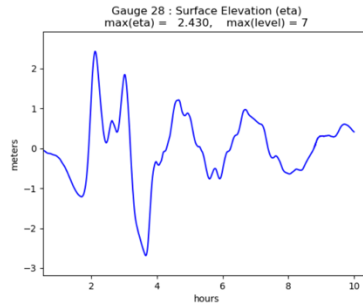
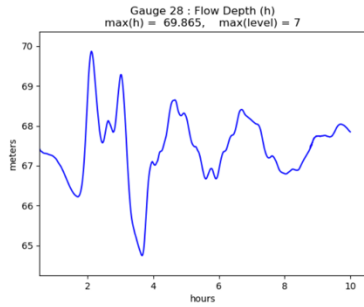


AKMaxWA MLW:

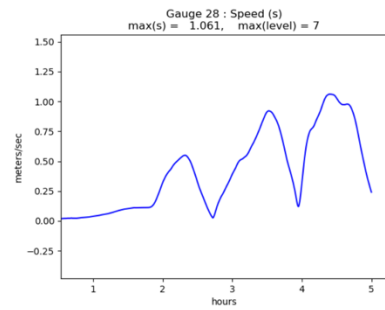
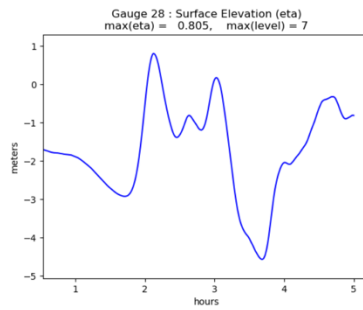
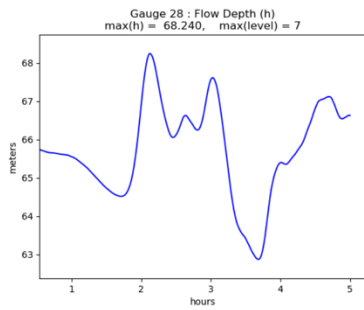


Gauge 28: South of Eliza Island

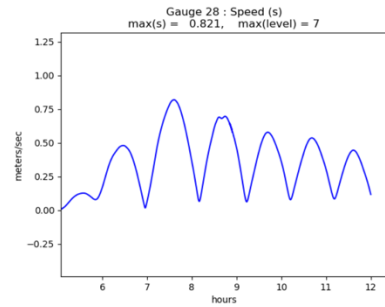
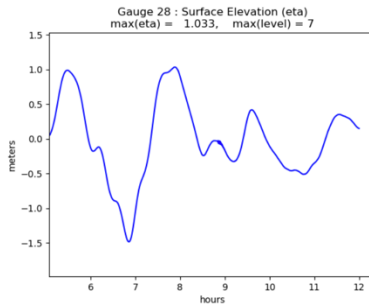
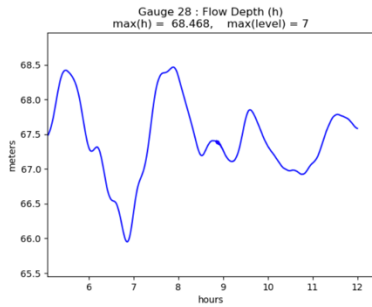
Cascadia-L1 MHW:



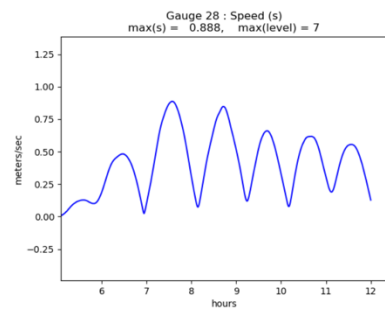
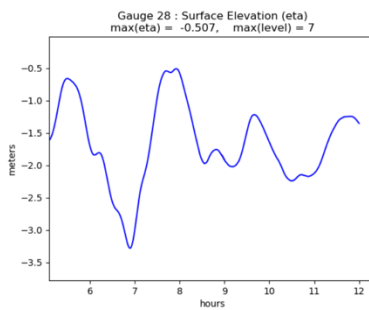
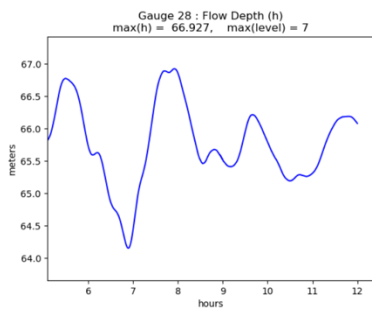
Cascadia-L1 MLW:



AKMaxWA MHW:

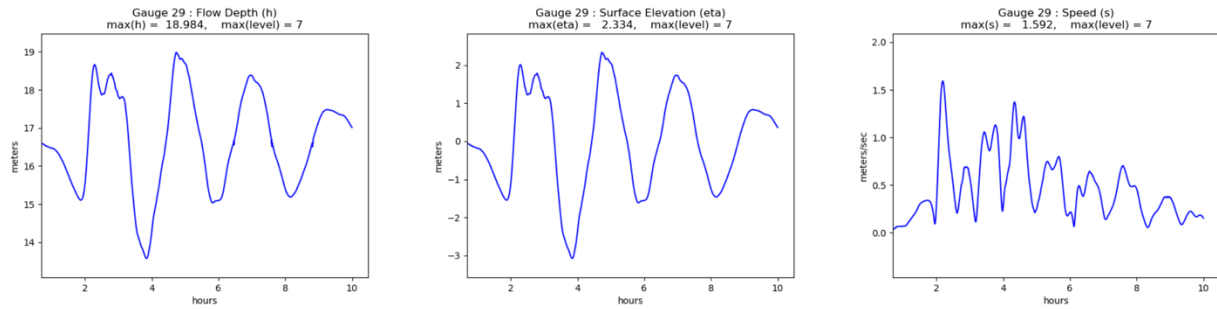


AKMaxWA MLW:

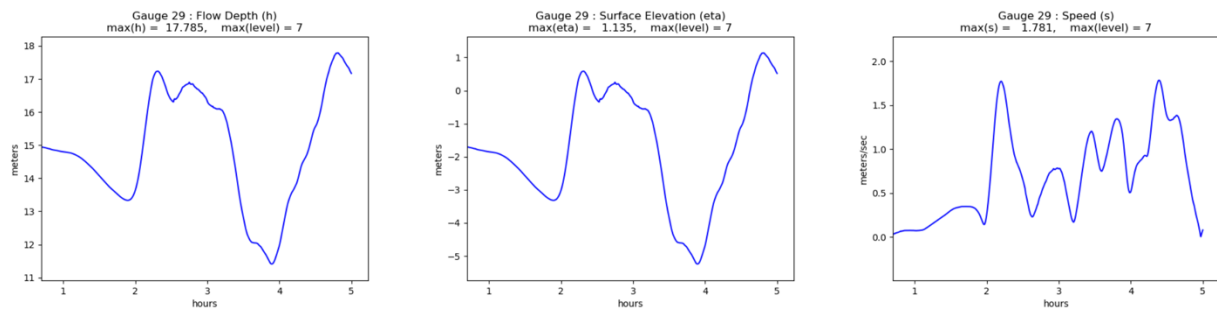


Gauge 29: North Samish Bay

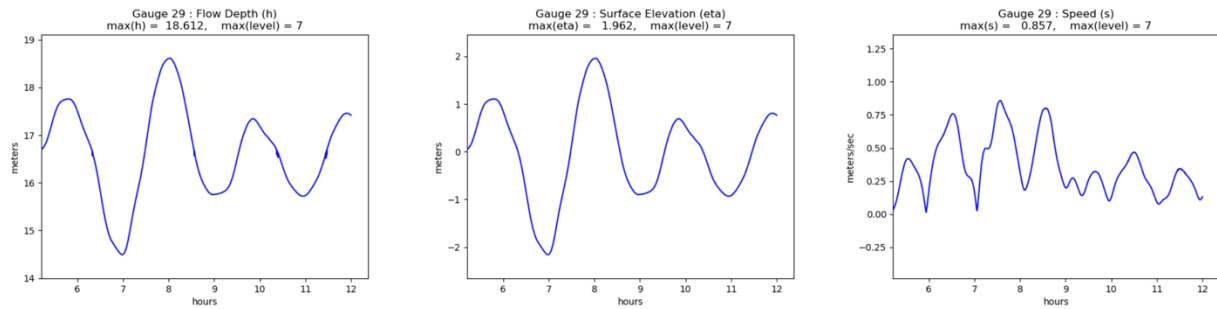
Cascadia-L1 MHW:



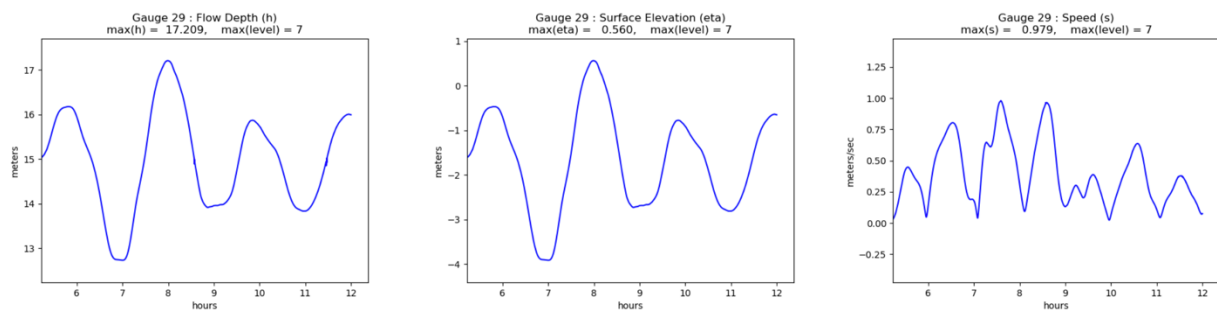
Cascadia-L1 MLW:



AKMaxWA MHW:

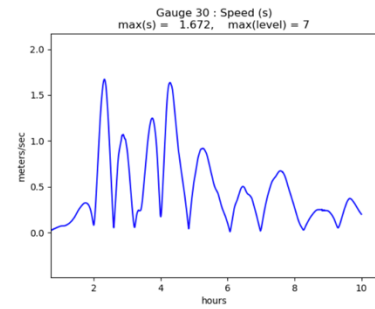
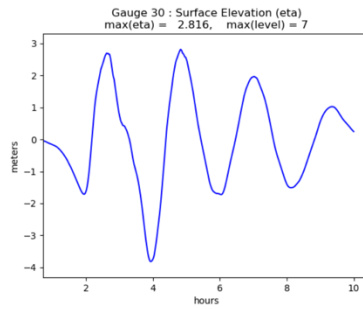
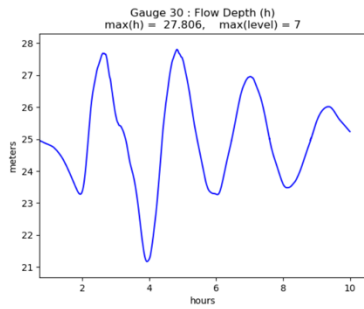


AKMaxWA MLW:

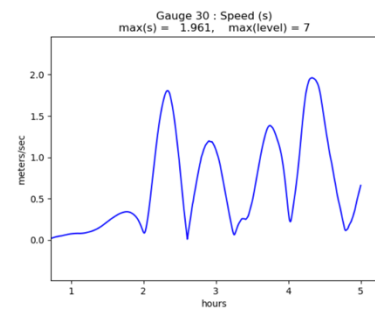
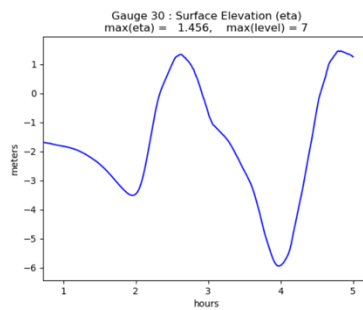
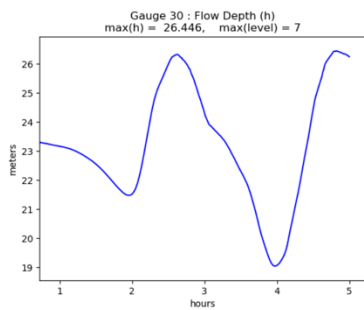


Gauge 30: Bellingham Bay

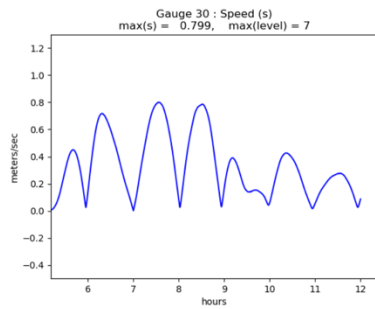
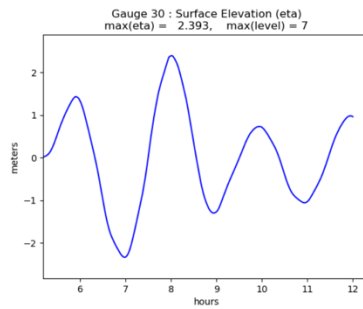
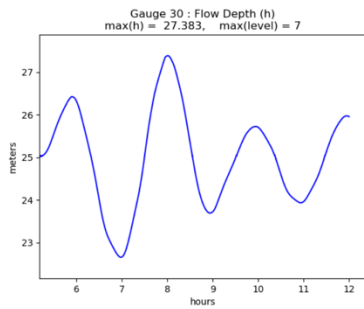
Cascadia-L1 MHW:



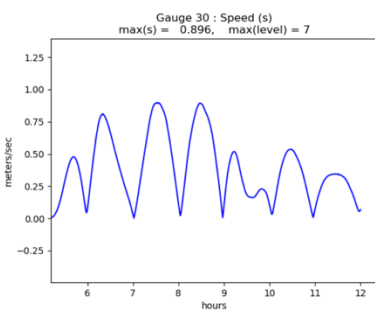
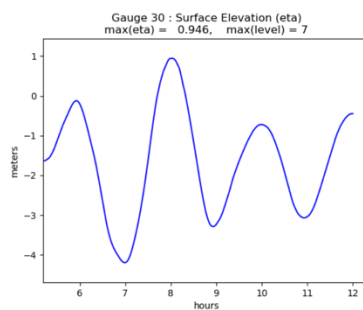
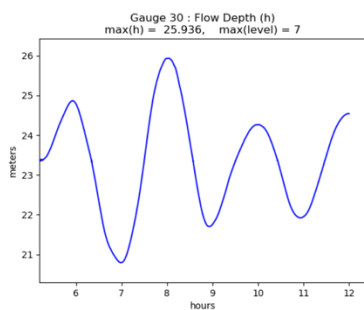
Cascadia-L1 MLW:



AKMaxWA MHW:

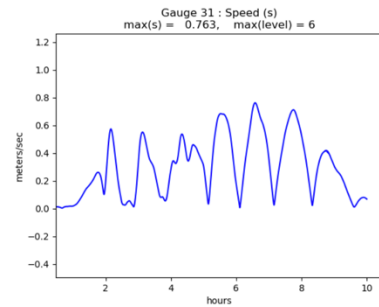
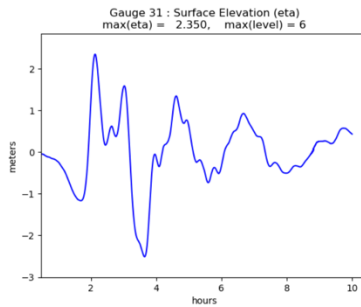
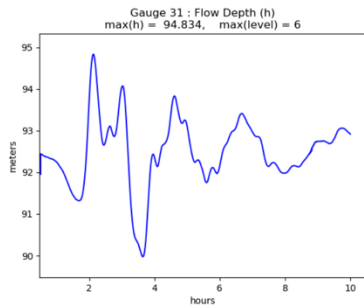


AKMaxWA MLW:

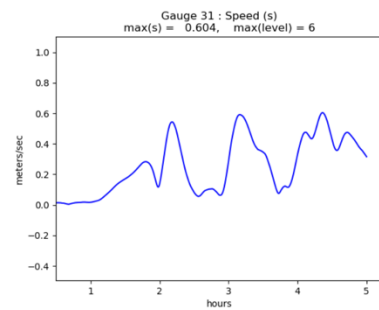
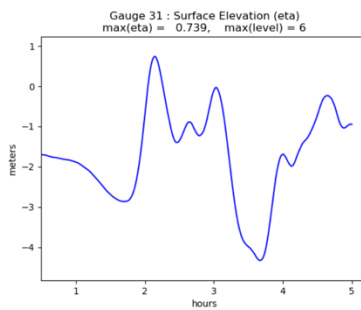
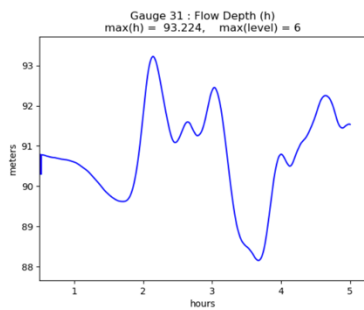


Gauge 31: Rosario Strait between Orcas and Lummi Islands

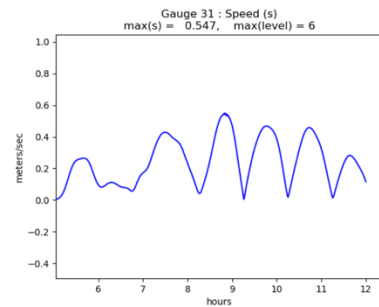
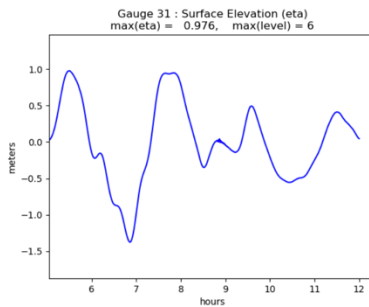
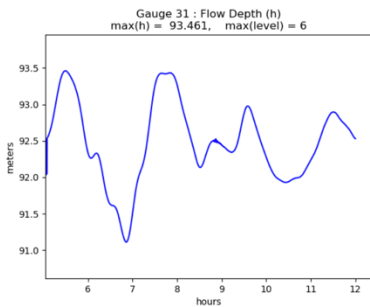
Cascadia-L1 MHW:



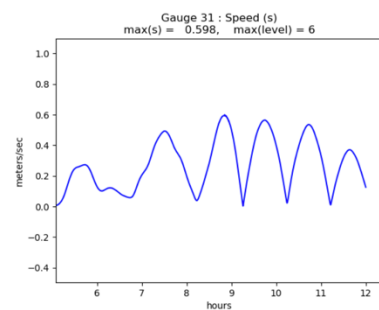
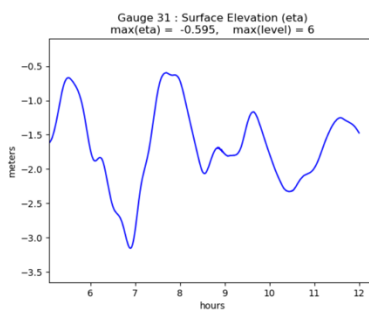
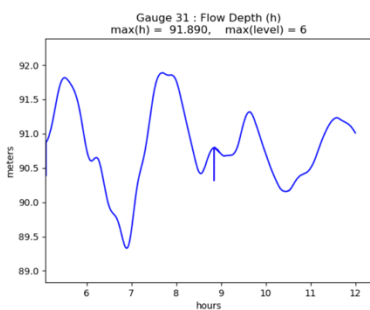
Cascadia-L1 MLW:



AKMaxWA MHW:

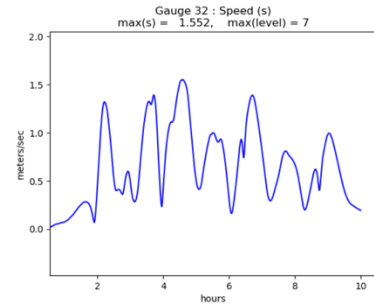
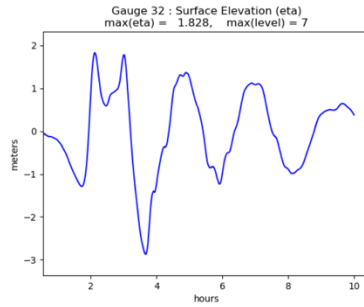
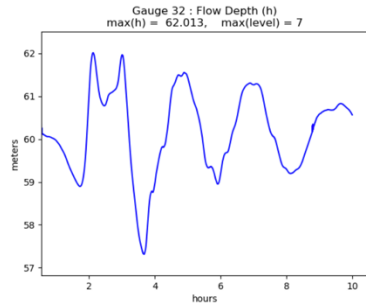


AKMaxWA MLW:

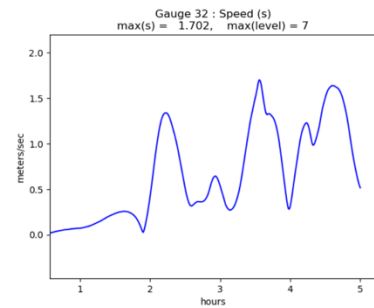
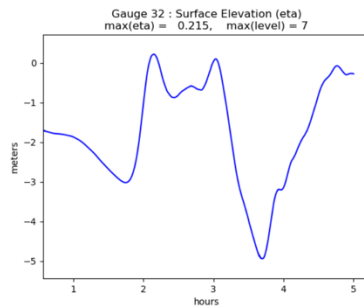
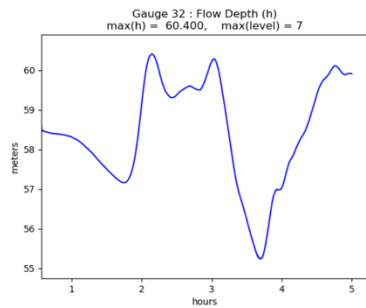


Gauge 32: Northeast of Sinclair Island

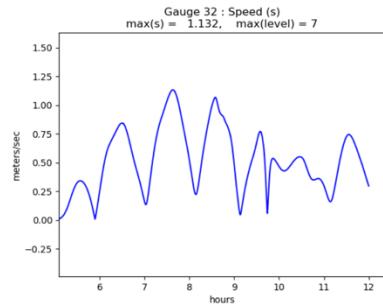
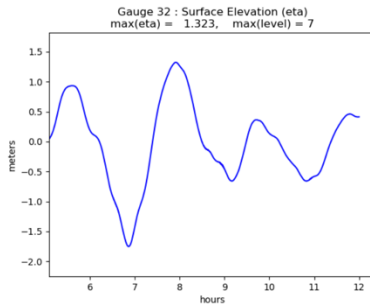
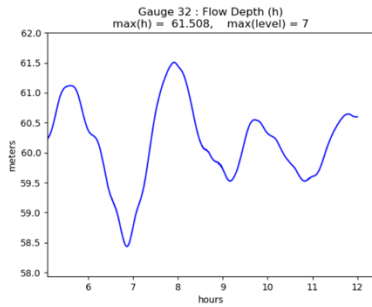
Cascadia-L1 MHW:



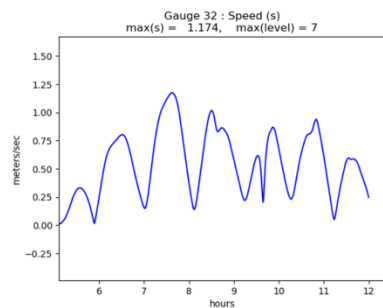
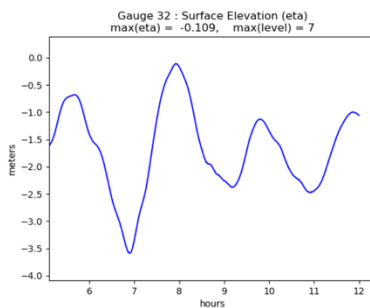
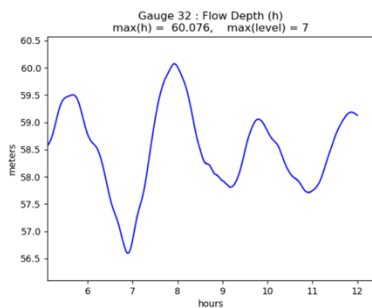
Cascadia-L1 MLW:



AKMaxWA MHW:

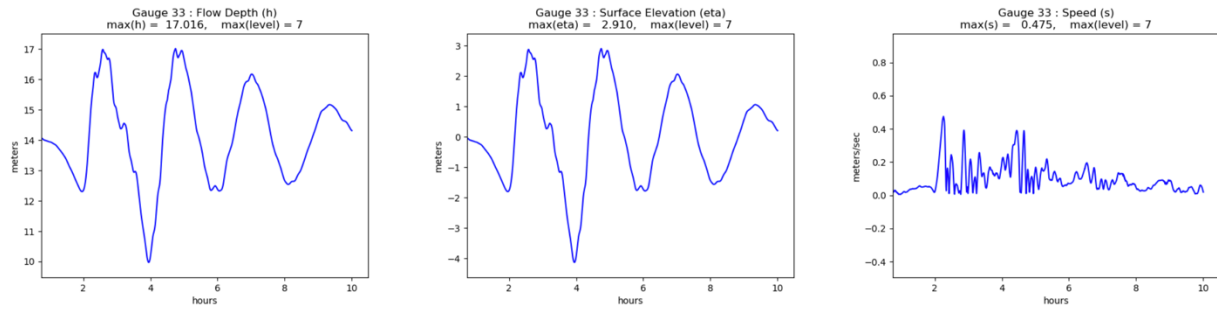


AKMaxWA MLW:

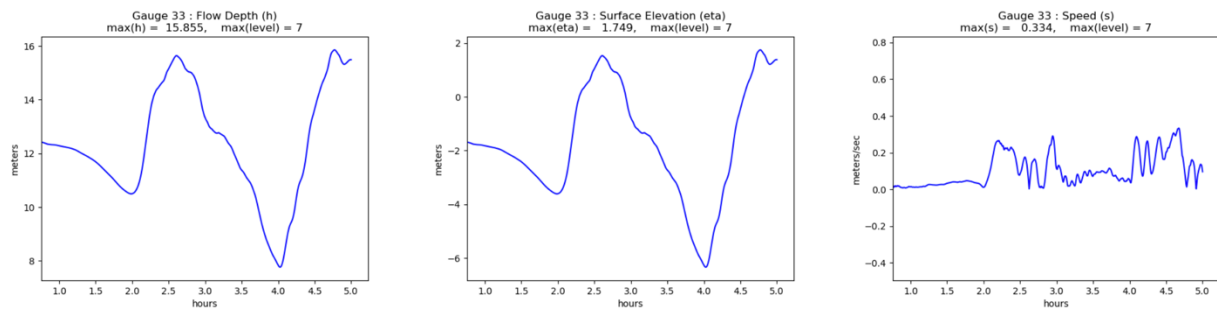


Gauge 33: North end of Chuckanut Bay

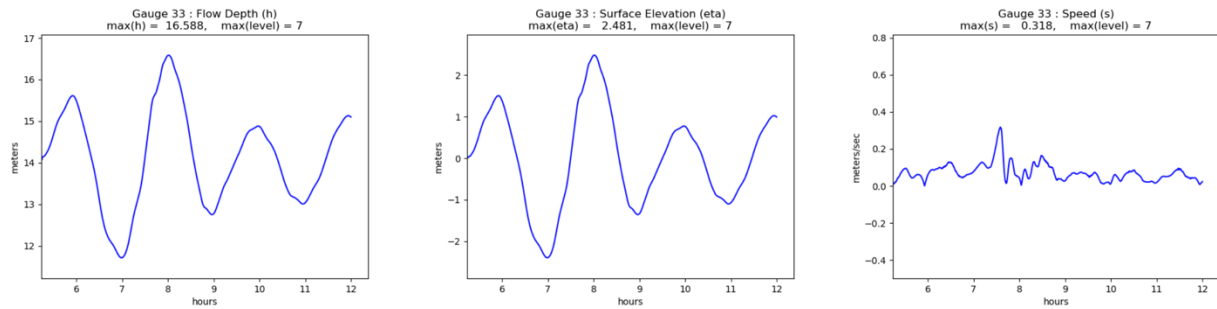
Cascadia-L1 MHW:



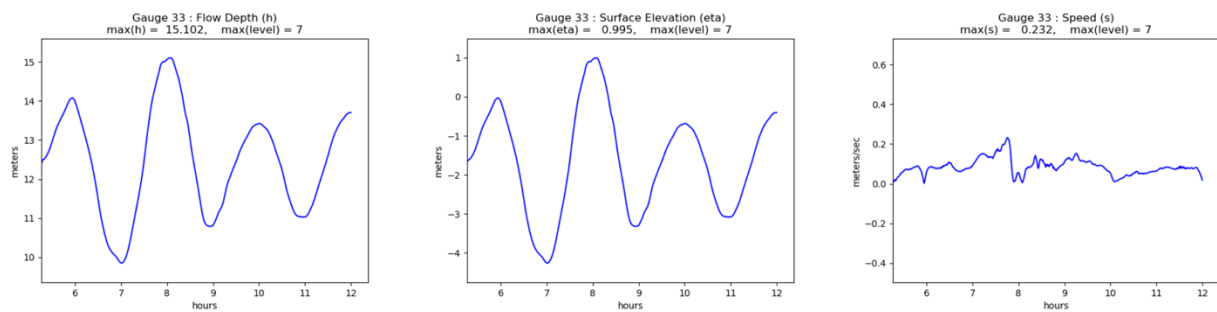
Cascadia-L1 MLW:



AKMaxWA MHW:

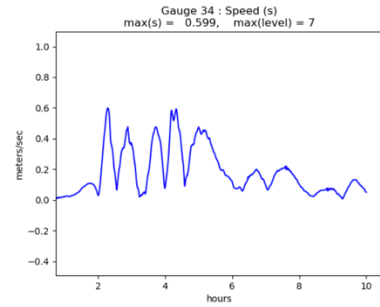
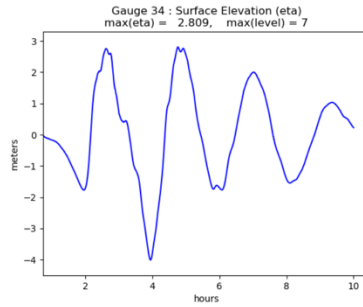
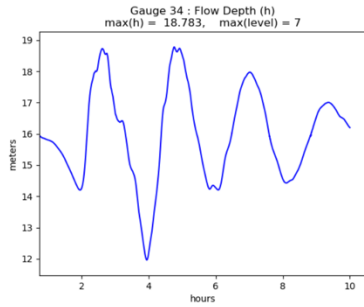


AKMaxWA MLW:

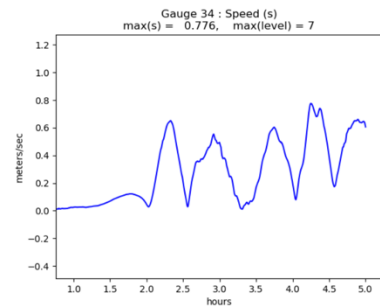
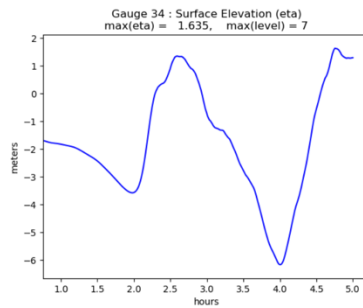
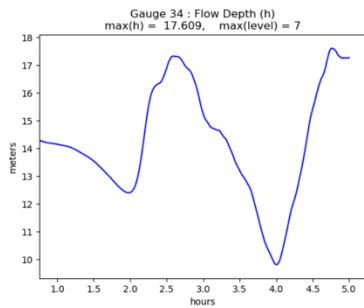


Gauge 34: Chuckanut Bay east of Chuckanut Island

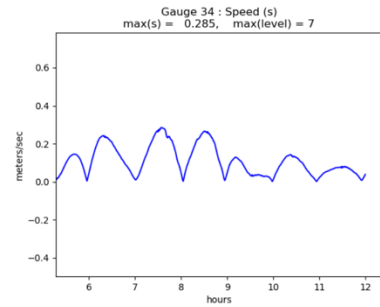
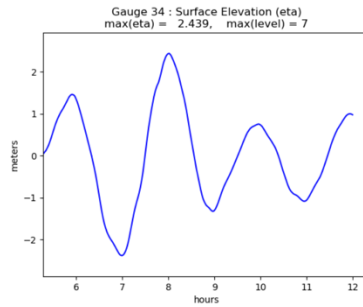
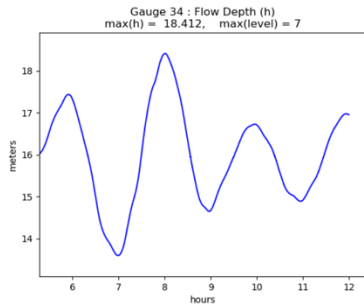
Cascadia-L1 MHW:



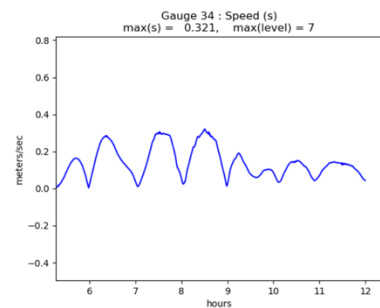
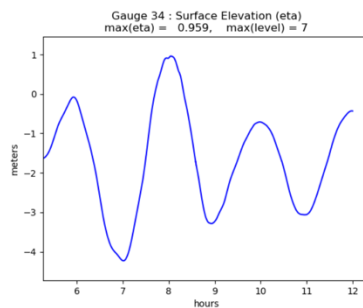
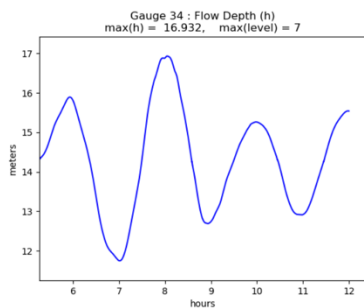
Cascadia-L1 MLW:



AKMaxWA MHW:

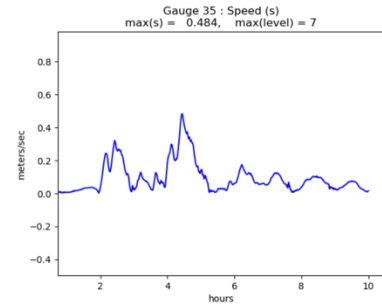
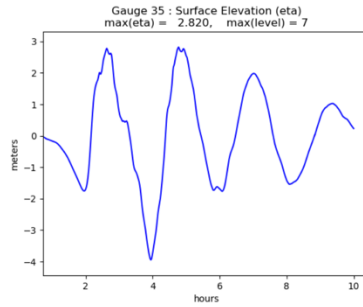
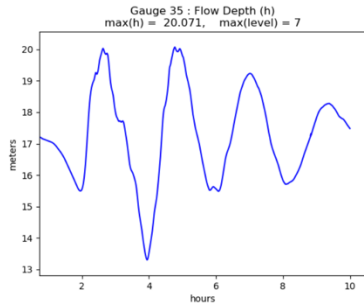


AKMaxWA MLW:

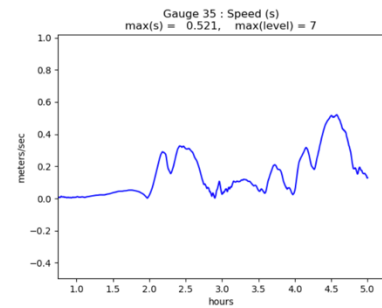
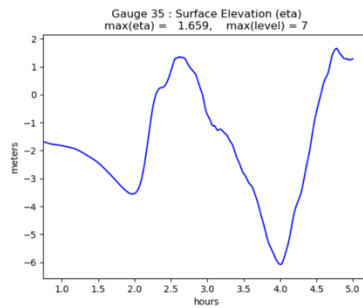
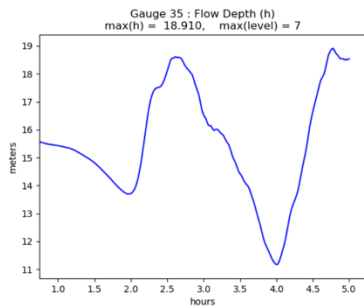


Gauge 35: Pleasant Bay

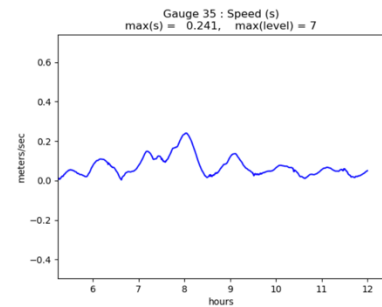
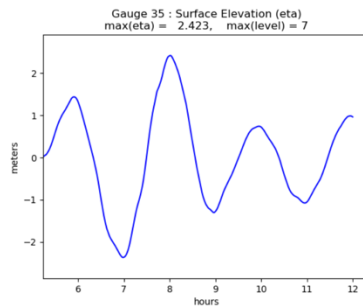
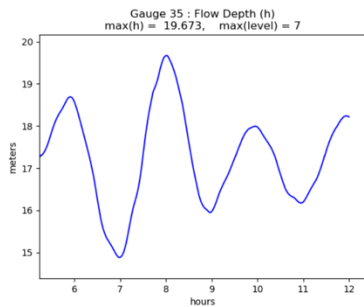
Cascadia-L1 MHW:



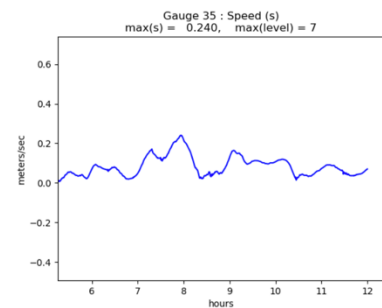
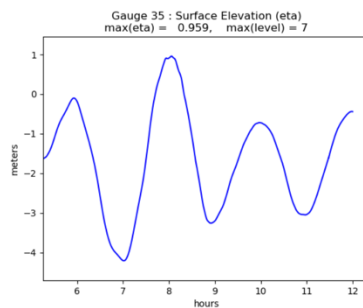
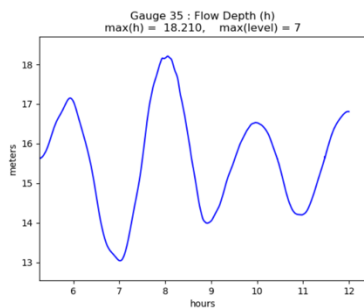
Cascadia-L1 MLW:



AKMaxWA MHW:

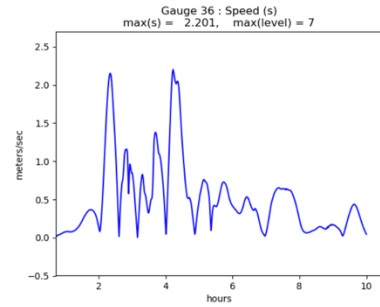
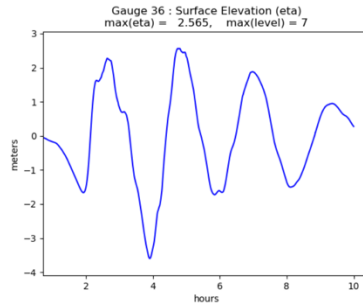
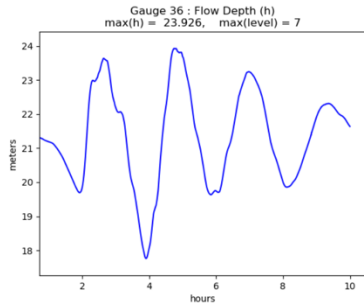


AKMaxWA MLW:

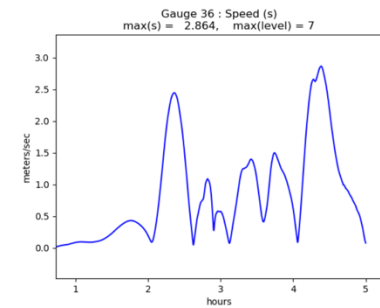
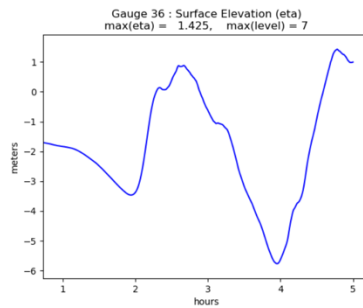
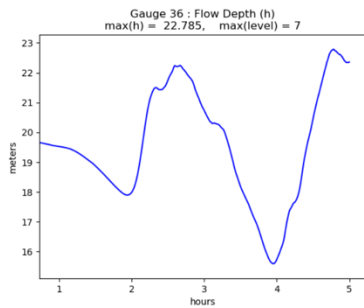


Gauge 36: West of Chuckanut

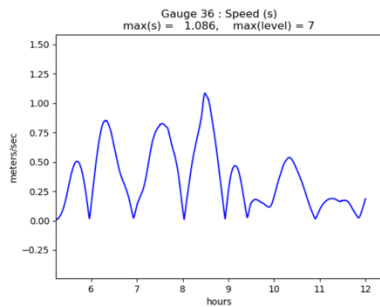
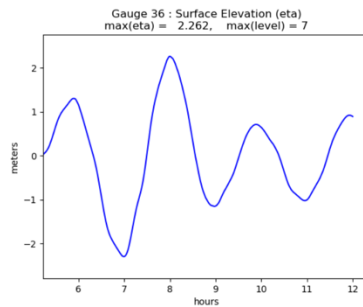
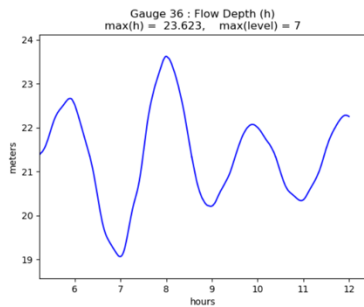
Cascadia-L1 MHW:



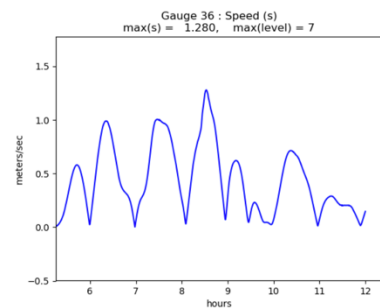
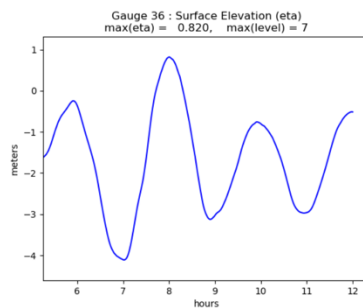
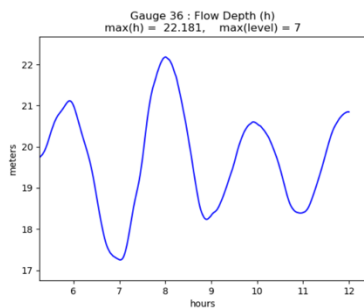
Cascadia-L1 MLW:



AKMaxWA MHW:



AKMaxWA MLW:



8. Future studies

Although other earthquake/tsunami sources including the South Whidbey Island fault (SWIF), the Darrington-Devils Mountain fault (D-DMF), and the Skipjack fault (SF) have the potential to generate hazardous tsunamis in the study area, they are not modeled in this study. When peer-reviewed models of earthquake events on these faults become available, further modeling of these events may be useful to identify additional tsunami hazards.

For future studies of potential tsunami hazards to the Port of Bellingham, a list of faults active in the Holocene (last 10,000 years) that cross bodies of water within 130 km (80 miles) of the Port of Bellingham are listed in Table 5. These faults either do not have associated deformation models, or have models that are currently in development.

Table 5. Active faults that may be capable of generating tsunamis that could reach the City of Bellingham waterfront. The column on the right lists the age range in calendar years before present of the last known earthquake on the corresponding fault.

Fault/source	Type	Reference	Most recent EQ Cal yr BP
Birch Bay fault	Reverse (?)	Kelsey et al., 2012*	1,280-1,070
Devils Mountain fault zone	Left-lateral	Barrie and Greene, 2015; Johnson et al., 2001; Personius et al., 2014*	2,300-1,500
Utsalady Point Fault	Left-lateral	Johnson et al., 2001; Johnson et al., 2004*	100-400
Sandy Point fault	Dip slip, unspecified	Kelsey et al., 2012	< 2,320
Drayton Harbor fault	Dip slip, unspecified	Kelsey et al., 2012	unknown
South Whidbey Island fault zone	Reverse/transpressional	Gower et al., 1985; Johnson et al., 2001; Johnson et al., 1996; Sherrod et al., 2008*	< 2,730
Seattle fault zone	Reverse	Blakely et al., 2002; Bucknam et al., 1992; Johnson et al., 1999; Nelson et al, 2014*	1,050-1,020 Restoration Point 1,040–910 EQ D 940–380 EQ E
Skipjack Island fault zone	Left-lateral	Greene et al., 2018*	> 6,130
Strawberry Point fault	Left-lateral	Johnson et al., 2001*	unknown
Fraser River fault (?)	Inferred alignment of scarps, pockmarks, and slumps	Greene et al., 2018*	unknown
Fraser River delta front failures	Scarps, slumps	Greene et al., 2018*	unknown
Orcas Island NE side	Landslide evidence	Greene et al., 2018*	unknown

*denotes the reference for the age

Acknowledgments

We acknowledge computing time on the CU-CSDMS High-Performance Computing Cluster to run the GeoClaw code, which used resources from the University of Colorado Boulder Research Computing Group, and is supported by the National Science Foundation (awards ACI-1532235 and ACI-1532236), the University of Colorado Boulder, and Colorado State University. The NOAA Center for Tsunami Research (NCTR) at the Pacific Marine Environmental Laboratory, in Seattle provided the earthquake deformation files for the Cascadia-L1 and AKMaxWA earthquake source models, as well as the unit source parameters of Table 1 for the AKMaxWA.

We thank NCEI for providing pre-publication versions of the newest 1/9" DEM tiles used for this study, which will eventually be available at <https://doi.org/10.25921/ds9v-ky35>. We also thank Washington Department of Natural Resources for the edits to the 1/9" DEM. This work was supported by an award from the National Science Foundation to the University of Washington M9 project and Washington Sea Grant.

Data Availability

The computer code and input data used in this study has been archived and is available on request from the Washington State Geological Survey. DEMs referenced to NAVD88 must be requested directly from the National Centers for Environmental Information (NCEI) at www.ncei.noaa.gov, or converted to MHW with NOAA's VDatum tool: <https://vdatum.noaa.gov/vdatumweb/>.

References

- Adams, L., González, F., and LeVeque, R., 2019, Tsunami Hazard Assessment of Whatcom County, Washington, Project Report – Version 2, <http://hdl.handle.net/1773/45586>.
- Atwater, B., Satoko, M.-R., Satake, K., Yoshinobu, T., Kazue, U., and Yamaguchi, D., 2005, USGS Professional Paper 1707.
- Barrie, J., & Greene, H. (2015). Active faulting in the northern Juan de Fuca Strait; implications for Victoria, British Columbia. Current Research - Geological Survey of Canada, Current Research - Geological Survey of Canada.
- Berger, M. J., George, D. L., LeVeque, R. J., & Mandli, K. T., 2011, The GeoClaw software for depth-averaged flows with adaptive refinement. *Advances in Water Resources*, 34(9), p. 1195-1206.
- Blakely, R. J., R. E. Wells, C. S. Weaver, and S. Y. Johnson (2002), Location, structure, and seismicity of the Seattle fault zone, Washington: Evidence from aeromagnetic anomalies, geologic mapping, and seismic reflection data, *Geol. Soc. Am. Bull.*, 114, 169–177, doi:10.1130/0016-7606(2002)114<0169:LSASOT>2.0.CO;2.
- Bucknam, R. C., E. Hemphill-Haley, and E. B. Leopold (1992), Abrupt uplift within the past 1700 years at southern Puget Sound, Washington, *Science*, 258, 1611–1614, doi:10.1126/science.258.5088.1611.
- Cooperative Institute for Research in Environmental Sciences, Continuously Updated Digital Elevation Model (CUDEM) – 1/9 Arc-Second Resolution Bathymetric-Topographic Tiles. NOAA National Centers for Environmental Information, Prepublication version provided by NCEI in 2020, <https://doi.org/10.25921/ds9v-ky35>.
- Clawpack Development Team, Clawpack software, 2020, Version 5.7.0, <http://www.clawpack.org>, <https://zenodo.org/record/3764278#.XupP-p5Kjdc>.
- Gica, E., M. Spillane, V. Titov, C. Chamberlain, and J. Newman, 2008, Development of the forecast propagation database for NOAA's Short-term Inundation Forecast for Tsunamis (SIFT), NOAA Technical Memorandum OAR PMEL-139, <https://www.pmel.noaa.gov/pubs/PDF/gica2937/gica2937.pdf>.
- González, F. I., LeVeque, R. J., & Adams, L. M., 2015, Tsunami Hazard Assessment of the Strait of Juan de Fuca, <http://hdl.handle.net/1773/36191>.
- Gonzalez, F., LeVeque, R. J., Varkovitzky, J., Chamberlain, P., Hirai, B., & George, D. L., 2011, GeoClaw results for the NTHMP tsunami benchmark problems, In Results of the 2011 NTHMP Model Benchmarking Workshop, <http://depts.washington.edu/clawpack/links/nthmp-benchmarks/geoclaw-results.pdf>.
- Gower, H. D.; Yount, J. C.; Crosson, R. S., 1985, Seismotectonic map of the Puget Sound region, Washington: U.S. Geological Survey Miscellaneous Investigations Series Map I-1613, 15 p., 1 plate, scale 1:250,000.
- Greene, H., Barrie, J., & Todd, B. (2018). The Skipjack Island fault zone: An active transcurrent structure within the upper plate of the Cascadia subduction complex. *Sedimentary Geology*, 378, 61-79.

- Jacoby, G.C., Bunker, D.E., and Benson, B.E., 1997, Tree-ring evidence for an A.D. 1700 Cascadia earthquake in Washington and northern Oregon, *Geology*, v. 25, no. 11, p. 999-1002.
- Johnson, Potter, Armentrout, & Miller. (1996). The southern Whidbey Island fault: An active structure in the Puget Lowland, Washington. Geological Society of America. Geological Society of America Bulletin, 108(3), 334-354.
- Johnson, S. Y., S. V. Dadisman, J. R. Childs, and W. D. Stanley (1999), Active tectonics of the Seattle fault and central Puget Sound, Washington: Implications for seismic hazards, *Geol. Soc. Am. Bull.*, 111, 1042–1053, doi:10.1130/0016 7606(1999)111<1042:ATOTSF>2.3.CO;2.
- Johnson, S. Y., Dadisman, S. V., Mosher, D. C., Blakely, R. J., & Childs, J. R. (2001). Active tectonics of the Devils Mountain fault and related structures, northern Puget Lowland and eastern Strait of Juan de Fuca region, Pacific Northwest. US Geological Survey Professional Paper, (1643), 1-45.
- Johnson, S., Nelson, A., Personius, S., Wells, R., Kelsey, H., Sherrod, B., . . . Harding, D. (2004). Evidence for late Holocene earthquakes on the Utsalady Point Fault, northern Puget Lowland, Washington. *Bulletin of the Seismological Society of America*, 94(6), 2299-2316.
- Kelsey, H., Sherrod, B., Blakely, R., & Haugerud, R. (2012). Holocene faulting in the Bellingham forearc basin: Upper-plate deformation at the northern end of the Cascadia subduction zone. *Journal of Geophysical Research: Solid Earth*, 117(B3).
- Kelsey, H. M., Sherrod, B. L., Nelson, A. R., & Brocher, T. M., 2008, Earthquakes generated from bedding plane-parallel reverse faults above an active wedge thrust, Seattle fault zone Reverse faults Seattle fault zone. *GSA Bulletin*, 120(11-12), p. 1581-1597.
- LeVeque, R. J., George, D. L., & Berger, M. J., 2011, Tsunami modelling with adaptively refined te volume methods. *Acta Numerica*, 20, p. 211-289.
- LeVeque, R., González, F., and Adams, L., 2018, Tsunami Hazard Assessment of Snohomish County, Washington, Project Report – Version 2, http://faculty.washington.edu/rjl/pubs/THA_Snohomish/index.html.
- LeVeque R.J., Adams, L.M., and González, F.I., 2019, Tsunami Hazard Assessment of Portions of Island and Skagit Counties, Washington, (website containing reports and data), http://depts.washington.edu/ptha/IslandSkagitTHA_2019/.
- Nelson, A. R., Personius, S. F., Sherrod, B. L., Kelsey, H. M., Johnson, S. Y., Bradley, L. A., & Wells, R. E., 2014, Diverse rupture modes for surface-deforming upper plate earthquakes in the southern Puget Lowland of Washington State. *Geosphere*, 10(4), 769-796.
- NOAA, SIFT propagation database metadata file. PMEL Tech report, http://sift.pmel.noaa.gov/ComMIT/compressed/info_sz.dat.
- NOAA National Centers for Environmental Information, 2013, British Columbia 3 arc-second Bathymetric Digital Elevation Model, [Accessed 2018] <https://www.ncei.noaa.gov/metadata/geoportal/rest/metadata/item/gov.noaa.ngdc.mgg.dem:4956/html>.

- NOAA National Geophysical Data Center, 2011, Port Townsend, Washington 1/3 Arc-second MHW Coastal Digital Elevation Model: NOAA National Centers for Environmental Information, [Accessed 2017]
<https://www.ncei.noaa.gov/metadata/geoportal/rest/metadata/item/gov.noaa.ngdc.mgg.dem:366/html>.
- NOAA National Geophysical Data Center, 2014, Puget Sound, Washington 1/3 Arc-second MHW Coastal Digital Elevation Model: NOAA National Centers for Environmental Information, [Accessed 2015]
<https://www.ncei.noaa.gov/metadata/geoportal/rest/metadata/item/gov.noaa.ngdc.mgg.dem:5164/html>.
- NOAA National Geophysical Data Center, 2015, Strait of Juan de Fuca, Washington 1/3 Arc-second NAVD88 Coastal Digital Elevation Model: NOAA National Centers for Environmental Information, [Accessed 2017]
<https://data.noaa.gov/metaview/page?xml=NOAA/NESDIS/NGDC/MGG/DEM//iso/xml/11514.xml&view=getDataView&header=none>.
- NOAA, National Geophysical Data Center. 2009: ETOPO1 1 Arc-Minute Global Relief Model. NOAA National Centers for Environmental Information, [Accessed 2016]
<https://www.ngdc.noaa.gov/mgg/global/>.
- Petersen, M. D., Cramer, C. H., & Frankel, A. D., 2002, Simulations of Seismic Hazard for the Pacific Northwest of the United States from Earthquakes Associated with the Cascadia Subduction Zone. *Pure and Applied Geophysics*, 159(9), p. 2147-2168.
- Personius, S., Briggs, R., Nelson, A., Schermer, E., Maharrey, J., Sherrod, B., . . . Bradley, L. (2014). Holocene earthquakes and right-lateral slip on the left-lateral Darrington-Devils Mountain fault zone, northern Puget Sound, Washington. *Geosphere*, 10(6), 1482-1500.
- Satake, K., Wang, K., & Atwater, B. F., 2003, Fault slip and seismic moment of the 1700 Cascadia earthquake inferred from Japanese tsunami descriptions. *Journal of Geophysical Research: Solid Earth*, 108(B11), <https://doi.org/10.1029/2003JB002521>.
- Sherrod, Brian L.; Blakely, Richard J.; Weaver, Craig S.; Kelsey, Harvey M.; Barnett, Elizabeth; Liberty, Lee; Meagher, Karen L.; Pape, Kristin, 2008, Finding concealed active faults--Extending the southern Whidbey Island fault across the Puget Lowland, Washington: *Journal of Geophysical Research*, v. 113.
- Sherrod, Brian L, Barnett, Elizabeth, Schermer, Elizabeth, Kelsey, Harvey M, Hughes, Jonathan, Foit, Jr, . . . Hyatt, Tim. (2013). Holocene tectonics and fault reactivation in the foothills of the north Cascade Mountains, Washington. *Geosphere* (Boulder, Colo.), 9(4), 827-852.
- University of Washington Tsunami Modeling Group (UWTMG),
<http://depts.washington.edu/ptha/projects/index.html>
- Witter, R. C., Zhang, Y., Wang, K., Priest, G. R., Goldfinger, C., Stimely, L. L., English, J.T., and Ferro, P. A., 2011, Simulating tsunami inundation at Bandon, Coos County, Oregon, using hypothetical Cascadia and Alaska earthquake scenarios. Oregon Department of Geology and Mineral Industries Special Paper, 43, 57 p.

Witter, R. C., Zhang, Y. J., Wang, K., Priest, G. R., Goldfinger, C., Stimely, L., English, J.T., and Ferro, P. A., 2013, Simulated tsunami inundation for a range of Cascadia megathrust earthquake scenarios at Bandon, Oregon, USA. *Geosphere*, 9(6), p. 1783-1803.

Yamaguchi, D.K., Atwater, B.F., Bunker, D.E., Benson, B.E., and Reid, M.S., 1997, Tree-ring dating the 1700 Cascadia earthquake: *Nature* [London], v. 389, no. 6654, p. 922-923.

Appendix A. Complete GeoClaw Model Results

GeoClaw Plots

URLs to plots for each of the four job runs in GeoClaw are available below. Descriptions of each section of the plots pages are below the links.

Cascadia L1 at Mean High Water:

http://depts.washington.edu/ptha/BellinghamBayMaritime/carrie_cu/port_19sec/CSZ_L1_cu_CSZ_L1_MHW_cu_job_9643485_Aug9_2020/_plots/PlotIndex.html

Cascadia L1 at Mean Low Water:

http://depts.washington.edu/ptha/BellinghamBayMaritime/carrie_cu/port_19sec/CSZ_L1_MLW_cu_CSZ_L1_MLW_cu_job_9643486_Aug9_20/_plots/PlotIndex.html

Alaska AKmaxWA at Mean High Water:

http://depts.washington.edu/ptha/BellinghamBayMaritime/carrie_cu/port_19sec/AK_cu_AK_MHW_cu_job_9643014_Aug9_2020/_plots/PlotIndex.html

Alaska AKmaxWA at Mean Low Water:

http://depts.washington.edu/ptha/BellinghamBayMaritime/carrie_cu/port_19sec/AK_MLW_cu_AK_MLW_cu_job_9643024_Aug9_2020/_plots/PlotIndex.html

Model animations

On each page of plots for the study (URLs above), “js Movies” shows a list of animations for the entire *Computational domain* (extent of model), *Inner Coast eta* (the variation in the water surface at the gauge location), *Greater Bellingham eta* (the variation in the water surface at the gauge location), *Bay speed* (current speeds in Bellingham Bay), *port speed* (current speeds along the Bellingham waterfront), and *marina speed* (current speeds zoomed in on Squalicum Harbor).

Gauges

The link to “Gauges” at the top of the page links down to gauge plots for all of the 36 gauges around Bellingham Bay and along the Bellingham waterfront used in the study. The gauge plots show *flow depth* (water depth at the gauge location), *gauge surface eta* (the variation in the water surface at the gauge location), and *speed* (current speeds at each gauge location).

See the Gauge Output section of this report for a map of gauge locations.

Other plots

The link to “Other plots” contains figures for *max depth* (for the fixed grid area—the maximum flow depth over land for the entire fixed grid area), *max speed* (for the fixed grid area—the maximum current speeds for the entire fixed grid area), *fgmax_results_port19s____.kmz* (a downloadable kmz file for Google Earth showing modeling results), and timing (information about computing time for the modeling).

Appendix B. GeoClaw technical information

Data output format

Output was delivered as NetCDF for each source (Cascadia-L1 and AKMaxWA), at high tide (MHW) and low tide (MLW). Hence, six netCDF files were provided with these results. The netCDF files are named by date prepared, source, and tidal level (e.g. Aug9_AK_MHW.nc for the Alaska Mean High Water results created on August 9, 2020).

The netCDF files contain multiple field variables. A pre-processing script generates a few variables before the initiation of the GeoClaw run based on the fgmax region as part of the input. Following the GeoClaw run, the fgmax output generates other variables. Note that all variables are stored on two-dimensional uniform grids as defined by the lon and lat arrays. Only the points on this grid where fgmax point == 1 are used as fgmax points and only at these points is fgmax output available.

Values created as part of the GeoClaw input:

- lon: longitude, x (degrees),
- lat: latitude, y (degrees),
- Z: topography value Z from the DEM, relative to MHW (m),
- fgmax point: 1 if this point is used as an fgmax point, 0 otherwise,
- allow_wet_init: 1 if this point is initialized as usual, 0 if this point is forced to be dry, regardless of initial topography value.

Values created based on the GeoClaw output:

- dz: Co-seismic surface deformation interpolated to each point (m),
- B: post-seismic topography value B from GeoClaw at gauge location (m),
- h: maximum depth of water over simulation (m),
- s: maximum speed over simulation (m/s),
- hss: maximum momentum hs^2 over simulation (m^3/s^2),
- hmin: minimum depth of water over simulation (m),
- arrival time: apparent arrival time of tsunami (s),

In addition, the netCDF files contain the following metadata values:

- tfinal: final time of GeoClaw simulation (seconds),
- history: record of times data was added to file,
- outdir: location of output directory where data was found,

- `run_finished`: date and time run finished,

The `fgmax` points align exactly with the 1/9" DEM points. The finest level computational finite volume grid also aligns so that cell centers are exactly at the `fgmax` points, and `Z` in the `netCDF` file is the value from the DEM at this point. However, by integrating a piecewise bilinear function that interpolates the 1/9" DEM obtains the topography value `B` used in a grid cell in GeoClaw, which is not exactly equal to `Z` initially. Moreover, `B` is the value after any co-seismic deformation associated with the event.

GeoClaw Version 5.7.0

The modeling for this project used a pre-release version of GeoClaw Version 5.7.0 (http://www.clawpack.org/new_features_for_v5.7.0/). GeoClaw is open source, part of the Clawpack software, and available at <http://www.clawpack.org>. The pre-released version 5.7.0 incorporates some modifications that sped up part of the code from version 5.6.1.

Many of the implemented modifications of the GeoClaw code used in this assessment, first debuted in a previous UW tsunami hazard assessment to tackle issues within the Island and Skagit county region (LeVeque and others, 2019). These modifications are briefly described in this appendix and available at: http://www.clawpack.org/new_features_for_v5.7.0/, with more documentation and examples in Jupyter notebooks.

Summary of changes to GeoClaw (FORTRAN code):

- Previous versions of GeoClaw (prior to 5.6.1) were not suitable to deal with millions of `fgmax` points. This updated version has sped the internal algorithms to better deal with millions of `fgmax` points, without changing the computational results.
- As part of speeding the code up, a new format for specifying `fgmax` points is now available. This format uses an ASCII raster file with a header identical to that used for topography files (`topo type==3` in GeoClaw). These files have data values equal to 1 at points that are selected and 0 at non-selected points. The code previously provided a list of all points. This does not change the capabilities in itself, but helps increase the speed (and reduces the file size of input data).
- The GeoClaw code now uses the boolean parameter, `variable_eta_init`. If true, then the sea level used to initialize grid cells to wet or dry when introducing new levels of grid refinement undergoes adjustment, if necessary, by the co-seismic surface displacement as defined by interpolating the `dtopo` file to the center of the grid cell. This is to account for the fact that when the shore subsides the water just offshore subsides as well. Failure to initialize properly can result in artificial flooding onshore. This has no effect for the Cascadia-L1 or AKMaxWA simulations and little effect for SF-L due to the small amount of subsidence in the study region.
- The GeoClaw code also now uses an array `force_dry_init` to indicate where the initial value is forced to be `h=0`, regardless of `topo` value. The `allow_wet_init` array described in Section 5.1, along with a parameter `t_stays_dry` is the basis of the `force_dry_init`.

Summary of new Python code:

GeoClaw 5.7.0 and 5.6.1 also use new Python code, also available here:

http://www.clawpack.org/new_features_for_v5.7.0/, and documented further within the GeoClaw GitHub repository. In particular, the repository contains:

- Code to subsample topography DEMs,
- `marching_front.py`, to implement the marching front algorithms described above.
- `Region_tools.py` implementing Ruled Rectangles.
- `Make_input_files.py` for each fgmax region, to pre-process DEMs and select fgmax points, define Ruled Rectangle flag regions for adaptive refinement around the fgmax points, and determine dry regions below MHW. The open-sourced web application, Jupyter notebook, generated these scripts.
- `fgmax_tools.py` contains tools for post-processing results and writing netCDF files, an updated version of the code in GeoClaw to handle the new style of fgmax files.
- `Process_fgmax_region.py` uses these tools for post-processing fgmax results and writing netCDF files for specific regions.

Appendix C. Modifications to Bellingham 1/9 arc-second DEM

Several minor edits were made to the Bellingham 1/9 arc-second DEM at the Port of Bellingham around Squalicum Harbor by the Washington Department of Natural Resources for the purposes of this study in July 2020. Entrances to the harbor, and breakwaters near the harbor were checked against air photos, and were edited to more accurately reflect the actual ground surface. These modifications were necessary because some parts of the original DEM had errors that influenced the behavior of the tsunami waves in test simulations, by artificially focusing waves, or by preventing them from flowing into or out of the harbor. One example of a modification is seen in Figure C1. Other similar modifications included closing gaps in breakers and removing bumps from the seabed (Figure C2).



Figure C1. An example of some of a modification done to the Bellingham 1/9 arc-second DEM by WA DNR. Left: Closeup of the west entrance to the Outer Squalicum Harbor (pink square). The breakwater shows a gap that does not exist in the actual breakwater.

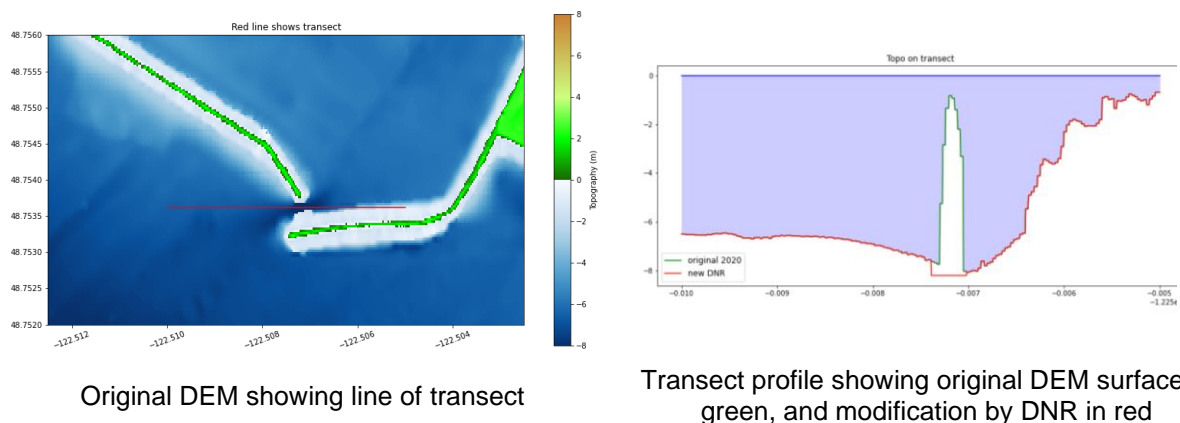


Figure C2. Another example of a modification done to the Bellingham 1/9 arc-second DEM by WA DNR. Left: the south entrance to Squalicum Harbor showing transect line in red. Right: two profiles along the line showing the original (green), and modified (red) topography.